Universidad de Oviedo

Programa de Doctorado en Biogeociencias

OLAS DE CALOR MARINAS EN EL GOLFO DE VIZCAYA: CARACTERIZACIÓN, TENDENCIAS E IMPACTOS

MARINE HEATWAVES IN THE BAY OF BISCAY: CHARACTERIZATION, TRENDS AND IMPACTS

Doctoranda:

Paula Izquierdo Muruáis

Oviedo, octubre de 2024

Universidad de Oviedo

Departamento de Biología de Organismos y Sistemas

Programa de Doctorado en Biogeociencias

OLAS DE CALOR MARINAS EN EL GOLFO DE VIZCAYA:

CARACTERIZACIÓN, TENDENCIAS E IMPACTOS

MARINE HEATWAVES IN THE BAY OF BISCAY:

CHARACTERIZATION, TRENDS AND IMPACTS

Doctoranda:

Paula Izquierdo Muruáis

Directores:

Dr. José Manuel Rico Ordás

Dr. Fernando González Taboada

Oviedo, octubre de 2024

Universidad de Oviedo

RESUMEN DEL CONTENIDO DE TESIS DOCTORAL

1.- Título de la Tesis	
Español: Olas de calor marinas en el Golfo de Vizcaya: caracterización, tendencias e impactos	Inglés: Marine heatwaves in the Bay of Biscay: characterization, trends and impacts

2.- Autor	
Nombre: Paula Izquierdo Muruáis	
Programa de Doctorado: Biogeociencias	
Órgano responsable: Centro Internacional de Postgrado	

RESUMEN (en español)

Las olas de calor marinas son episodios transitorios de temperaturas oceánicas extremadamente altas que pueden causar impactos profundos y duraderos en la estructura y el funcionamiento de los ecosistemas marinos, así como en los medios de vida humanos y las actividades económicas que dependen de sus recursos. La incidencia, intensidad y duración de las olas de calor marinas han aumentado en todo el mundo a consecuencia del calentamiento oceánico, y las simulaciones de modelos climáticos proyectan un aumento en su frecuencia y gravedad en los próximos años. Los análisis globales brindan una comprensión amplia de las tendencias de las olas de calor marinas, pero la investigación regional sigue siendo crucial para captar impactos localizados y entender la realidad experimentada por los ecosistemas marinos. Este trabajo se centra en caracterizar las olas de calor marinas, analizar sus tendencias y evaluar sus impactos en el Golfo de Vizcaya, una región con ecosistemas marinos diversos y socioeconómicamente importantes donde el conocimiento sobre estos eventos extremos está comenzando a desarrollarse. En primer lugar, analizamos tendencias en la ocurrencia de olas de calor marinas y sus características clave en dos ubicaciones costeras en el Mar Cantábrico central utilizando datos de temperatura in situ recopilados entre 1998 y 2019. Si bien la corta duración y la presencia de lagunas en las series de temperatura impidieron la detección de tendencias significativas, encontramos una correlación positiva entre la incidencia de olas de calor marinas y la fase positiva del patrón del Atlántico este, así como una posible asociación con cambios documentados de poblaciones de macroalgas formadoras de hábitat. En segundo lugar, realizamos un análisis comparativo de la incidencia y las características clave de las olas de calor marinas derivadas de registros de temperatura in situ y aquellas detectadas mediante productos de detección remota. Descubrimos que las estimaciones satelitales tendían a pasar por alto el afloramiento costero estival y, en consecuencia, conducían a una sobreestimación de la incidencia y duración de las olas de calor marinas cerca de la costa. Para corregir estos sesgos, desarrollamos un enfoque de reducción de escala basado en modelos de regresión que consigue reconciliar las mediciones in situ y satelitales considerando el afloramiento costero y los flujos de calor aire-mar. Este método nos permitió predecir con precisión la incidencia de las olas de calor marinas costeras en un ámbito espaciotemporal prolongado y revelar una sextuplicación de su ocurrencia en el sur del Golfo de Vizcaya durante las últimas cuatro décadas. Los análisis de tendencias basados en umbrales de detección estáticos versus dinámicos indican que más de la mitad de este aumento es atribuible a la tendencia subyacente del calentamiento oceánico. Por último, examinamos las tendencias a largo plazo en la temperatura media de la superficie del mar, el afloramiento, la turbulencia, las olas de calor y las olas de frío marinas en la plataforma continental del Golfo de Vizcaya durante las últimas cuatro décadas y evaluamos su influencia en la supervivencia temprana de cuatro especies clave de pequeños peces pelágicos: la anchova, la caballa, el chicharro y la sardina. Reportamos un aumento general de la temperatura de la superficie del mar, una intensificación de las olas de calor marinas y un debilitamiento de las olas de frío. También encontramos que los procesos relacionados con el viento ejercen impactos variados según la especie y la región. Las aguas más cálidas y las olas de calor marinas fomentan la supervivencia de la caballa pero perjudican la del chicharro en todo el Golfo, mientras que las olas de frío marino afectan negativamente a la anchoa y la caballa. En conjunto, nuestro trabajo destaca la importancia del seguimiento continuado de las olas de calor marinas en el Golfo de Vizcaya y subraya la necesidad de incluir proyecciones climáticas en próximas investigaciones para anticipar futuras

tendencias en la región. Desde una perspectiva metodológica, aporta modelos estadísticos para mejorar la detección y caracterización de olas de calor marinas en mares costeros y de plataforma que pueden complementar instrumentos de monitoreo in situ de alta resolución. Finalmente, nuestro trabajo pone el foco en el impacto de las olas de calor marinas en las comunidades de macroalgas y pequeños peces pelágicos de la región y enfatiza la necesidad de realizar nuevos esfuerzos de conservación y gestión que se adapten al clima y que tengan como objetivo lograr la resiliencia de los ecosistemas en un mundo que se calienta.

RESUMEN (en inglés)

Marine heatwaves are transient episodes of extremely high ocean temperatures that can cause profound, long-lasting impacts on the structure and functioning of marine ecosystems, as well as on human livelihoods and economic activities reliant on their resources. The incidence, intensity, and duration of marine heatwaves have been increasing worldwide as a response to ocean warming, and climate model simulations project an upcoming rise in their frequency and severity in forthcoming years. Global analyses provide a broad understanding of marine heatwave trends, but regional research remains crucial for capturing localized impacts and addressing the actual experiences of marine ecosystems. This work focuses on characterizing marine heatwaves, analyzing their trends, and assessing their impacts in the Bay of Biscay—a region with diverse and socioeconomically important marine ecosystems where knowledge on these extreme events is beginning to unfold. First, we analyzed trends in marine heatwave occurrence and key features at two coastal locations in the central Cantabrian Sea using in situ temperature data gathered within 1998-2019. While the short length and of the presence of gaps in the temperature series prevented the detection of significant trends, we found a positive correlation between marine heatwave incidence and the positive phase of the East Atlantic pattern, as well as a potential association with reported population shifts of habitat-forming macroalgae. Second, we conducted a comparative analysis of the incidence and key features of marine heatwaves derived from in situ temperature records and those detected via remotely-sensed products. We found that satellite estimates tended to overlook summer coastal upwelling and consequently led to overestimated marine heatwave incidence and duration nearshore. To amend these biases, we developed a downscaling approach based on regression modeling that achieves to reconcile in situ and satellite measurements by considering coastal upwelling and air-sea heat fluxes. This method allowed us to accurately hindcast coastal marine heatwave incidence over a prolonged spatiotemporal scope and reveal a six-fold increase in their occurrence across southern Bay of Biscay over the last four decades. Trend analyses based on static vs. dynamic detection thresholds indicate that over half of this increase is attributable to the underlying ocean warming trend. Lastly, we examined long-term trends in average sea surface temperature, upwelling, turbulence, marine heatwaves and cold-spells across the continental shelf of the Bay of Biscay over the last four decades and assessed their influence on the early life survival of four key small pelagic fish species: anchovy, mackerel, horse mackerel and sardine. We report an overall rise in sea surface temperature, an intensification of marine heatwaves and a weakening of cold-spells. We also found that wind-related processes exert varied impacts depending on the species and region. Warmer waters and marine heatwaves foster mackerel survival but hamper that of horse mackerel across the entire Bay, whereas marine cold-spells negatively affect anchovy and mackerel. Altogether, our work highlights the importance of continued marine heatwave monitoring in the Bay of Biscay and stresses the need to include climate projections in upcoming research to anticipate future trends in the region. From a methodological perspective, it contributes statistical models to improve the detection and characterization of marine heatwaves in coastal and shelf seas that can complement high-resolution, in situ monitoring instruments. Finally, our work brings into light the impact of marine heatwaves on macroalgae and small pelagic fish communities in the region and emphasizes the urge for new, climate-adaptive conservation and management efforts aimed at achieving ecosystem resilience in warming world.

SR. PRESIDENTE DE LA COMISIÓN ACADÉMICA DEL PROGRAMA DE DOCTORADO EN BIOGEOCIENCIAS

Contents

List of figures

List of tables

Acknowledgements

This work has been made possible thanks to the dedicated efforts of many individuals and organizations. I would like to extend my gratitude to the following organizations and their personnel for the public availability of the databases used in this study:

- NOAA National Centers for Environmental Information (NCEI) for providing and maintaining the NOAA Optimum Interpolation 0.25º Daily Sea Surface Temperature Analysis (OISST version 2).
- Ocean Observatory of Asturias (OMA) for producing, maintaining, and providing *in situ* water temperature data.
- NASA Global Modeling & Assimilation Office (GMAO) for the availability and maintenance of the Modern-Era Retrospective analysis for Research and Applications, Version 2 (MERRA-2).
- Copernicus Climate Change Service (C3S) Climate Data Store (CDS) for the production and maintenance of ERA5 0.25° reanalysis data.
- General Bathymetric Chart of the Oceans (GEBCO) for developing and providing bathymetric grids.
- International Commission for the Exploration of the Sea (ICES), especially the Working Group on Southern Horse Mackerel, Anchovy and Sardine (WGHANSA) and the Working Group on Widely Distributed Stocks (WGWIDE), for the production and availability of fish abundance data.

This work was also possible thanks to a "Severo Ochoa" Grant Program for training in research and teaching of the Principality of Asturias (AYUD0029T01, Gobierno del Principado de Asturias). I would also like to acknowledge the crew from the IMBRSea Program and the Chair of Climate Change at the University of Oviedo (CuCC) for providing ongoing learning opportunities through their support, resources, and commitment to advancing knowledge in marine science, both in Asturias and abroad. On a more academic note, I have also benefited from the generous assistance of several anonymous and known referees; please receive my heartfelt thanks. I also owe gratitude to the many individuals who have selflessly addressed queries on mailing lists associated with R, LaTeX, GitLab and Stack Overflow.

On a more personal level, several key events have brought me to this point. Throughout my academic journey from school to university I have been fortunate to benefit from the guidance of exceptional teachers, to whom I extend my deepest gratitude. After earning my degree in Biology, I pursued a MSc in Marine Conservation at the University of Oviedo, where I had the opportunity to learn from notable professors such as José Luis Acuña, Julio Arrontes, Yaisel Borrell, and

many others involved in the program. Their expertise and support played a significant role in shaping my academic journey, and I am grateful for their valuable contributions. It was during this period that I was introduced to marine heatwaves at the hands of José Manuel Rico. Under his supervision, I explored this area further in my MSc Thesis. His mentorship played a crucial role in motivating me to pursue a PhD, and I am thankful for his support during this significant phase of my academic career. As a doctoral student at the Department of Biology of Organisms of Systems (BOS), I would like to thank all those within the department, with special recognition to both current and former members of the Marine Ecology group. I am also grateful to professors Alfredo Fernández-Ojanguren and Nicolás Weidberg for their collaboration in teaching endeavors and their continued good humor. A special mention goes to María Aida González for her assistance in keeping everything working properly and for her boundless patience. Lastly, I would like to extend my thanks to Ricardo González-Gil for his invaluable research contributions and for generously sharing his expertise in code, manuscript writing, marine science, and indispensable advice and support.

I have set aside this penultimate paragraph to express my sincere thanks to José Manuel Rico and Fernando González Taboada for their steadfast supervision, mentorship, and support throughout this journey. I am truly grateful for their expertise and dedication, and I aspire to embody at least a part of their qualities in my own endeavors.

Finally, I want to thank my partner Jorge, my longstanding friends Sara, Aida, and Carol, and, most importantly, my family. My deepest gratitude goes to my parents for their unwavering love, encouragement and belief, which have fueled my determination and resilience in achieving this milestone.

Chapter 1

Introduction

Global change stands as one of the defining issues of our time (IPCC, 2023). Human activities have been the unequivocal driver of this phenomenon, mainly through the emission of greenhouse gases by unsustainable practices such as fossil fuel burning, exploitative land use and consumption-centered lifestyles. Its effects have been vividly apparent in the last few decades with rising global temperatures, shifting weather patterns, melting ice caps, rising sea levels and an increasing frequency and intensity of extreme weather events, among other manifestations. These impacts hold far-reaching, multifaceted repercussions that transcend environmental domains, permeating into the stability of present and future economies and social structures.

The ocean plays a crucial role in supporting human well-being. Economically, it contributes 2.5% of global gross domestic product (GDP), employs 1.5% of the global workforce, and is projected to reach an estimated output of US$3 trillion by 2030 (Organization for Economic Co-operation and Development, 2016). Ecologically, it regulates the global climate by absorbing and storing vast amounts of carbon dioxide (Gruber et al., 2023), maintains the functioning, resilience, and services provided by ecosystems (Costanza et al., 2014) and hosts vital habitats for a wide range of biodiversity (Costello et al., 2017), among many other essential functions. As a whole, sustainable and healthy oceans are key in meeting climate and societal goals for a resilient and equitable future (Hoegh-Guldberg et al., 2019) – a future that is currently at a crossroads.

Model projections under different greenhouse gas emission scenarios predict unprecedented changes in ocean conditions throughout the 21st century, *i.e.* increased temperatures, greater upper ocean stratification, acidification, deoxygenation and altered net primary production (Kwiatkowski et al., 2020). Although the rates and magnitudes of these changes are expected to be smaller under low emission scenarios, they are nonetheless foreseen to induce consistent declines in the biomass and species richness of marine animal communities (Tittensor et al., 2021; Penn & Deutsch, 2022). As of today, 66% of the global oceans are already experiencing increasing cumulative impacts from a variety of drivers (IPBES, 2019a). These impacts heighten the risk of marine ecosystem disruption worldwide and directly compromises the ocean's role in sustaining essential goods and services for human welfare (Ruckelshaus et al., 2013). Consequently, there has been a notable rise in the prominence of ocean governance, emphasizing international collaboration and the development of comprehensive management strategies to tackle the complexities of marine ecosystems and anticipate future challenges (Haas et al., 2022).

The success of such strategies relies on scientific research aimed at exploring the complexities and drivers of stressed oceanic systems, along with their associated impacts and repercussions.

Global ocean warming has emerged as a central focus in environmental scientific research due to its profound implications for marine ecosystems and the planet as a whole (Cheng et al., 2022, 2023). Within this context, extreme temperature events have garnered considerable attention in recent years for their disruptive effects on marine biodiversity, ecosystems, and associated socioeconomic activities (Frölicher, 2019). Marine heatwaves are periods of extremely high temperatures that can last for days to months, can extend up to thousands of kilometers, and can penetrate multiple hundreds of meters deep into the ocean (Oliver et al., 2021). While marine heatwaves are not a new phenomenon and can occur naturally, their frequency and intensity have increased globally over the past century driven by the growing influence of climate change (Oliver et al., 2018; Laufkötter et al., 2020). Given the escalating concern over their associated impacts, quantifying trends and patterns of marine heatwaves has become a pressing issue.

The term ‘marine heatwave’ was first coined by Pearce et al. (2011) to describe an anomalously warm water event in Western Australia in 2011, marking the inception of research in this field. Consensus on qualitative marine heatwaves definition was not achieved until 2016 by Hobday et al. (2016), who described them as "discrete, prolonged anomalously warm water events" and provided quantitative criteria for their identification. First, marine heatwave detection must be based on a sufficiently long, temporally consistent climatological baseline (Hobday et al., 2016; Schlegel et al., 2019) that can be either seasonally varying or fixed, depending on the research objectives at hand (Chiswell, 2022). Second, to be considered as such, marine heatwaves must surpass a threshold set at the 90th percentile of the climatological baseline and last for at least 5 consecutive days (Hobday et al., 2016). This common framework paved the way for retrospective comparisons between marine heatwave episodes worldwide and enabled the mechanistic understanding of their role in diverse marine ecosystems.

The occurrence of marine heatwaves is modulated by a complex interplay of local and remote drivers operating across different spatial and temporal scales (Holbrook et al., 2019). Locally, marine heatwave emergence is attributed to changes in the surface mixed layer temperature budget, driven by processes such as air–sea heat fluxes and oceanic advection currents on the horizontal (*e.g.* geostrophic boundary currents and wind-driven Ekman flows) and the vertical (*e.g.* upwelling and downwelling) (Oliver et al., 2021). The spatiotemporal reach of these processes can be amplified through the influence of large-scale climate variability modes and remote sources via teleconnections, which can potentially result in longer, wider-reaching, and more intense marine heatwaves (Hobday et al., 2023). On a broader scale, increasing trends in marine heatwaves incidence and intensity across global oceans are largely attributed to long-term changes in mean sea surface temperatures (Oliver, 2019). As ocean warming continues to

accelerate in the coming decades, future projections point towards more frequent and prolonged marine heatwaves worldwide (Frölicher et al., 2018; Oliver et al., 2019). This trend poses a significant threat to the sustainability of marine communities and directly jeopardizes the vital goods and services they provide (Smale et al., 2019).

In recent years, several high-impact marine heatwave events have garnered attention due to the severity and breadth of their repercussions, which have been extensively researched and documented within the scientific community (Benthuysen et al., 2020). Some of the longest, most intense events recorded include low-latitude marine heatwaves linked to the El Niño in the Coral Sea (2016, 2017, and 2020; Benthuysen et al., 2021) and off the Australian coast (2011, 2015/16 and 2017/18; Kajtar et al., 2021), high-latitude events in the northwest Atlantic (2012 and 2016; Pershing et al., 2018) and multiyear, persistent episodes in the northeast Pacific (2014/16 and 2019/21; Barkhordarian et al., 2022), including the longest marine heatwave on record, 'the Blob' (Di Lorenzo & Mantua, 2016).

The ecological and socioeconomic impacts stemming from the occurrence of these and other extreme marine heatwaves worldwide are diverse and profound. Mass mortality events, loss of seagrass and kelp forests, extended coral bleaching, harmful algal blooms, depleted zooplankton biomass, species tropicalization, distribution range shifts, and the overall restructuring and/or depletion of marine ecosystems ultimately reverberate in the economy through decreased tourism, potential health risks, reduced catch quota, fisheries closure, and civil unrest (Smith et al., 2021). As marine heatwaves deepen the conflict between humans and wildlife (Samhouri et al., 2021), understanding ecosystem-specific responses becomes imperative for effective conservation and management efforts across different regions of the world (Thoral et al., 2022).

The preceding overview provides a little glimpse into the current state of the art in marine heatwave research, offering insights into the latest advancements in understanding their dynamics, drivers and associated impacts. This work presents contributions that delve into the characterization, detectability, and repercussions of marine heatwaves in ecologically significant regions, aiming to contribute additional pieces to the larger puzzle of comprehending and addressing marine heatwaves in a changing global ocean. Our focus lies on the temperate marine environment of the Bay of Biscay, which constitutes a unique setting for marine environmental science that, beyond its longstanding tradition of research and exploration, presents a significant gap in marine heatwave monitoring and assessment. The major features of the Bay of Biscay include i) weak circulation patterns mostly shaped by the influence of Atlantic waters, ii) pronounced seasonal mixing and stratification of water masses, and iii) coastal upwelling, river discharge, and tidal dynamics across the continental shelf that contribute to substantial fluctuations in primary production and phytoplankton biomass (Borja et al., 2019). Taking advantage of this setting, we studied recent trends in marine heatwave incidence in coastal and

shelf areas of the Bay making use of both *in situ* and remote sensing data. We begin by characterizing marine heatwaves off central Cantabrian Sea, while also examining the influence of the East Atlantic pattern and identifying their potential impact on intertidal macroalgae communities (Chapter 2). Then, we present a novel downscaling approach based on regression modeling that reconciles discrepancies between field and satellite coastal temperature measurements by considering the influence of alongshore upwelling and air-sea heat fluxes. This method improves coast-level marine heatwave detection accuracy while retaining satellite resolution, which enabled the reconstruction of past temperatures and the analysis of marine heatwave trends along the northern coast of Spain over the last four decades (Chapter 3). In the last chapter, we examine how environmental forcing and extreme temperature events affect the early life survival of four pelagic fish species of both ecological and commercial relevance in the Bay of Biscay (Chapter 4). Each chapter can be read independently and provides a detailed introduction and discussion. The final chapter (Chapter 5) synthesizes the main findings and results, presenting a comprehensive overview and highlighting the key conclusions reached.

1.1. Objectives

- Examine the frequency, intensity and duration of marine heatwaves in two intertidal locations in central Cantabrian Sea and assess mechanistic links between marine heatwave occurrence, changes in large-scale, atmospheric circulation, and documented shifts in the abundance and distribution of dominant macroalgae species.
- Develop a statistical downscaling approach to enhance the detection of marine heatwaves in coastal shelf ecosystems. Taking advantage of this approach, analyze marine heatwave trends along the northern coast of Spain spanning four decades using static (no trend) vs. dynamic (incorporating a linear warming trend) detection thresholds to distinguish potential impacts of ocean warming.
- Assess long-term trends in sea surface temperature, coastal upwelling, wind turbulence, marine heatwave and marine-cold spells across the continental shelf of the Bay of Biscay over the last four decades, and examine their potential impact on the early life survival of commercially exploited small pelagic species (anchovy, mackerel, horse mackerel and sardine).

Chapter 2

Marine heatwave characterization in southern Bay of Biscay

Abstract

The trend towards an increased incidence of marine heatwaves (MHWs) due to climate change poses a serious threat to the health of coastal ecosystems. Here, we characterized MHWs based on daily *in situ* water temperature measurements collected from 1998 to 2019 in two intertidal coves, Oleiros and La Franca, located in the central Cantabrian Sea coast, N Spain. The two study locations cover the transition zone between cold- and warm-temperate benthic communities that characterizes the biogeography of intertidal assemblages along the SW Bay of Biscay. We examined the incidence, duration and magnitude of MHWs, and assessed the emergence of trends towards more frequent, prolonged and intense MHWs during the study period. We further assessed mechanistic links with modes of climate variability by examining the association between MHW occurrence and the East Atlantic pattern (EA). We detected 78 MHW events between Jan. 1998 and Mar. 2019 (40 in Oleiros, 38 in La Franca) and more than half were synchronous among study locations. The incidence, duration, and intensity of MHWs were higher during the positive phase of the EA, which is associated with air pressures above normal and southwesterly winds during summer. The recorded MHWs also coincided with documented shifts in the abundance and distribution of dominant macroalgae species that triggered abrupt changes in the structure of intertidal communities of the region. Our findings and the present scenario of climate change emphasize the need to enhance research around the trends in the occurrence of MHWs in the coast of northern Spain, and the NE Atlantic Ocean coast in general.

Keywords: Marine heatwaves, sea surface temperature, *in situ* measurements, East Atlantic pattern, Bay of Biscay, coastal environment

2.1. Introduction

Marine heatwaves (MHWs) are transient episodes of extreme ocean temperatures that can cause serious, long-lasting impacts on the structure and function of marine ecosystems (Hobday et al., 2016). These authors define MHWs as lasting for at least 5 days and being warmer than the 90th percentile of the climatological observations. Parallel to the general trend in global ocean warming, MHWs have become more intense and frequent in recent years under the influence of anthropogenic climate change (Fox-Kemper et al., 2021; Laufkötter et al., 2020). Extreme temperature events like MHWs often exert stronger impacts than gradual changes associated with ocean warming (Oliver et al., 2018), and often promote abrupt changes in the composition of marine ecosystems (Wernberg et al., 2016). These impacts entail changes in natural communities and considerable losses of the local ocean's goods and services, leading to serious socioeconomic issues (Smale et al., 2019). Analyzing trends and patterns in MHW occurrence has become a pressing issue, especially under their imminent increase in likelihood and severity around the world, according to future predictions (Frölicher et al., 2018; Collins et al., 2019).

In this global context, within the North-East Atlantic Ocean, the Cantabrian Sea is a narrow (~30km) temperate coastal shelf sea that comprises the northern coast of Spain (southern Bay of Biscay). The Cantabrian coastal waters have experienced an unabated increase in sea surface temperature (SST) from the 1970s onwards by 0.22ºC decade^{-1} (deCastro et al., 2009; Chust et al., 2022), which exceeds the global trend [~0.15ºC decade^{-1}, Rhein et al., 2013]. Increases in mean SSTs have been identified as one of the main reasons for the worldwide increase in MHW frequency and duration over the past century (Oliver et al., 2018). The occurrence of MHWs at a global scale has recently been addressed through multiproduct analyses relying on satellite data (Marin, Feng, et al., 2021; Varela et al., 2021). However, the incidence of MHWs in northern Spain using field temperature data has only been recently assessed in Izquierdo et al. (2022). The projected increase in MHW severity (Oliver et al., 2019) and the ecological impacts witnessed by the scientific community (Smale et al., 2019) bring out the relevance of their study in the region.

The occurrence of MHWs has been linked to large-scale atmospheric circulation patterns (Holbrook et al., 2019). In the Bay of Biscay, the East Atlantic pattern (EA) is the dominant mode of climate variability (Borja et al., 2019). According to previous studies, it is among the most representative regional patterns of atmospheric variation in the Northern Hemisphere (Rodriguez-Puebla et al., 1998; Lorenzo et al., 2007). Modes of climate variability remotely modulate SSTs through the alteration of sea surface energy fluxes and oceanic advection currents (Holbrook et al., 2019). Their occurrence may hence prompt anomalous patterns in SST at a local-regional scale (Deser et al., 2010; deCastro et al., 2011). The occurrence of MHWs is attributed to the influence of different atmospheric and oceanic physical processes (Schlegel, Oliver, et al., 2021)

that directly affect SST variations (Oliver et al., 2021). As a mode of large-scale atmospheric circulation pattern, the assessment of the EA's association with the incidence of MHWs in the Cantabrian coast is of considerable interest for quantifying trends and patterns of their occurrence in the region, as well as their impacts on different habitats.

Among these habitats, vegetated coasts form highly productive ecosystems that contribute important services (Barbier, 2017), including its role as a net carbon sink of anthropogenic emissions (Duarte, 2017). MHWs pose a serious risk to marine ecosystems dominated by macroalgae, altering the distribution and abundance of their populations and the associated community (Wernberg et al., 2016). Canopy-forming species (kelp, fucoids) play an essential role as habitat-forming species and primary producers of the coastal marine ecosystems of the Cantabrian Sea (Martínez et al., 2015). In the past few years, numerous authors have reported significant and progressive changes in the distribution of the main coastal seaweed species in northern Spain (Fernández & Anadón, 2008; Müller et al., 2009; Fernández, 2011; Viejo et al., 2011; Duarte et al., 2013; Voerman et al., 2013; Fernández, 2016; Piñeiro-Corbeira et al., 2016; Casado-Amezúa et al., 2019; Des et al., 2020). These shifts have been mostly associated with the observed increase in SST in the region, among other factors (Gómez-Gesteira et al., 2008). The intensification of MHWs due to climate change compromises the endurance of these key organisms and that of the very ecosystem (Smale et al., 2019). Their disappearance entails a negative environmental impact for coastal communities and poses a threat to the maintenance of the highly valuable goods and services they provide.

Here, we analyzed the incidence and characteristics of MHWs over the period Jan. 1998 – Mar. 2019 at two intertidal locations in central Cantabrian Sea, SW Bay of Biscay. To assess the influence of large-scale climatic anomalies on MHW incidence, we compared MHW records with the historical series of an atmospheric index capturing variability in the EA pattern. Finally, we screened the literature to identify potential impacts of MHWs on intertidal communities along the central Cantabrian coast. Our analyses bring to light the incidence and severity of MHWs on the Cantabrian coast while, in parallel, connect their occurrence to the influence of climate variability modes and address their impacts on local marine ecosystems.

2.2. Materials and methods

2.2.1. Study area

The study was conducted in the central Cantabrian Sea, SW Bay of Biscay (NE Atlantic). The Cantabrian coast is subjected to a marked thermal gradient from a cooler western area with an oceanic influence towards a warmer, more continental regime towards the inner Bay of Biscay (Lavín et al., 2006). Cape Peñas influences regional coastal circulation and alongshore upwelling

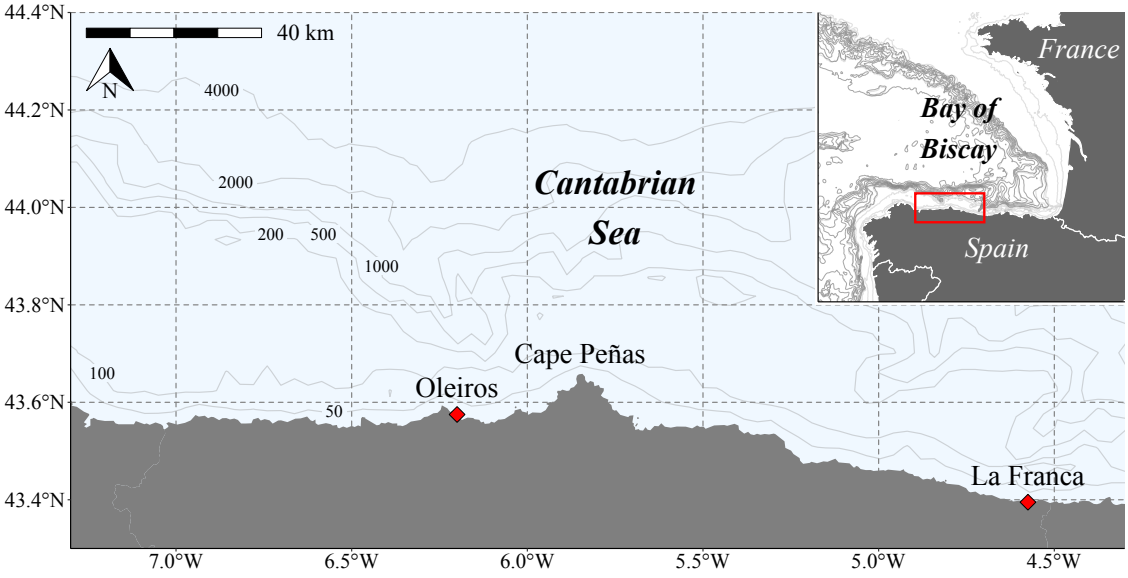

Figure 2.1. Map showing the two study locations of Oleiros and La Franca, which are separated by Cape Peñas. Bathymetry data were extracted from the (GEBCO Compilation Group, 2021). Depth is expressed in meters.

patterns, which come ultimately defined by the prevailing seasonal winds (Valencia et al., 2004; Llope et al., 2006). Oleiros (6.200W 43.575N) and La Franca (4.575W 43.395N) constitute two coastal locations separated by ~100 km and by Cape Peñas, which represents an abrupt transition in average temperature in the westward warming trend of the Cantabrian Sea (Fig. 2.1). Altogether, the area represents a well-defined biogeographical transition zone between cold- and warm-temperate waters.

2.2.2. *In situ* temperature data

Daily *in situ* temperature measurements were collected from Jan. 1998 to Mar. 2019 (~21 years) at Oleiros and La Franca using TidbiT V2 water temperature dataloggers (ONSET Company). The data were retrieved with a reader HOBO Optic USB Base Station and converted to text files through the program HOBOWare Pro v.3.7.10 (ONSET Company). *In situ* water temperature dataloggers were fixed onto solid rock between 0.5-1m above minimum tidal level, ensuring that they will always stay submerged at high tide. Loggers were programmed to record water temperature twice per hour. We filtered the series to retain two daily records corresponding to the semidiurnal high tides, from which we took the average value as a measure of daily mean sea temperature.

The resulting time series misses daily temperature data during 6% of the study period in Oleiros and 18% in La Franca. In terms of length and temporal consistence the temperature series would be considered sub-optimal according to Hobday et al. (2016) but remains nonetheless suitable for MHW research (Schlegel et al., 2019). The time series is framed within a warming period of the

SSTs in the Cantabrian coast that began in the 1970s (deCastro et al., 2009). Ideally, the series should span its overall length to thoroughly assess MHW impacts upon natural communities within that period, as well as the evolution in their incidence (see Izquierdo et al., 2022). However, no *in situ* records prior to 1998 are available and although the series remains adequate for MHW characterization, the frequency, intensity and duration of the events detected in the present study might be underestimated.

Trends in sea temperature based on the *in situ* records were obtained from Gaussian regression coefficients based on Generalized Linear Models (GLM; Gelman & Hill, 2006) to assess the presence of warming or cooling trends in the respective study locations.

2.2.3. East Atlantic pattern (EA) historical series

The EA pattern, first described by Wallace & Gutzler (1981), is one of the most important modes of atmospheric variability in the north Atlantic/European sector. It consists of a north–south dipole in sea level pressure anomalies that spans the entire North Atlantic Ocean, with the centers located near 55°N, 20–35°W and 25–35°N, 0–10°W (Barnston & Livezey, 1987). Its structure resembles the North Atlantic Oscillation, although the EA pattern is associated with atmospheric circulation across the subtropical Atlantic that influence storm tracks and air mass transport towards southern Europe. The positive phase of the EA is associated with above-average SSTs and precipitation in the northeast Atlantic margin, including the Bay of Biscay (Rodriguez-Puebla et al., 1998; deCastro et al., 2008). The EA pattern has also been reported to have a notable impact over maximum atmospheric temperatures over the Iberian Peninsula (Frías et al., 2005). We extracted the monthly teleconnection index of the EA from the Climate Prediction Center of the NOAA's National Weather Service for the period 1998-2019. Northern Hemisphere teleconnection indices are calculated based on the Rotated Principal Component Analysis used by Barnston & Livezey (1987) applied to monthly mean standardized 500-mb height anomalies obtained from the Climate Data Assimilation System in the analysis region 20°N-90°N between Jan. 1950 – Dec. 2000. The anomalies are standardized by the 1950-2000 base period monthly means and standard deviations. We examined the relationship between MHW incidence and the occurrence of either phase of the EA pattern through a Chi-squared test.

2.2.4. Characterization of marine heatwaves (MHWs)

We characterized MHWs following Hobday et al.'s (2016) criteria, which state that a MHW i) must last for at least 5 days ii) must be warmer than the 90th percentile of the climatological observations and iii) must be based, at least, on a 30-year historical baseline period. Although our time series is 21 years long, Schlegel et al. (2019) state that series as long as 10 years produce acceptable MHW metrics that may be used with some caution. We used *in situ*

temperature data to create an annual climatological mean and a 90th percentile threshold, which allowed us to set up the framework to detect MHWs. We considered the total number of MHWs and MHW days to assess MHW incidence throughout time in both study locations. We also described and classified each MHW according to the following set of summary statistics: maximum intensity (highest temperature anomaly value during the MHW [i_{max}, ºC]), mean intensity (mean temperature anomaly during the MHW [i_{mean}, ºC]), cumulative intensity (sum of daily intensity anomalies [i_{cum}, ºC days]) and duration (consecutive period of time [D, days]) (Table 2.A.1 in the Appendix). The former temperature anomalies refer to the temperature that exceeds the annual climatological mean. Trends in MHW frequency, number of MHW days and MHW duration -discrete variables, *i.e.*, counts of events during some period of time- were estimated using Poisson GLMs (*e.g.*, Gelman & Hill, 2006). For this purpose, MHW duration and the number of MHW days were both fixed by the yearly possible number of MHW days in order to deal with missing data. MHW trends were examined both annually and seasonally for spring-summer [Mar-Aug] and autumn-winter months [Sep-Feb] (Table 2.A.2 in the Appendix). We assessed model adequacy through standard residual checks and accounted for overdispersion of discrete data counts when necessary.

2.2.5. Technical implementation details

All analyses were implemented in R version 4.0.5 (R Core Team, 2021). MHW characterization and analysis were performed using the library *heatwaveR* (Schlegel & Smit, 2018), which applies the MHW definition from Hobday et al. (2016). We made extensive use of the libraries *tidyverse* (Wickham et al., 2019), *lubridate* (Grolemund & Wickham, 2011), *plyr* (Wickham, 2011) and *readxl* (Wickham & Bryan, 2019) to perform all calculations and regression analyses. We also used the R packages *cowplot* (Wilke, 2020), *rnaturalearth* (Massicotte et al., 2017), *rnaturalearthdata* (South et al., 2017), *ggspatial* (Dunnington et al., 2021), *mapSpain* (Hernangómez, 2021), *scales* (Wickham et al., 2020), *metR* (Campitelli, 2021), *png* (Urbanek, 2013) and *extrafont* (Chang, 2014) for graphical design and the generation of the map of the study location.

2.3. Results

The analysis of sea temperature trends revealed a general, steady increase (slope = 0.009ºC year^{-1}; p-value = 0.012). Separately, Oleiros displayed an increasing trend (slope = 0.023ºC year^{-1}; p-value < 0.001); but no trend was detected in La Franca (slope = -0.004ºC year^{-1}; p-value = 0.456).

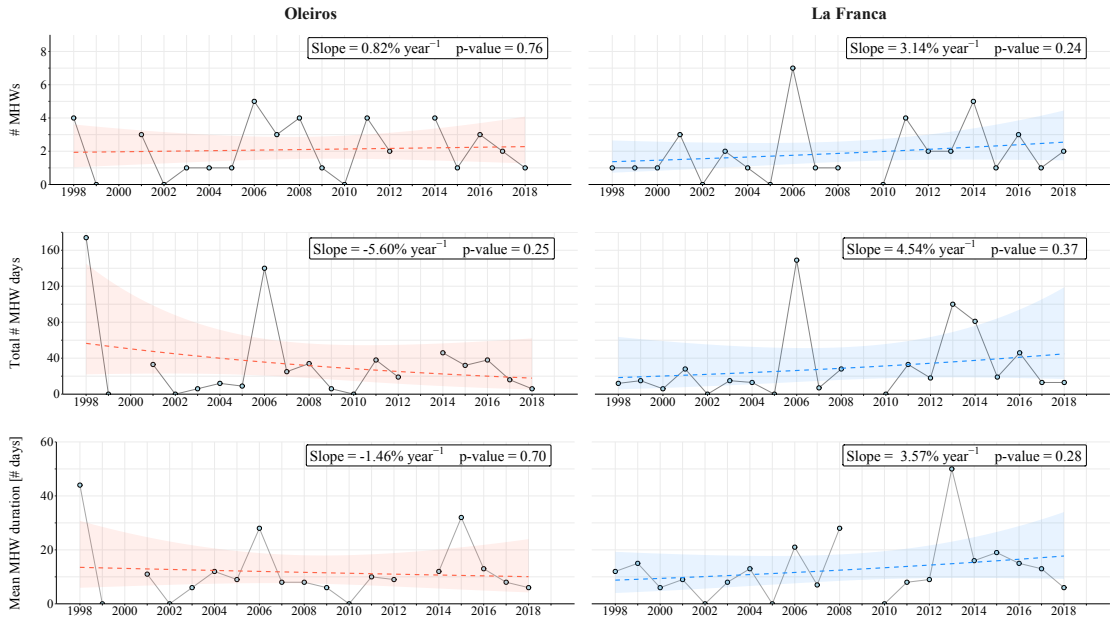

Figure 2.2. Time series of marine heatwave frequency (1st row), total number of marine heatwave days (2nd row) and yearly averaged duration (3rd row) of marine heatwaves detected between 1998 and 2019 in Oleiros and La Franca. The slope and p-value of each trend are shown. Dashed lines represent the linear regression trend in Oleiros (red) and La Franca (blue). Shaded areas represent 95% confidence intervals.

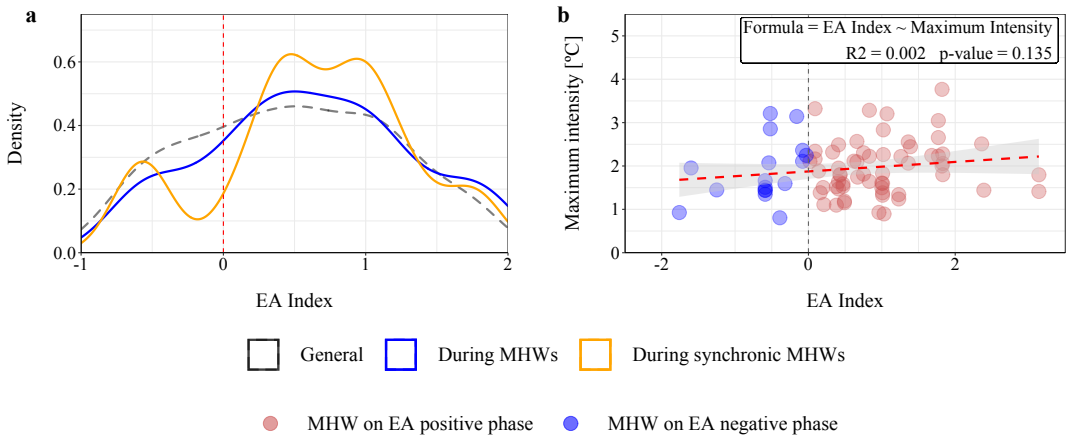

Figure 2.3. (a) Statistical distribution of marine heatwaves according to current East Atlantic Index at their occurrence; (b) relationship between marine heatwave maximum intensity [i_{max}] and the East Atlantic pattern index.

A total of 78 MHW events were detected between Jan. 1998 and Mar. 2019; 40 in Oleiros and 38 in La Franca, which comprised 557 and 498 MHW days respectively (~7% and ~6% of the total length of the series in days). Over half of the events registered were synchronous between study locations, with 22/40 MHWs for Oleiros and 21/38 MHWs for La Franca, which is ~55% for both cases (Table 2.A.1).

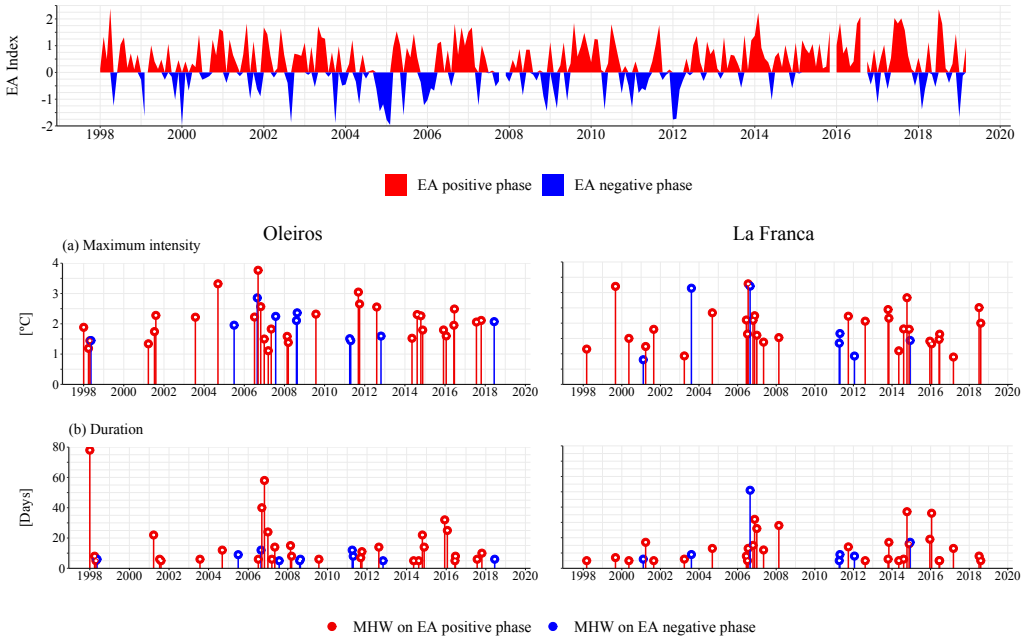

Figure 2.4. Concurrence between marine heatwave events and the phases of the East Atlantic pattern. First row: historical series of the East Atlantic pattern. Second row: (a) maximum intensity [i_{max}] and (b) duration [D] of the marine heatwaves detected in the time series from Oleiros and La Franca, classified according to their occurrence within the phases of the East Atlantic pattern. Results from marine heatwave mean [i_{mean}] and cumulative intensities [i_{cum}] are not shown here due to their big resemblance to marine heatwave maximum intensity and duration plots, respectively. Most of the detected marine heatwaves and, in general, the largest episodes of each metric took place within East Atlantic pattern positive phases at both locations.

Both annual and seasonal MHW trend analyses failed to reveal an increase in any of the MHW features examined at both study locations (Table 2.A.2; p-value > 0.05 in every computation). Trends in MHW frequency presented estimates of increase, whereas those for the number of MHW days and MHW duration were mostly negative. Individually, no significant trends were found either (Table 2.A.2; Fig. 2.2). Annual estimates were of increase for all variables at both study locations, except for the number of MHW days and MHW duration at Oleiros. The occurrence of MHWs of great duration in 1998, together with the short length of the temperature series, are probably the cause for the annual decreasing estimates for most variables at Oleiros (and for the number of MHW days for both sites combined). The year 2006 had the highest number of MHWs (5 at Oleiros, 7 at La Franca) and some of most severe, long-lasting episodes at both locations (*i.e.*, $i_{max} \geq 3$ºC; $i_{mean} \geq 2$ºC; $i_{cum} \geq 100$ºC days; $D = 50$ days; see Table 2.A.1). Importantly, 25% and ~30% of the MHW days in Oleiros (140/557) and La Franca (149/498), respectively, took place during within this year (Fig. 2.2).

The EA pattern was predominately positive during the study period. The Chi-squared test revealed that the EA pattern influences the incidence of MHW episodes at Oleiros (X-squared = 128.73; df = 1; p-value < 0.001) and La Franca (X-squared = 46.791; df = 1; p-value < 0.001). The

comparative analysis with the historical series of the EA revealed that ~88% and ~79% of the MHWs detected at Oleiros and La Franca respectively occurred during positive phases (95% confidence interval = [0.44, 0.80], Fig. 2.3). Furthermore, we found that >85% of the MHWs that were synchronous between Oleiros and La Franca took place during positive phases too (19/22 MHWs at Oleiros; 18/21 MHWs at La Franca; 95% confidence interval = [0.53, 0.97] (Fig. 2.3). Most importantly, the warm phase of the EA entailed the occurrence of some of the most severe MHWs from both study locations, with episodes that registered $i_{max} \geq 3$ºC and $D \geq 1$ month (Fig. 2.4).

2.4. Discussion

Our analyses failed to acknowledge any significant trends in the incidence and duration of MHWs in two coastal locations located in the central Cantabrian Sea, SW Bay of Biscay, from Jan. 1998 to Mar. 2019. The incidence of MHWs in the region, on the other hand, seems to be related to the positive phase of the EA pattern, which involves above-average SSTs.

Since the late 20th century, the global upper ocean (0-700 m) has dramatically increased its warming rate, a fact that is mainly attributed to anthropogenic influences (Gulev et al., 2021). The surface temperatures over the coastal zone of northern Spain have experienced a noticeable rise during the last four decades, especially during spring-summer (Gómez-Gesteira et al., 2008; Koutsikopoulos et al., 1998; Voerman et al., 2013). Despite the amount of missing data and/or the limited extent of our temperature series -which does not span the overall length of the warming period undergone in the region-, the steady temperature increase revealed in this research for the two study locations combined supports the general warming trend in northern Spain. The former drawbacks, nonetheless, likely contributed to the discrepancies found in the significance of the temperature trends of each study location individually and the inconclusive trends observed in MHW frequency and duration (*i.e.,* see MHW trends in Izquierdo et al., 2022). Global-scale shifts in mean SST drive changes in MHW occurrence (Frölicher et al., 2018), and the current human-induced global warming scenario increases the probability for large and severe MHWs to take place (Laufkötter et al., 2020). Above average SST anomalies had been previously registered in the region for the years 1999, 2003 and 2006 (Duarte et al., 2013; Voerman et al., 2013). In our investigation, MHWs with $i_{max} \geq 3$ºC were detected in all three years at La Franca, and only in 2006 for Oleiros (Table 2.A.1). Besides the occurrence of the European heatwave in July 2006 (Chiriaco et al., 2014), Le Cann & Serpette (2009) reported an unusually warm water inflow during autumn-winter in that year. Both events probably relate to the incidence of high-impact MHWs observed at both locations from summer through winter. This also contributes to explain the synchrony of the MHW episodes from both study locations in 2006 (5/5 [5/7] of the MHWs in Oleiros [La Franca] in that year were synchronous, Table 2.A.1).

The evidence provided in the present study shows that around three quarters-75% of the detected MHWs took place under the influence of the positive phase of the EA pattern. Climate variability modes such as the EA remotely modulate the inter-annual variation of a number of climate elements (*i.e.*, air temperatures, SSTs, precipitation, wind; Deser et al., 2010) and thus have a noticeable influence on important local atmospheric and/or oceanic processes. In general, these processes have a direct effect upon SST variations, which ultimately influences the likelihood of MHW occurrence. The EA pattern has been reported to be the most important variation explaining atmospheric temperature variability and around 25% of the SST variability in northern Spain (Sáenz et al., 2001; deCastro et al., 2011; Borja et al., 2019). Our observations reveal that most of the synchronous MHWs occurred during warm phases of the EA. Modes of climate variability act on a synoptic scale and its effect manifest after a few days on a large range of spatial and temporal scales (Holbrook et al., 2019) and are often responsible for abnormal weather patterns occurring simultaneously over seemingly vast distances (deCastro et al., 2008). This implies that, in essence, the observed synchrony in MHW incidence at Oleiros and La Franca is most likely due to the influence of the EA pattern acting over a range of ~100km at least. Most likely, the positive phase of the EA affects SST variations through air-sea heat fluxes, which have proven to be a physical driver responsible for setting MHW properties in regions susceptible to atmospheric forcing (Oliver et al., 2021). Nonetheless, it would be desirable to consider new physical parameters (*i.e.*, wind or atmospheric pressure) in future investigations to look further into the possible mechanisms by which the EA pattern might be prompting the occurrence of MHWs in the region.

It has been recently predicted that the incidence and intensity of MHW will increase in the coming years, regardless of the global warming scenario, which further threatens global marine ecosystems and biodiversity (Oliver et al., 2019). Biological and ecological impacts derived from MHW occurrence have been thoroughly reported worldwide, which range from population regime shifts and algal blooms to coral bleaching, mass mortality and re-structuring of entire ecosystems (Ummenhofer & Meehl, 2017). Specifically, MHW impacts upon macroalgae communities and their repercussions have been widely addressed in literature (Smale & Wernberg, 2013; Wernberg et al., 2016; Arafeh-Dalmau et al., 2019; Smale et al., 2019; Benthuysen et al., 2020). Although the distribution changes experienced by coastal seaweed populations off the coast of northern Spain in recent years have been widely addressed (Fernández & Anadón, 2008; Müller et al., 2009; Fernández, 2011; Viejo et al., 2011; Duarte et al., 2013; Voerman et al., 2013; Fernández, 2016; Piñeiro-Corbeira et al., 2016; Casado-Amezúa et al., 2019; Des et al., 2020), the influence of extreme temperature events upon them has not yet been assessed. Thus, abrupt changes in the abundance and distribution of habitat-forming seaweed communities

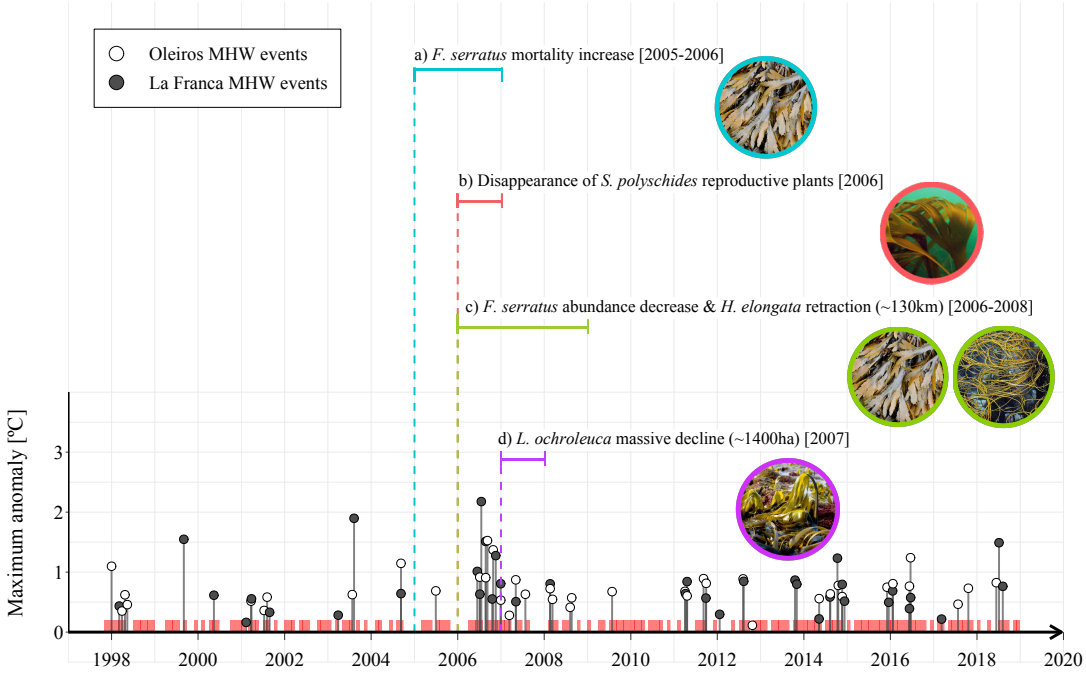

Figure 2.5. Maximum temperature anomaly -interpreted as the temperature exceeding the 90th percentile threshold, not the climatological baseline- of the marine heatwaves detected in the time series from Oleiros (open dots) and La Franca (solid dots) overlapped with periods of severe population shifts of local macroalgae communities documented in (a) Viejo et al. (2011), (b) Fernández (2011), (c) Duarte et al. (2013) and (d) Voerman et al. (2013). Red bars at the bottom represent the positive phases of the East Atlantic pattern.

recently documented in the literature provide good candidates to assess the impact of MHWs in the Cantabrian Sea.

Viejo et al. (2011) documented a general decrease in the reproductive capacity of *Fucus serratus* and a dramatic increase in their mortality from 2005 to 2006 towards the west of Cape Peñas. Fernández (2011) observed a progressive abundance decrease and growth issues in *Sacchoriza polyschides* populations in the central Cantabrian coast from the year 2000 on and reported the disappearance of reproductive plants by 2006. Duarte et al. (2013) observed a sharp decline in the abundance of *Fucus serratus* in the area west to Cape Peñas, as well as a 130 km westwards retreat of *Himanthalia elongata* between 2004-2006 and 2008-2009. Finally, Voerman et al. (2013) detected a massive decline of nearly ~1400 hectares of *Laminaria ochroleuca* west of Cape Peñas in 2007. All of the former population shifts were reported to occur between 2005-2009 and seem to coincide with MHW incidence periods (Fig. 2.5). Nearly 30% of the total MHWs detected in the present study took place within these years (23/78 MHWs; 14 at Oleiros and 9 at La Franca), half of them during 2006 (12/24 MHWs; 5 at Oleiros and 7 at La Franca). Straub et al. (2019) recently argued that the differential responses over time and space of macroalgae species to the effect of a MHW are likely subjected to a number of factors (*e.g.*, physiological versatility, ecological resilience and genetic diversity of macroalgae populations,

MHW extent and magnitude; see Wernberg et al., 2018). Thus, MHW impacts upon macroalgae communities may not be immediately evident and might even present long time-lags. This implies that the extreme temperatures derived from the occurrence of MHWs probably contributed to the range shifts and abundance decreases in the canopy-forming algae communities documented in the literature above.

SSTs in the Bay of Biscay have been warming at a considerable rate since the 1970s (deCastro et al., 2009). The disappearance of canopy-forming algae species in the Cantabrian Sea began to be described from that moment on (Fernández, 2016), although it has been especially noticeable since the turn of century (Casado-Amezúa et al., 2019; Fernández, 2011). Alongside with human-derived pressures, a number of environmental agents have been described in the Bay of Biscay that can influence the maintenance of canopy-forming macroalgae populations (*i.e.*, temperature, sunlight, wave exposure, storms, changes in biogeochemical cycles; see Borja et al., 2013; Borja et al., 2018), although temperature is usually the main factor used to assess distribution change scenarios (Franco et al., 2018). Temperature is known to strongly influence the spatial distribution of canopy-forming algae species, with extreme temperatures directly affecting their physiological and ecological performance (Straub et al., 2019). Species distributions might indeed be more sensitive to extreme conditions than to average longer-term trends (Sanz-Lázaro, 2016), considering the rapid shifts and long-term impacts that discrete events drive in ecosystems (O′Leary et al., 2017; Smale et al., 2019). Hence, the recently documented shifts in macroalgal communities in the central Cantabrian Sea may be related to the incidence of MHWs reported here, especially during 2005-2009. Extreme temperatures associated with MHWs erode the resilience of seaweeds adapted to cool conditions like *Fucus serratus* and may ultimately lead to their eventual loss as their biogeographical distribution range continues to shrink.

The results in this study are unavoidably conditioned by the short duration and narrow spatial extent of our analysis, which represent a major weakness of our approach. Though Oleiros and La Franca provide the longest and most complete *in situ* temperature record in an intertidal rocky shore in the central Cantabrian Sea, a spatiotemporally longer, more comprehensive record should provide a broader perspective and reveal different trends both in SST and MHW incidence in the region (see Izquierdo et al., 2022), considering the general warming trend that affects the Bay of Biscay and the world oceans (Fox-Kemper et al., 2021; Chust et al., 2022). Our findings suggest, nonetheless, a warming trend in central Cantabrian Sea manifested as a steady increase in water temperature and through prolonged MHWs with extreme temperatures. Moreover, the positive association between MHW incidence and the EA implies that large scale patterns of atmospheric forcing may act dominating variability in the incidence of MHWs. However, further research is needed on how the EA pattern may be operating on local-scale oceanic physical processes to prompt MHW conditions (*i.e.*, air-sea heat fluxes or ocean advection; Schlegel et al., 2017).

Future investigations might consider taking into account other European modes of climate variability to look into their influence on the occurrence of MHWs in the Bay of Biscay (Borja et al., 2019). Finally, the match between recently documented shifts in the abundance and distribution of canopy-forming macroalgae and severe MHW episodes suggests that MHWs might have played a part in the regression of macroalgae species in the coast of northern Spain in recent years. Under the escalating pressure of global warming, and in light of the ecological consequences reported in the scientific literature (Smale et al., 2019), our study stresses the need to reinforce coastal monitoring efforts to analyze the impact of extreme temperature events like MHWs.

Appendix

2.A. Supporting tables

Table 2.A.1. Marine heatwaves (MHWs) detected within the period Jan. 1998 - Mar. 2019. at Oleiros and La Franca, classified in chronological order. For each MHW episode, the following set of summary statistics are reported: start/peak/end dates, maximum intensity (highest temperature anomaly value during the MHW [i_{max}, ºC]), mean intensity (mean temperature anomaly during the MHW [i_{mean}, ºC]), cumulative intensity (sum of daily intensity anomalies [i_{cum}, ºC days]), and duration (consecutive period of time [D, days]). Pairs of episodes highlighted in grey represent synchronic MHWs (notice the similar start/peak/end dates among locations). We noticed that some MHWs were detected as a very long event in one location and as two separate events in the other. According to the definition of MHWs in Hobday et al. (2016), "gaps between events of two days or less with subsequent five days or more events will be considered as a continuous event". The local peculiarities of each study location might cause the MHWs to be detected differently, even for long-lasting episodes. Nonetheless, if the overall start/end dates of the two shorter MHWs from location 1 virtually comprise those of the complementary MHWs from location 2, it will be considered as a single synchronic event between study locations (MHW trios highlighted in light green). The East Atlantic patten Index (EA Index) for synchronic episodes is highlighted in red when positive (warm phase) and in blue when negative (cold phase).

Site	Year	Start date	Peak date	End date	D (days)	i_{max} (ºC)	i_{mean} (ºC)	i_{cum} (ºC days)	EA Index
Oleiros	1998	1998-01-01	1998-03-07	1998-03-19	78	1.8839	1.4012	109.2907	0.14
La Franca	1998	1998-03-07	1998-03-08	1998-03-11	5	1.1536	1.0534	5.2670	0.49
Oleiros	1998	1998-03-30	1998-04-02	1998-04-06	8	1.1954	1.0258	8.2061	0.49
Oleiros	1998	1998-04-24	1998-04-25	1998-04-28	5	1.4469	1.2307	6.1537	2.39
Oleiros	1998	1998-05-14	1998-05-17	1998-05-19	6	1.4525	1.2685	7.6112	-1.25
La Franca	1999	1999-09-03	1999-09-08	1999-09-09	7	3.2029	2.8268	19.7877	1.07
La Franca	2000	2000-05-14	2000-05-15	2000-05-18	5	1.5036	1.2503	6.2514	0.20
La Franca	2001	2001-02-10	2001-02-13	2001-02-15	6	0.8055	0.7347	4.4081	-0.39
Oleiros	2001	2001-03-23	2001-04-06	2001-04-13	22	1.3401	1.0535	23.1779	1.23
La Franca	2001	2001-03-27	2001-04-06	2001-04-12	17	1.2434	0.9155	15.5639	1.23
Oleiros	2001	2001-07-12	2001-07-17	2001-07-17	6	1.7479	1.5624	9.3741	0.67
Oleiros	2001	2001-08-06	2001-08-09	2001-08-10	5	2.2728	2.0784	10.3919	1.83
La Franca	2001	2001-08-27	2001-08-27	2001-08-31	5	1.7995	1.6970	8.4850	1.83
La Franca	2003	2003-03-29	2003-03-29	2003-04-03	6	0.9349	0.8092	4.8552	0.96
Oleiros	2003	2003-07-26	2003-07-28	2003-07-31	6	2.2179	1.9886	11.9317	1.26
La Franca	2003	2003-08-10	2003-08-16	2003-08-18	9	3.1476	2.5413	22.8719	-0.16
Oleiros	2004	2004-09-09	2004-09-11	2004-09-20	12	3.3210	2.9720	35.6646	0.09
La Franca	2004	2004-09-09	2004-09-10	2004-09-21	13	2.3402	1.9460	25.2975	0.09
Oleiros	2005	2005-06-30	2005-07-01	2005-07-08	9	1.9545	1.6331	14.6982	-1.60
La Franca	2006	2006-06-15	2006-06-18	2006-06-22	8	2.1037	1.5762	12.6095	0.02
Oleiros	2006	2006-07-06	2006-07-08	2006-07-11	6	2.2234	1.8013	10.8080	0.83
La Franca	2006	2006-07-07	2006-07-10	2006-07-11	5	1.6497	1.3609	6.8043	0.83
La Franca	2006	2006-07-19	2006-07-23	2006-07-31	13	3.2846	2.4764	32.1928	0.83
Oleiros	2006	2006-08-25	2006-08-30	2006-09-05	12	2.8612	2.5281	30.3367	-0.52
La Franca	2006	2006-08-26	2006-09-10	2006-10-14	50	3.2102	2.1514	107.5689	-0.52
Oleiros	2006	2006-09-09	2006-09-18	2006-10-18	40	3.7669	2.6301	105.2059	1.82
La Franca	2006	2006-10-19	2006-10-23	2006-11-02	15	2.1000	1.8317	27.4761	0.66
Oleiros	2006	2006-10-27	2006-12-04	2006-12-23	58	2.5663	1.8415	106.8086	0.66

Site	Year	Start date	Peak date	End date	*D* (days)	i_{max} (ºC)	i_{mean} (ºC)	i_{cum} (ºC days)	EA Index
La Franca	2006	2006-11-18	2006-12-05	2006-12-19	32	2.2426	1.5841	50.6927	1.68
Oleiros	2006	2006-12-30	2007-01-06	2007-01-22	24	1.4922	1.2505	30.0126	1.00
La Franca	2006	2006-12-30	2007-01-02	2007-01-24	26	1.6056	1.2625	32.8251	1.00
Oleiros	2007	2007-03-13	2007-03-16	2007-03-18	6	1.1111	0.9540	5.7242	0.21
Oleiros	2007	2007-05-06	2007-05-11	2007-05-19	14	1.8229	1.3864	19.4098	1.01
La Franca	2007	2007-05-12	2007-05-13	2007-05-18	7	1.3813	1.1317	7.9222	1.01
Oleiros	2007	2007-07-26	2007-07-29	2007-07-30	5	2.2408	1.9854	9.9272	-0.03
Oleiros	2008	2008-02-20	2008-03-01	2008-03-05	15	1.5809	1.1845	17.7679	0.47
La Franca	2008	2008-02-20	2008-03-03	2008-03-18	28	1.5291	1.0732	30.0505	0.47
Oleiros	2008	2008-03-11	2008-03-14	2008-03-18	8	1.3844	1.1390	9.1117	0.16
Oleiros	2008	2008-08-07	2008-08-09	2008-08-11	5	2.1078	1.9444	9.7221	-0.08
Oleiros	2008	2008-08-20	2008-08-22	2008-08-25	6	2.3570	2.0886	12.5315	-0.08
Oleiros	2009	2009-07-27	2009-07-31	2009-08-01	6	2.3215	1.8356	11.0138	0.33
Oleiros	2011	2011-04-03	2011-04-11	2011-04-14	12	1.5130	1.1805	14.1665	-0.59
La Franca	2011	2011-04-08	2011-04-10	2011-04-12	5	1.3506	1.1168	5.5838	-0.59
Oleiros	2011	2011-04-21	2011-04-28	2011-04-28	8	1.4395	1.1433	9.1467	-0.59
La Franca	2011	2011-04-21	2011-04-28	2011-04-29	9	1.6649	1.3653	12.2873	-0.59
La Franca	2011	2011-05-05	2011-05-06	2011-05-09	5	1.5551	1.1802	5.9008	-0.67
Oleiros	2011	2011-09-07	2011-09-10	2011-09-13	7	3.0475	2.6631	18.6417	1.77
La Franca	2011	2011-09-27	2011-10-01	2011-10-10	14	2.2255	1.8606	26.0481	1.77
Oleiros	2011	2011-09-29	2011-10-07	2011-10-09	11	2.6603	2.2515	24.7664	1.77
La Franca	2012	2012-01-21	2012-01-26	2012-01-28	8	0.9217	0.7501	6.0008	-1.76
Oleiros	2012	2012-08-06	2012-08-13	2012-08-19	14	2.5603	2.1908	30.6714	1.36
La Franca	2012	2012-08-11	2012-08-12	2012-08-15	5	2.0627	1.7903	8.9517	1.36
Oleiros	2012	2012-10-23	2012-10-23	2012-10-27	5	1.5940	1.5161	7.5807	-0.32
La Franca	2013	2013-10-18	2013-10-21	2013-10-23	6	2.4397	2.0028	12.0167	1.39
La Franca	2013	2013-11-02	2013-11-07	2013-11-18	17	2.1647	1.6501	28.0512	0.09
La Franca	2014	2014-05-09	2014-05-11	2014-05-13	5	1.0995	0.9860	4.9301	0.38
Oleiros	2014	2014-05-10	2014-05-13	2014-05-14	5	1.5238	1.3378	6.6888	0.38
La Franca	2014	2014-08-09	2014-08-10	2014-08-14	6	1.8097	1.5540	9.3240	0.75
Oleiros	2014	2014-08-12	2014-08-13	2014-08-16	5	2.3098	2.1077	10.5384	0.75
La Franca	2014	2014-10-11	2014-10-19	2014-11-16	37	2.8289	1.9640	72.6679	1.02
Oleiros	2014	2014-10-18	2014-10-22	2014-11-08	22	2.2678	1.7718	38.9788	1.02
Oleiros	2014	2014-11-20	2014-11-30	2014-12-03	14	1.7903	1.5707	21.9899	0.43
La Franca	2014	2014-11-20	2014-11-29	2014-12-05	16	1.7974	1.4757	23.6116	0.43
La Franca	2014	2014-12-10	2014-12-22	2014-12-26	17	1.4315	1.0876	18.4890	-0.59
Oleiros	2015	2015-12-04	2015-12-24	2016-01-04	32	1.7912	1.4625	46.8008	3.14
La Franca	2015	2015-12-18	2015-12-23	2016-01-05	19	1.4088	1.2040	22.8755	3.14
La Franca	2016	2016-01-20	2016-02-13	2016-02-24	36	1.3275	1.0009	36.0324	1.01
Oleiros	2016	2016-01-22	2016-01-27	2016-02-15	25	1.5947	1.2937	32.3420	1.01
Oleiros	2016	2016-06-10	2016-06-12	2016-06-14	5	1.9518	1.5751	7.8755	0.41
La Franca	2016	2016-06-10	2016-06-11	2016-06-14	5	1.4730	1.2326	6.1630	0.41
Oleiros	2016	2016-06-19	2016-06-21	2016-06-26	8	2.4848	1.8298	14.6382	0.41
La Franca	2016	2016-06-20	2016-06-21	2016-06-24	5	1.6389	1.4120	7.0600	0.41
La Franca	2017	2017-03-08	2017-03-16	2017-03-20	13	0.8951	0.7722	10.0387	1.03
Oleiros	2017	2017-07-25	2017-07-28	2017-07-30	6	2.0564	1.8293	10.9756	1.83
Oleiros	2017	2017-10-20	2017-10-28	2017-10-29	10	2.1124	1.8590	18.5902	0.62
Oleiros	2018	2018-06-13	2018-06-18	2018-06-18	6	2.0719	1.5688	9.4131	-0.54
La Franca	2018	2018-07-06	2018-07-11	2018-07-13	8	2.5056	1.7851	14.2808	2.36
La Franca	2018	2018-08-07	2018-08-08	2018-08-11	5	2.0031	1.6429	8.2143	1.82

Table 2.A.2. Annual and seasonal trends in marine heatwave (MHW) features for the study locations of Oleiros and La Franca together (first row group) and individually (second and third row group).

	MHW frequency [% year^{-1}]		Total MHW days [% year^{-1}]		MHW mean duration [% year^{-1}]	
	Slope	p-value	Slope	p-value	Slope	p-value
Both locations together						
Annual	1.99	0.29	-0.58	0.87	1.26	0.61
Spring-summer (Mar-Aug)	0.48	0.84	-2.41	0.47	-0.25	0.92
Autumn-winter (Sep-Feb)	4.50	0.15	0.41	0.92	-1.33	0.77
Oleiros						
Annual	0.82	0.76	-5.60	0.25	-1.46	0.70
Spring-summer (Mar-Aug)	-1.29	0.69	-4.09	0.24	0.10	0.97
Autumn-winter (Sep-Feb)	4.92	0.30	-6.40	0.33	-8.34	0.20
La Franca						
Annual	3.14	0.24	4.54	0.37	3.57	0.28
Spring-summer (Mar-Aug)	2.41	0.50	-0.83	0.89	-0.63	0.87
Autumn-winter (Sep-Feb)	4.16	0.32	7.82	0.18	7.36	0.11

Chapter 3

Towards an improved detection of marine heatwaves: a coast-level assessment

Abstract

Analyses of long-term temperature records based on satellite data have revealed an increase in the frequency and intensity of marine heatwaves (MHWs) in the world oceans, a trend directly associated with global change according to climate model simulations. However, these analyses often target open ocean pelagic systems and rarely include local scale, field temperature records that are more adequate to assess the impact of MHWs close to the land-sea interface. Here, we compared the incidence and characteristics of open ocean MHWs detected by satellites with those observed in the field over two decades (1998-2019) at two temperate intertidal locations in the central Cantabrian Sea, southern Bay of Biscay. Satellite retrievals tended to smooth out cooling events associated with intermittent, alongshore upwelling, especially during summer. These biases propagated to the characterization of MHWs and resulted in an overestimation of their incidence and duration close to the coast. To reconcile satellite and field records, we developed a downscaling approach based on regression modelling that enabled the reconstruction of past temperatures and analyze MHW trends. Despite the cooling effect due to upwelling, the temperature reconstructions revealed a six-fold increase in the incidence of MHWs in the Cantabrian Sea over the last four decades. A comparison between static (no trend) vs. dynamic (featuring a linear warming trend) MHW detection thresholds allowed us to attribute over half of the increase in MHW incidence to the ocean warming trend. Our results highlight the importance of local processes to fully characterize the complexity and impacts of MHWs on marine coastal ecosystems and call for the conservation of climate refugia associated with coastal upwelling to counter the impacts of climate warming.

Keywords: Sea surface temperature, global warming, ocean remote sensing, climate refugia, shelf seas, Bay of Biscay.

3.1. Introduction

Marine heatwaves (MHWs) are transient episodes of extreme water temperatures that leave a detrimental and long-lasting impact on the structure and functioning of marine ecosystems (Hobday et al., 2016; Oliver et al., 2021). Analyses of long-term satellite temperature records have revealed an increase in the frequency, intensity and duration of MHWs during the last century (Oliver et al., 2018). Such trends parallel the gradual increase in ocean temperature due to anthropogenic greenhouse gas emissions (Gulev et al., 2021), which lies behind the dramatic increase in the occurrence and intensity of MHWs in recent decades (Laufkötter et al., 2020). In fact, projections under different socioeconomic development scenarios foresee a sustained increase in the likelihood and severity of MHWs around the world in coming years (Fox-Kemper et al., 2021; Frölicher et al., 2018).

Discrete events like MHWs often pose a more serious threat to marine life than changes in mean state due to the sudden and long-lasting consequences triggered by extreme perturbations (O'Leary et al., 2017). Fluctuations and extremes in water temperature are an intrinsic component of environmental variability that shapes the structure and functioning of marine ecosystems (Denny et al., 2009; Clarke, 2017). In practice, despite growing concerns, analyzing the impact of MHWs becomes a complex task. Temperature extremes leading to MHWs are by definition rare, short-lived warming episodes above normal conditions that often last for a few days. As a consequence, the detection and characterization of MHWs remains challenging and demands sustained records of high-frequency observations.

Long-term temperature records are necessary to define a meaningful baseline and characterize extremes, while high-quality, frequent observations are important to avoid biases and ensure the proper detectability of MHW events (Hobday et al., 2016; World Meteorological Organization, 2018). Such constraints become more acute when attempting to characterize changes in the incidence and intensity of MHWs. High data demands make that most MHW studies tend to rely on satellite or model-based datasets, and to focus on open ocean pelagic environments away from the coastline, where the presence of land and local processes like river runoff and coastal upwelling limit indirect approaches (Smit et al., 2013; Stobart et al., 2015; Schlegel, 2017). These biases may extend to the detection of small-scale variability and temperature extremes (Smale & Wernberg, 2009; Smit et al., 2013). In fact, it has been recently shown that remotely-sensed products may overestimate coastal SSTs in upwelling prone locations (Meneghesso et al., 2020) as a result of the differences between the warming rates in offshore *vs.* nearshore waters (Varela et al., 2018), which may ultimately lead to the overestimation of MHW trends (Varela et al., 2021). This raises concerns about the actual impact of MHWs in coastal areas.

Intertidal and shallow coastal areas disproportionately contribute valuable ecosystem services to humankind (Costanza et al., 2014). These highly diverse and productive habitats control land erosion and buffer coastal pollution through carbon sequestration and nutrient cycling (Barbier, 2017). They also provide commodities ranging from fertilizers and foods to compounds of industrial use, which are harvested from algae and fisheries or collected from aquaculture. MHWs compromise the sustained provision of these services and the restoration of currently degraded ecosystems (Duarte et al., 2020) and represent a threat to blue carbon nature-based solutions that may contribute to mitigate climate change (Macreadie et al., 2021). Together, these issues call for an improved monitoring and assessment of the impact of MHWs in coastal areas as a way to guide the sustainable use and conservation of living marine resources.

Here, we analyze the incidence of MHWs along the coasts of the central Cantabrian Sea, in the Northeast Atlantic. This stretch covers a sharp biogeographical transition from cool to warm conditions where temperature extremes have prompted abrupt changes in the structure of coastal marine communities in recent years (Fernández, 2011; Viejo et al., 2011; Voerman et al., 2013; Fernández, 2016). Taking advantage of high-frequency, two-decade long temperature field records, we assessed the reliability of coarse scale satellite data to monitor MHWs in coastal areas. The analyses revealed important biases that resulted in the overestimation of the incidence of MHWs by satellites during periods of intense upwelling. To reconcile satellite and field measurements we developed a statistical downscaling approach, a technique often used to obtain finer-scale climate information from coarse resolution products (see Wilby & Wigley, 1997). Such approach enabled us to account for the impact of upwelling on nearshore temperatures, exploit the prolonged coverage of the satellite record and hindcast the incidence of MHWs during the last four decades. We characterized MHWs using two different baseline periods: static (based on the climatological seasonal cycle) *vs.* dynamic (featuring a linear warming trend). The comparison of both approaches provides useful insight on the potential contribution of climate warming to the increased incidence of MHW. Our results highlight the contribution of upwelling to buffer the impact of open ocean MHWs in coastal areas, but in parallel reveal a concerning increase in the incidence and intensity of MHWs due to climate warming.

3.2. Materials and methods

3.2.1. Study area

We analyzed the occurrence and intensity of MHWs in the central Cantabrian Sea (Fig. 3.1), a narrow (30-40 km) temperate coastal shelf sea located in the southern Bay of Biscay (NE Atlantic, Gil et al., 2002). To this end, we combined data from large scale ocean reanalysis and satellite monitoring of the temperature of the ocean surface with field measurements at two

selected coastal locations —Oleiros (6.200W 43.575N) and La Franca (4.575W 43.395N)— which enabled us to assess and calibrate satellite data (Fig. 3.1).

Large scale gradients in ocean conditions anticipate spatial variability in the incidence and characteristics of MHWs along the entire Cantabrian Sea. Water temperatures increase eastwards as climatic conditions become less oceanic and more continental due to the proximity of the Eurasian landmass (Koutsikopoulos et al., 1998). Atmospheric circulation further presents a marked seasonality, with prevailing southwesterly winds during autumn and winter, and northeasterly winds during spring and summer that are more intense towards the west. The easterly component flows parallel to the coast and causes intermittent upwelling events that, especially during summer, bring cool waters to the surface and erode the seasonal thermal stratification of the upper layer (Gil et al., 2002), further contributing to accentuate the eastward gradient in temperature (Botas et al., 1990).

Oleiros and La Franca are representative of large-scale gradients in environmental conditions in the Cantabrian Sea and their effect on marine life. The two locations are separated by just ~100 km of coast but, halfway amid them, the presence of Cape Peñas alters the predominant east-west orientation of the coastline (Fig. 3.1). This headland juts 10 km into the sea, affecting coastal circulation by deflecting internal waves and enhancing the gradient towards more intense seasonal alongshore upwelling in the west (Lavín et al., 2006; Llope et al., 2006). As a consequence, the cape marks the approximate location of a sharp biogeographical transition from cool to warm adapted intertidal communities towards the interior of the Bay of Biscay (Anadón & Niell, 1981). Both locations are otherwise similar; they are rocky shores exposed to the open ocean, located away of any known anthropogenic heat source, and experiencing moderate semidiurnal tides with a range of up to 4.5 m during the spring tides.

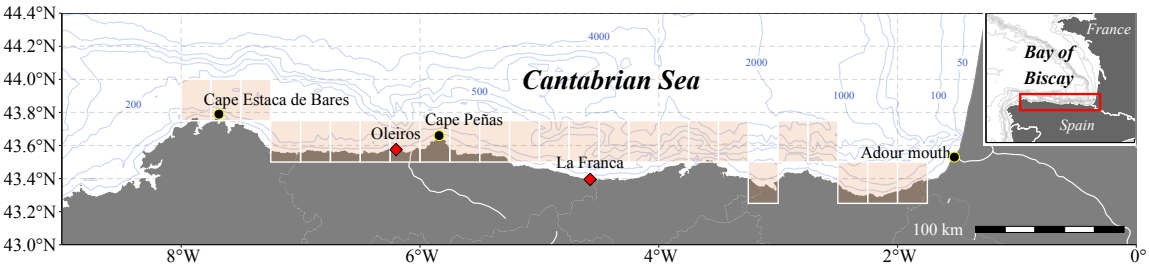

Figure 3.1. Map of the Cantabrian Sea showing the study areas of Oleiros and La Franca, where the field observations were collected. Salmon-coloured rectangles represent the 0.25º localities covering the spatial extent of the extended modelled temperature series (n=25). The locations of Cape Estaca de Bares and the mouth of the Adour River serve as reference to indicate the edges of the extended series. Bathymetry data were extracted from the GEBCO 2021 Grid (GEBCO Compilation Group, 2021).

3.2.2. Temperature time series and ancillary datasets

The incidence of MHWs was analyzed based both on field and remote sensing temperature time series data. To examine potential biases among the two data sources, we further retrieved time series of alongshore upwelling and of heat fluxes across the air-sea interface, which provided a proxy of water column stratification.

Field temperature data

Daily field temperature measurements were collected at Oleiros and La Franca from Jan. 1998 to Mar. 2019 (~21 years) using TidbiT V2 water temperature dataloggers (Onset Computer Corp). The loggers were attached to the rock and protected from wave action by a steel mesh. Temperature data were retrieved with a HOBO Optic USB Base Station reader and converted to text files using HOBOWare Pro v.3.7.10 (Onset Computer Corp). These devices have a maximum sustained temperature range of 0-30°C in water and an accuracy of ± 0.21°C over 0-50°C. The dataloggers were programmed to retrieve a single datum per hour before attaching them at depths 0.3-0.6 m above the lowest astronomical tide to ensure they were always submerged at high tide. The time series was filtered to retain the two records per day that correspond to water temperature at semidiurnal high tides. Then the average of high tide values was calculated to estimate daily mean sea temperature and applied a backward 5-day moving average to smooth out high frequency noise. The resulting daily series was 21 years long but presented ~6% and ~18% missing data at Oleiros and La Franca, respectively. Though time series with these features would be considered sub-optimal according to Hobday et al.'s (2016) recommendations, they remain suitable for MHW research (Schlegel et al., 2019).

Satellite temperature data

Sea surface temperature (SST) data were retrieved for the entire coast of the Cantabrian Sea from the NOAA Optimum interpolation 0.25° daily sea surface temperature analysis (oiSST version 2, Sep. 1981-2019, see Banzon et al. (2016), Reynolds et al. (2007) and www.ncdc.noaa.gov/oisst for further details). The assessment with field observations used data for the nearest pixel locations to the study sites (6.125ºW 43.625ºN for Oleiros; 4.625ºW 43.625ºN for La Franca). To ensure temporal homogeneity (Reynolds & Chelton, 2010), we used the Advanced Very High-Resolution Radiometer (AVHRR-only) product from the Pathfinder Version 5 dataset (Casey et al., 2010). This dataset includes an optimal interpolation step to fill gaps and aggregate fine scale high resolution retrievals (~1 km) that effectively smooths original observations and avoids biases in measurements close to the land-sea interface. Therefore, satellite-based SSTs provide a reliable temperature record for monitoring MHW incidence in open ocean waters (Hobday et al., 2016).

Coastal winds and upwelling

Hourly wind speed vectors over the ocean surface were extracted from ERA5 0.25º reanalysis data from the nearest pixel locations to the study sites (6.25ºW 43.75ºN for Oleiros; 4.5ºW 43.5ºN for La Franca), for the period Jan. 1981 - Dec. 2019. Data were retrieved from the Copernicus Climate Change Service (C3S) of the Climate Data Store (CDS) (Hersbach et al., 2020). Wind stress, τ [N m^{-2}], was calculated from neutral wind speed vectors at 10 m (U_{10} [m s^{-1}]) using the bulk formula; $\tau = \rho_{air} \cdot C_D \cdot U_{10} \cdot |U_{10}|$, where ρ_{air} is air density (taken as 1.223 kg m^{-3}) and C_D is a non-dimensional drag coefficient. C_D was estimated as a function of U_{10} based on Large et al. (1994):

$$10^3 C_D = \frac{2.70}{U_{10}} + 0.142 + 0.0764 U_{10}$$

Alongshore coastal upwelling was then calculated based on estimates of the seaward Ekman transport (T [m^2 s^{-1}]) along a segment of coast of a given length (L = 1 m), which gives Bakun's (1973) upwelling index, $bui = TL = \frac{\tau_a L}{\rho_{sw} f}$ [m^3 s^{-1}]. Transport depends on the alongshore component of wind stress, τ_a, which was estimated assuming a prevailing east-west orientation of the coastline; seawater density, ρ_{sw}, set to 1025 kg m^{-3}, and the Coriolis parameter f = 9.96 10^{-5} s^{-1}, corresponding to 43°N. An 11-day simple moving average was applied on the resulting *bui* estimates to integrate the cumulated impact of high frequency wind variability on cross-shore transport (García-Reyes & Largier, 2010; Otero & Ruiz-Villarreal, 2008). Positive *bui* values correspond to the upwelling of deep waters and leads to surface cooling, whereas negative values correspond to downwelling, sinking and warming.

Air-sea heat fluxes and stratification

Time series of ocean surface net heat flux, Q_i [W m^{-2}], were calculated based on data from the Modern-Era Retrospective analysis for Research and Applications version 2 (MERRA-2) V5.12.4 ocean surface diagnostics product (M2T1NXOCN, Global Modeling & Assimilation Office [GMAO], 2015). Hourly estimates were retrieved for each 0.5° × 0.625º grid cell corresponding to the nearest pixel locations to the study sites (6.2500ºW 43.75ºN for Oleiros; 4.6875ºW 43.5ºN for La Franca), for the period Jan. 1980 - Oct. 2020.

Surface waters in the Cantabrian Sea follow the characteristic seasonal cycle of temperate shelf seas (*e.g.*, Simpson & Sharples, 2012). During winter (Dec-Feb), convective mixing leads to the formation of a deep homogeneous layer that lasts until spring (Mar-May), when favorable weather conditions eventually generate a shallow, mixed layer that persists throughout summer (Jun-Aug) until autumn (Sep-Nov) storms break stratification (Lavín et al., 2006). Surface heat exchange is the dominant buoyancy source for seasonal mixing in most shelf seas, so the net heat flux (Q_i)

was used as a proxy for thermally driven seasonal stratification (with positive [negative] Q_i matching seasonal stratification [mixing]). Net heat flux was calculated as $Q_i = Q_s(1\text{-}A) - Q_b - Q_e - Q_c$, where Q_s represents solar inputs to the ocean surface, A is albedo, Q_b is back radiation, Q_e and Q_c are sensible and latent heat fluxes respectively. An 81-day simple moving average was applied to smooth out a signal to distinguish seasonal stratification *vs.* mixing periods.

3.2.3. Detectability and trends in coastal marine heatwaves (MHWs)

The analysis was structured in three steps. First, a set of regression models was developed to downscale and calibrate the satellite time series against field observations, which allowed us to explore potential biases among the two series due to the proximity to land. Then, the impact of deviations among satellite and local field measurements on the detection and characterization of MHWs was examined. In a third set of analyses, the models were used to reconstruct past temperatures and assess the contribution of the underlying warming trend on the incidence of MHWs in the Cantabrian Sea.

Assessment and downscaling of satellite temperatures

In the first analysis, we tested a set of nested statistical downscaling models to assess and reconcile potential deviations between satellite temperatures and those recorded in the field (Table 3.1). Downscaling is a technique that allows to derive finer-scale projections of climate variables affected by local processes not captured by coarse resolution products (see Wilby & Wigley, 1997). All models initially assumed that field temperatures are linearly related to satellite retrievals. Such relationship accounts for the expected offset between field point measurements and the large areas averaged by the satellite. Local site effects account for extra deviations due to the unique characteristics of each location, from local bathymetry and circulation to the degree of land contamination in satellite retrievals.

The baseline model featured the above defined assumption of a simple linear relationship between field and satellite temperature measurements with a different intercept on each site ($T_f = \beta_0 + \beta_1 site + \beta_2 T_s$, Mod_1 in Table 3.1). Deviations between both series may grow during coastal upwelling and downwelling depending on water column stratification, so we tested two extra models, Mod_2 and Mod_3, which feature an interaction between *bui* as a proxy of cross-shore transport and net heat flux (Q_i) as a proxy of stratification. The interaction term accounts for the varying impact of upwelling on surface temperature; coastal upwelling (downwelling) may cool (further warm) surface waters when the column is stratified. However, upwelling may not alter surface temperatures when the column is fully mixed in winter, though downwelling may still transport slightly warmer waters from deeper areas offshore.

Table 3.1. Model selection table summarizing the assessment of alternative hypotheses about the best strategy to reconcile satellite and field temperature measurements. Models with a lower AIC score were favored. T_f stands for field measurements [ºC]. Predictor variables are *site* (study area), T_s (satellite measurements [ºC]), *bui* (Bakun Upwelling Index [10^3 m^3 s^{-1} km^{-1}]) and *Qi* (net heat flux [W m^{-2}]). The coefficient β_0 denotes the intercept, whereas the other β measure the effect of each predictor separately. Mod_1 and Mod_2 are linear models, Mod_3 is a Generalized Additive Model (GAM). In Mod_3, *s(x)* stands for a regular smooth term (specifically a thin-plate regression spline) featuring a flexible relationship between T_f and the covariate *x*, while *ti*(*x*,*y*) represents a tensor smooth allowing a nonlinear interaction between covariates *x and y,* which may have different measurement units (Wood, 2017).

Name	Description	Equation	logLik	dLogLik	df	AIC	dAIC	AIC weights
Mod_1	Linear effect of satellite temperature series (T_s) and different intercept depending on *site*.	$T_f = \beta_0 + \beta_1 site + \beta_2 T_s$	-18030	0	4	36067	7304	0
Mod_2	T_s linear effect and linear interactive effect between coastal up/downwelling (*bui*) and net heat flux at the sea surface (Q_i).	$T_f = \beta_0 + \beta_1 site + \beta_2 T_s + \beta_3 bui + \beta_4 Q_i + \beta_5 bui * Q_i$	-15564	2465	7	31143	2380	0
Mod_3	T_s linear effect and non-linear interactive effect between *bui* and Q_i at the sea surface.	$T_f = \beta_0 + \beta_1 site + \beta_2 T_s + s_1(bui) + s_2(Q_i) + ti(bui, Q_i)$	-14354	3676	27	28763	0	1

Mod_2 and Mod_3 attempt to capture potential differences in surface water temperatures near the shore *vs.* more oceanic conditions. Mod_2 is a linear regression model where the interaction between cross-shore transport and net heat flux is assumed to be linear (*i.e.*, a multiplicative, symmetric effect see Mod_2 in Table 3.1). On the other hand, Mod_3 is a generalized additive model (GAMs; Hastie & Tibshirani, 1986; Wood, 2017), a type of model especially useful to describe non-linear effects of independent variables without an a priori specification of the functional relationships (see Mod_3 in Table 3.1). In particular, Mod_3 includes regular smooth terms (*s*, specifically a thin-plate regression spline) to describe individual non-linear effects of *bui* and Q_i, and a tensor product smooth (*ti*) to incorporate their interactive non-linear effect and account for their different units (Wood, 2017). Such interaction enables a varying effect of cross-shore transport on deviations between satellite and field temperatures across net heat flux levels. The complexity of smooth terms in GAMs is determined through cross-validation to avoid overfitting (Wood, 2017).

Mod_3 assumes that the effect of upwelling on satellite deviations is homogeneous along the coast. To assess the reliability of this assumption, we reconstructed the field signal at La Franca using satellite, *bui* and *Qi* data from the closest pixel and the parameters derived from fitting of Mod_3 only using data from Oleiros, and viceversa. As shown in Figs. 3.A.1 and 3.A.2 in the Appendix, these analyses result in predictions i) that reproduce near-shore SSTs more reliably than the satellite (Fig. 3.A.1) and ii) comparable to those based on a model trained using all data and featuring a local upwelling effect (Fig. 3.A.2), suggesting that Mod_3 may provide a reasonable description of the effect of upwelling along the coast.

Model fits were checked for Mod_1, Mod_2 and Mod_3 for the presence of any non-random pattern in the residuals, and then ranked them using the Akaike's Information Criterion (AIC, Burnham & Anderson, 2002).

Detection and characterization of marine heatwaves (MHWs)

We analyzed the incidence and magnitude of MHWs following Hobday et al.'s (2016) criteria, who defined MHWs as warm periods that last for five or more consecutive days during which temperature rises above a seasonal climatology of the 90th percentile (P_{90}) of the temperature at a given location. Previous studies estimated P_{90} threshold climatologies using a centered 30-day moving window. Such an approach introduces a directional lag by pooling temperatures consistently increasing or decreasing along the seasonal cycle. For instance, P_{90} estimates for late July are partially based on warmer temperatures from early August, making it more difficult to detect actual MHWs. To avoid potential biases, we implemented a parametric Monte Carlo approach to estimate P_{90}. For each SST time series, we fitted a GAM featuring a constant seasonal cycle and a linear trend. Then, we randomly sampled 10000 model parameter vectors from their fitted mean and covariance using a multivariate normal random number generator. Sample parameters were used to simulate daily surrogate time series, providing a large sample to retrieve unbiased estimates of P_{90} for each simulated date. Surrogates incorporating only the constant seasonal cycle term result in a static threshold that does not vary between years, but adding simulated trends result in a time-moving P_{90} threshold. This dynamic threshold is useful to assess the impact of long-term trends in MHWs (see section '*Temperature reconstruction and association of MHWs to climate warming*' below). Resulting thresholds were further smoothed using a 15-day central moving average to avoid wiggles.

Assessment of MHWs based on field observations

The second analysis focused on the incidence of MHWs at the two study locations of Oleiros and La Franca. The incidence and characteristics of MHWs were compared based on field, satellite and model-based reconstructions of coastal sea surface temperature during the period Jan. 1998 - Mar. 2019. MHW detection thresholds were calculated using all available data to characterize overall changes in the incidence of MHWs. We constructed presence-absence confusion matrices to assess the ability of each temperature series to detect MHWs, setting field observations as reference (Allouche et al., 2006). Additionally, we analyzed other MHW features such as duration (*dur*) and maximum, mean and accumulated intensity of detected events (i_{max}, i_{mean}, i_{cum}, respectively; Hobday et al., 2016). To ensure a fair comparison, missing dates in temperature field records were masked on both satellite and model-based temperature reconstructions before the analysis and separately at each station.

Temperature reconstruction and association of MHWs to climate warming

In the third analysis we used the best fitting model (Mod_3 in Table 3.1, based on AIC scores) to hindcast coastal temperature variability based on satellite and ocean reanalysis data. This approach enabled us to extend the analysis back in time and to examine trends in the incidence of MHWs during the last four decades (Sep. 1981 - Dec. 2019). Also, the spatial extent was broadened to cover the entire Cantabrian Sea from Cape Estaca de Bares in the west to the mouth of the Adour River in the east (n = 25, Fig. 3.1). Upwelling index (*bui*) and heat flux (Q_i) reanalysis fields were aligned with SST data using first-order, conservative interpolation.

Finally, we assessed changes in trend estimates for the incidence and features of MHWs resulting when using a static detection threshold based on the climatological seasonal cycle *vs.* a dynamic baseline incorporating a linear warming trend (Oliver et al., 2021). For i_{max}, i_{mean}, i_{cum} and *dur* of detected MHWs, these trends were estimated using simple linear regression. MHW frequency and the number of MHW days per year are discrete variables (*i.e.*, counts of events during some period of time) whose residuals are usually skewed following a Poisson distribution, so these trends were estimated using Poisson generalized linear models (*e.g.*, Gelman & Hill, 2006). We performed standard residual checks and tests to assess model adequacy and accounted for overdispersion of MHW counts when necessary (Gelman & Hill, 2006).

Technical implementation details

Statistical model fitting was implemented in *R* version 4.1.2 (R Core Team, 2021) making extensive use of libraries *mgcv* (Wood, 2017) for GAMs, *caret* (Kuhn, 2008) and *bbmle* (Bolker et al., 2020) for confusion matrices and model predictions. MHW events were detected and characterized using the library *heatwaveR* (Schlegel & Smit, 2018), which implements the definition of MHW proposed by Hobday et al. (2016). Libraries *tidyverse* (Wickham et al., 2019), *ncdf4* (Pierce, 2019), *lubridate* (Grolemund & Wickham, 2011), *plyr* (Wickham, 2011), *zoo* (Zeileis & Grothendieck, 2005), *gratia* (Simpson & Singmann, 2021), *reshape2* (Wickham, 2007), *fields* (Nychka et al., 2017), *data.table* (Barrett et al., 2021), *sf* (Pebesma, 2018), *RColorBrewer* (Neuwirth, 2014), *cowplot* (Wilke, 2020), *rnaturalearth* (Massicotte et al., 2017) and *extrafont* (Chang, 2014) were also used in the analyses and to prepare graphs and other summaries.

3.3. Results

Satellite and field records of the ocean surface confirmed the predominance of cooler conditions in the westernmost station of Oleiros than in La Franca (Table 3.2). Differences in surface water temperatures between the two stations further increased during spring and summer coinciding with the upwelling season (Apr-Sep; Lavín et al., 2006), which is also stronger at Oleiros. The analysis also revealed large deviations between field and satellite temperature

records (root mean square error, *i.e.* RMSE > 1.22ºC at both Oleiros and La Franca), which increased again during the upwelling season, when satellite temperatures tended to overestimate field temperatures by up to 5ºC (Table 3.2, Fig. 3.2, Fig. 3.A.3 & Fig. 3.A.4 in the Appendix). Satellite retrievals also resulted in smoother time series that lacked sudden temperature fluctuations associated with upwelling and downwelling events in field series.

3.3.1. Assessment and downscaling of satellite temperatures

Table 3.1 summarizes the assessment of models reconciling field and satellite temperature time series. Model selection based on AIC scores favored model Mod_3, which features a nonlinear interaction between upwelling and time-integrated heat. In essence, Mod_3 lowers and raises satellite temperatures during upwelling and downwelling events when $Q_i > 0$, respectively (Fig. 3.3). The same model further suggests that satellite temperatures tend to overestimate coastal field measurements in the absence of water column stratification ($Q_i < 0$ in Fig. 3.3). The model resulted nonetheless in an excellent skill (r = 0.97; r2 = 0.94), so we proceeded to reconstruct a gap-free temperature time series at the two study locations for the period Jan. 1998 – Mar. 2019 (Fig. 3.2, Fig. 3.A.3 & Fig. 3.A.4). As expected, the reconstructed time series amended biases between field and satellite records due to wind-driven, cross-shore transport, especially during spring and summer (RMSE < 0.67ºC between field and reconstructed temperatures at both Oleiros and La Franca; see Table 3.2 for complementary metrics).

Table 3.2. Annual and seasonal estimates of mean sea surface temperature and of the Bakun Upwelling Index values at Oleiros and La Franca for the period 1998-2019.

			Oleiros			La Franca		
			Field	Satellite	Model	Field	Satellite	Model
Annual	Sea surface temperature [ºC]	Mean	15.13	15.73	15.19	15.48	16.14	15.47
		SD	1.14	1.24	1.10	1.23	1.32	1.23
	Bakun Upwelling Index [$10^3 m^3 s^{-1} km^{-1}$]	Mean	-	-0.10	-	-	-0.20	-
		SD	-	0.77	-	-	0.88	-
Spring-summer (Mar-Aug)	Sea surface temperature [ºC]	Mean	15.61	16.11	15.50	15.89	16.53	15.92
		SD	1.23	1.27	1.19	1.31	1.40	1.23
	Bakun Upwelling Index [$10^3 m^3 s^{-1} km^{-1}$]	Mean	-	-0.01	-	-	-0.11	-
		SD	-	0.65	-	-	0.73	-
Autumn-winter (Sep-Feb)	Sea surface temperature [ºC]	Mean	14.65	15.35	14.73	15.09	15.77	15.03
		SD	1.04	1.20	1.01	1.15	1.25	1.04
	Bakun Upwelling Index [$10^3 m^3 s^{-1} km^{-1}$]	Mean	-	-0.20	-	-	-0.29	-
		SD	-	0.89	-	-	1.04	-

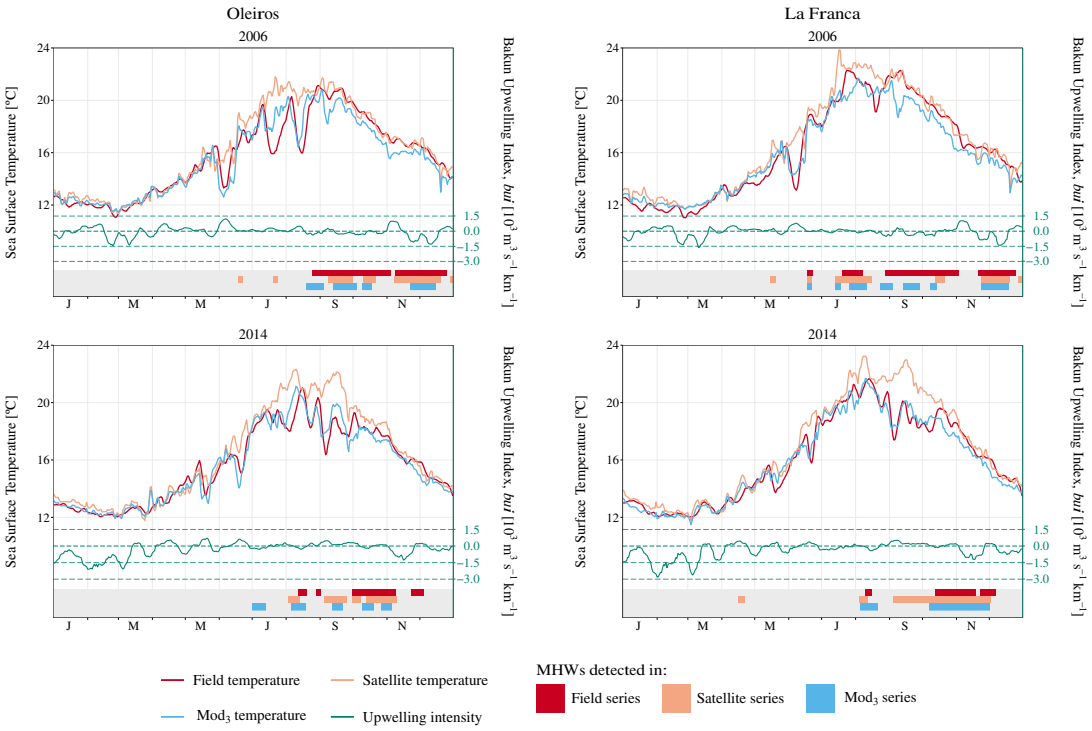

Figure 3.2. Seasonal sea surface temperature variations at Oleiros (*left column*) and La Franca (*right column*) in 2006 (*top row*) and 2014 (*bottom row*). Colored bars in red (field), orange (satellite) and light blue (best selected model [Mod_3, Table 3.1]) show marine heatwave days detected with each temperature series. The years shown here are among those with the most remarkable marine heatwaves in number and/or intensity and/or duration in the entire series (1998-2019). The rest of the years are further illustrated in Fig. 3.A.3 & Fig. 3.A.4 in the Appendix.

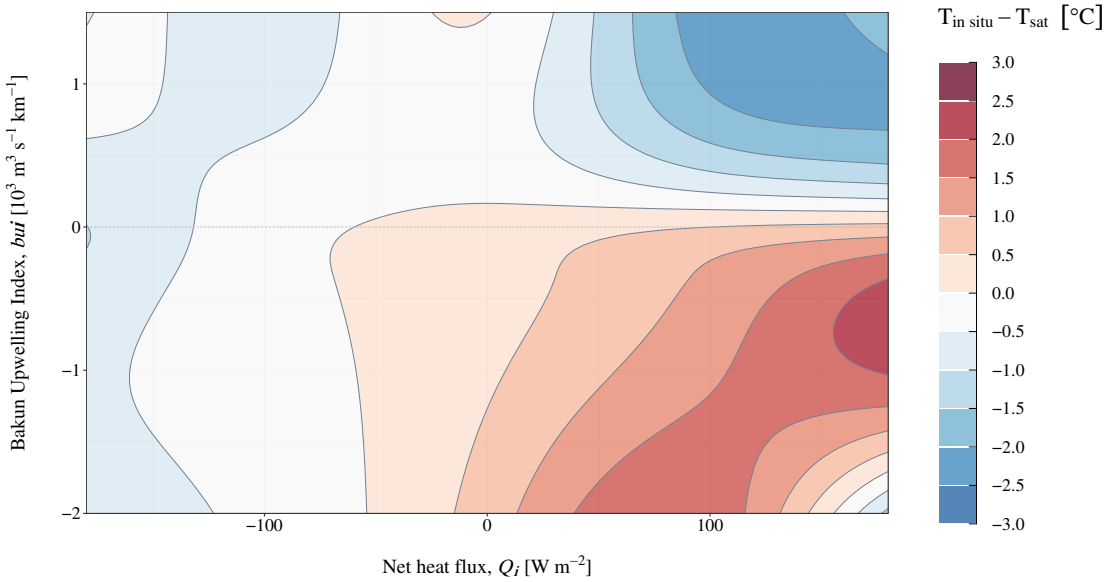

Figure 3.3. Non-linear interaction between the Bakun Upwelling Index (*bui*) and net heat flux (Q_i) based on the best selected model (Mod_3, Table 3.1) on the difference between field and satellite temperatures.

3.3.2. Detection of MHWs in field, satellite and model-based reconstructions

Deviations between temperature time series propagated to the detection of MHW, and both the number and characteristics of the MHWs showed consistent differences between the two locations in the field, satellite and reconstructed temperature time series. The overall number of MHWs detected in the field series was 42 and 30 at Oleiros and La Franca, respectively, suggesting regional scale asynchrony in the occurrence of MHWs. The number of MHWs detected was similar and slightly larger both in the satellite and modelled series than in the field, with smaller differences with respect to MHW counts in Oleiros (41 and 46, respectively) than in La Franca (35 and 36, respectively). The satellite and the reconstructed series also failed to detect a large proportion of MHW days (above a half in Oleiros, Table 3.3). However, the modelled series improved the detection of MHW with respect to the raw satellite series, both in terms of MHW and non-MHW days (Table 3.3). The satellite series resulted in an overestimation of the incidence of MHWs, with a large proportion of false positive MHW days during upwelling episodes (*i.e.,* ~73% and ~76% of the non-MHW days classified as MHW days at Oleiros and La Franca, respectively). The same fraction is reduced at least by a half in the model-based, reconstructed series (17% and 37% of false positives during upwelling events).

3.3.3. Trends in MHWs based on temperature reconstructions

The extended series reconstructed from satellite and reanalysis data (Sep. 1981 - Dec. 2019) revealed an average rate of warming of 0.16ºC per decade along the coasts of the Cantabrian Sea (Table 3.A.1 in the Appendix). Such rate exceeds mean surface warming in the global ocean (0.11-0.13ºC per decade, Rhein et al., 2013), but it is still considerably below the estimate based on the satellite series (0.23ºC per decade, Table 3.A.1). Warming rates increase eastwards towards the inner Bay of Biscay (Fig. 3.A.5 in the Appendix).

Table 3.3. Assessment of detected MHW in satellite and model-based reconstructions of coastal temperatures with respect to those detected based on field observations. Presence-absence confusion matrices were built to compare the number of non-MHW and MHW days detected with the field measurements [reference] *vs.* those from the satellite and the best selected model -Mod_3, Table 3.1-, respectively [tests], within Jan. 1998 - Mar. 2019 at Oleiros and La Franca. For each approach, each date is classified as a *presence* (MHW) or as an *absence* (non-MHW) to calculate the numbers of true positives (both test and reference are *presences*), false positives (*presence* in the test but *absence* in the reference), true negatives (both test and reference are *absences*) and false negatives (test is an *absence* but the reference is a *presence*).

Confusion matrices									
		Oleiros				La Franca			
		Satellite		Model		Satellite		Model	
		MHW	Non-MHW	MHW	Non-MHW	MHW	Non-MHW	MHW	Non-MHW
Field	MHW	235	379	251	363	190	234	213	211
	Non-MHW	277	6364	202	6439	330	5775	210	5895

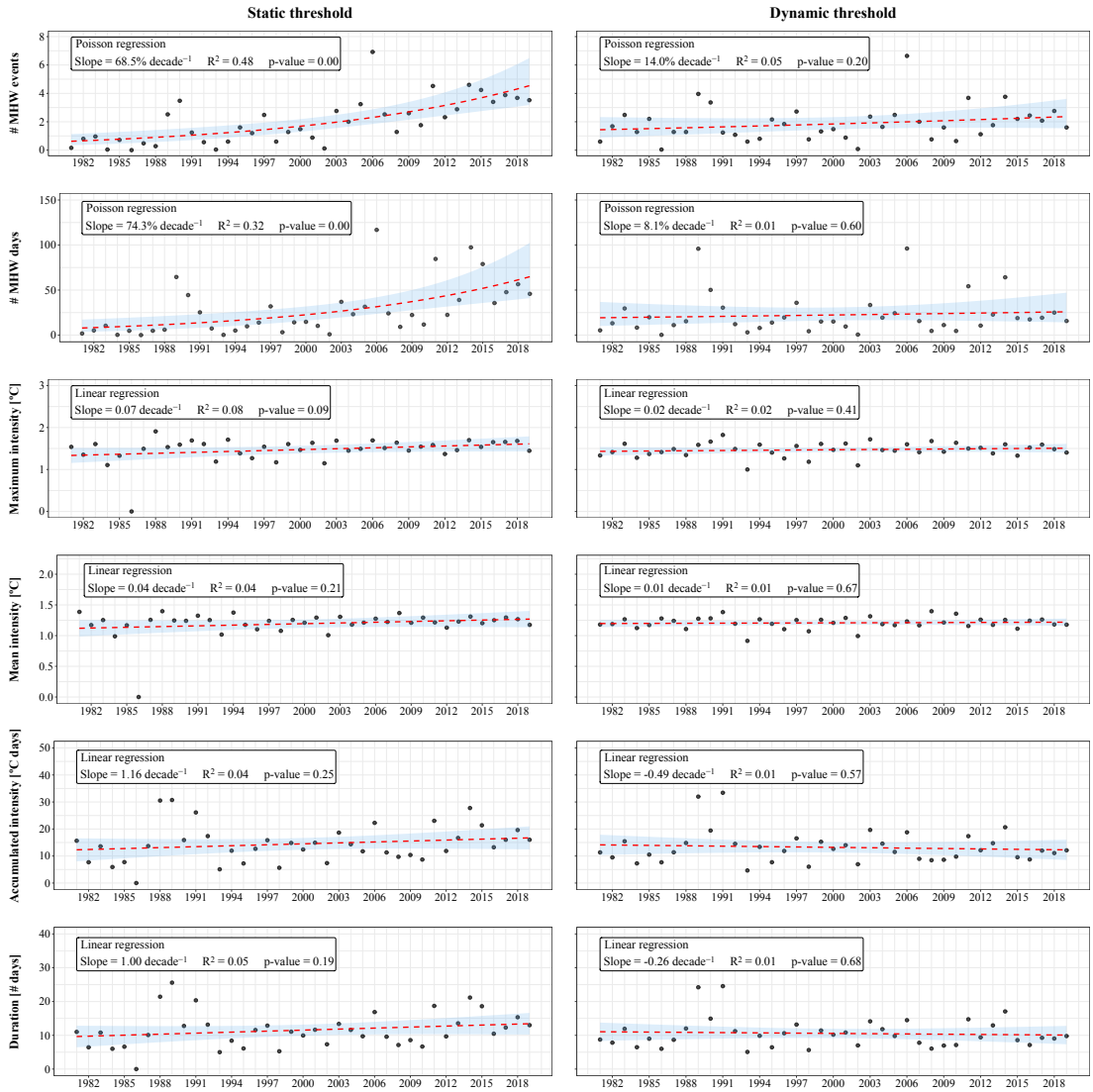

Figure 3.4. Annual values -on average for all 25 localities along the Cantabrian coast- of the features of the marine heatwaves detected with the extended modelled series using a static (*left*) *vs.* a dynamic (*right*) baseline period. Red dashed lines indicate the estimate linear trend for each marine heatwave feature. The slope, proportion of variance explained (R^2), and p-value of each trend are shown. Shaded areas account for 95% confidence intervals.

The comparative analysis of MHW features based on static *vs.* dynamic detection thresholds pointed towards a potential role of long-term ocean warming in enhancing MHWs in the Cantabrian Sea in the past 40 years (Fig. 3.4). When using a static MHW detection threshold (left column in Fig. 3.4) both the number of MHW events and MHW days per year revealed an increase by a factor of ~1.9 per decade (*i.e.,* doubling each 11 years). No significant trends were found for i_{max}, i_{mean}, i_{cum} and *dur* (p-value > 0.05 in every computation), though all estimates were positive. When using a dynamic MHW detection threshold incorporating a linear warming trend in surface temperature (right column in Fig. 3.4), all trends became non-significant and estimates substantially decreased.

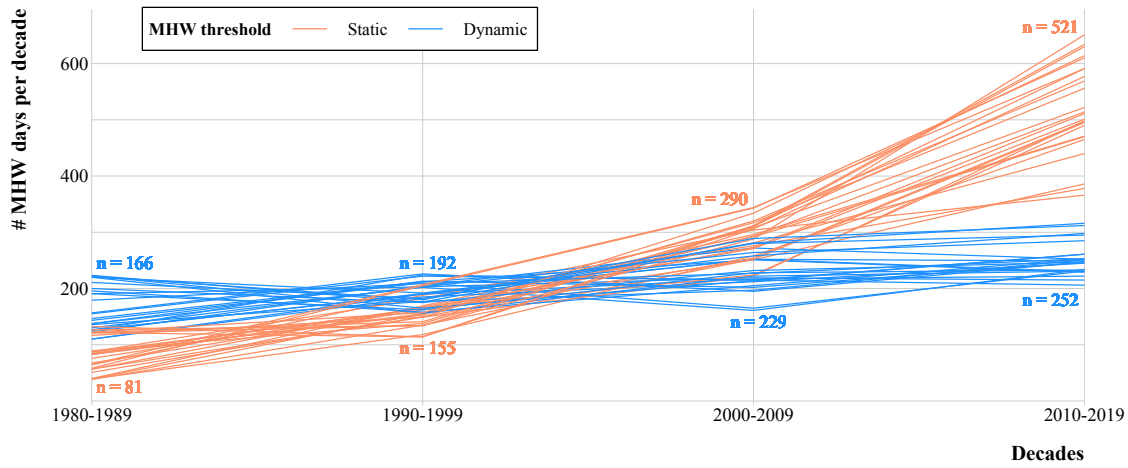

Figure 3.5. Progression of the number of marine heatwave days decade^{-1} detected with the extended modelled temperature series when calculated using static (blue) *vs.* dynamic (orange) detection thresholds (see left and middle columns in Fig. 3.A.6 in the Appendix). Note that we adjusted the estimates by the total number of days per decade to compensate lack of data in the early 1980s. Each line -for each color- represents one locality of the 25 examined along the Cantabrian coast. Numeric values indicate the average number of marine heatwaves per decade calculated using all 25 localities for each marine heatwave detection threshold approach.

To ease the interpretation of the increase in MHW incidence throughout the past 40 years, we arranged by decades the number of MHW days detected in the extended series (Fig. 3.5) and mapped them to illustrate spatial gradients along the Cantabrian coast (Fig. 3.A.6 in the Appendix). On average for all 25 localities covering the spatial extent of the extended series, a total of 1047 *vs.* 839 MHW days per decade were detected in the past four decades when using static *vs.* dynamic detection thresholds, respectively (Fig. 3.5). This may be interpreted as 80% of MHW days (839/1047) taking place regardless of the underlying warming trend, while the remaining ~20% (208/1047) occurring because of it. The proportions increase to 60-40% for the period 2000-19, and to 50-50% for 2010-2019. The analysis also revealed considerable interannual and interdecadal variability, with some years having a remarkably high number of MHW days (*i.e.,* 2006, 2011 or 2014; Fig. 3.4). Overall, the analysis based on a static baseline period reveals a six-fold increase in the incidence of MHWs during the last four decades, which exceeds the two-fold, steady increase observed in the series derived using a dynamic threshold.

3.4. Discussion

This study combines two decades of field temperature measurements with long term reanalysis and satellite data in a statistical downscaling approach based on regression modelling, which allowed to reconstruct past coast-level temperatures and hindcast the incidence of MHW in the last four decades. By including the effect of coastal upwelling and air-sea heat fluxes, our method enabled us to predict an improved temperature series that i) reliably reproduces near-

shore sea surface temperatures, ii) retains the satellite's spatial and temporal resolution and iii) improves MHW detection near-shore. Also, the assessment of trends using static *vs.* dynamic detection thresholds suggested that the underlying ocean warming trend contributed to enhance the incidence, intensity and duration of MHWs along the coasts of the Cantabrian Sea during the last four decades.

Downscaling of satellite data enabled the reconstruction of a temperature series to fairly capture temperature variation close to the coast, enhancing the detection and characterization of MHW nearshores. However, some aspects of this approach limit its possible application in other areas and require further refinement. The proposed downscaling approach relies on long-term field records of water temperature that are seldom available (Oliver et al., 2021). Data from meteorological station networks provide a potential alternative, with the added challenge of modeling water temperature dynamics (*e.g.*, Somavilla Cabrillo et al., 2011). Another caveat lies on the number of stations needed to properly characterize downscaling transfer functions. The two stations, Oleiros and La Franca, may not be fully representative of upwelling regimes along the southern Bay of Biscay, which tend to be weaker towards the inner part of the Bay (Lavín et al., 2006).

Our approach has room to improve by considering additional physical processes modulating water temperatures along the Cantabrian shelf, like the incidence of the Iberian Poleward Current (IPC, Garcia-Soto et al., 2002). This current conveys subtropical, warm waters along the Cantabrian continental shelf and slope during winter, which result in milder conditions that might favor the occurrence of MHWs. In other areas, it may be more important to account for the impact of river discharge or tidal currents on temperature. Nevertheless, the approach provides reasonable, robust predictions and reassures the use of downscaling approaches to extend the applicability of coarse satellite and reanalysis products near the shore.

Disparities between field and satellite temperature records are compatible with those reported in prior studies regarding the reliability of near-shore satellite temperature data (Smit et al., 2013; Stobart et al., 2008, 2015). The importance of these biases depends on the specific context and the question at hand. Analyses of short-term temperature extremes like MHWs, which entail fine-scale recording of swift temperature variations, may be compromised by small scale biases (Smale & Wernberg, 2009). On the other hand, satellites provide a reliable approach to assess the incidence and impact of surface MHWs in the open ocean (Fewings & Brown, 2019). Downscaling methods are routinely used to project climate variables from coarse-resolution climate models to a local-scale (*e.g.*, Gaitán et al., 2014; Gaitán, 2016; Muhling et al., 2018) and to reproduce historical records of specific events (Hirsch et al., 2021). Our approach relies on analyses of air-sea heat fluxes and estimates of wind-induced cross-shore transport to calibrate satellite estimates against field measurements through regression modelling.

Deviations between satellite and field temperature records during coastal upwelling events depend on water column stratification (Botas et al., 1990; Lavín et al., 2006; Llope et al., 2006), but they mainly reflect the coarse resolution of the satellite product employed here. First, temperature variability close to the land-sea margin occurs at smaller spatial scales than offshore and, as a result, the effect of local physical processes such as coastal upwelling might go unnoticed to it (Smit et al., 2013). Second, the coarse size of the satellite pixel entails an unavoidable interpolation with temperatures more offshore. In general, open ocean waters have a greater inertia and vary at a slower pace than shallow waters (Marin, Bindoff, et al., 2021). In particular, upwelling-prone coastal areas tend to present significant differences in warming rates when comparing trends in nearshore and offshore waters. Coastal cooling due to upwelling weakens trends in surface temperature (Fewings & Brown, 2019; Gentemann et al., 2017) and enhances differences in warming rates between coastal and oceanic waters. Offshore waters remain unaffected by the cold-deep-water pump and experience higher warming rates (deCastro et al., 2014; Santos et al., 2001). In fact, Varela et al. (2018) found that SST warming has been more intense in offshore than nearshore waters in ~92% of the upwelling locations worldwide. During upwelling events, satellite retrievals of offshore temperatures may result in warmer measurements than those recorded by the field loggers close to the shore. Indeed, Meneghesso et al. (2020) revealed that Level 4 remotely-sensed products (blended satellite and/or *in situ* observations, interpolated to fill data gaps like those used here) can overestimate coastal SST in upwelling prone locations. This warm bias may consequently lead to the overestimation of MHW events. Varela et al. (2021) recently showed that trends in the number of MHW days were lower near the coast than in adjacent offshore areas in the Eastern Boundary Upwelling systems. Our results add to previous evidence showing a similar buffering effect in a system with weak seasonal upwelling and highlight how satellite-derived SSTs may overestimate MHW incidence near the coast.

All available estimates agree that the Bay of Biscay has been warming at rates above 0.10ºC per decade since the 1970s (Table 3.A.1). The increase in SST observed in the present study in all 25 localities along the coast of northern Spain within Sep. 1981 - Dec. 2019 confirms previous findings and results in trend estimates similar to those of Gómez-Gesteira et al. (2008), who revealed a warming of 0.15-0.25ºC per decade along the Cantabrian coast. This temperature increase might be linked to the general warming trend in the North Atlantic Ocean, which is attributed to global climate change (Harris et al., 2014).

The combined use of static and dynamic detection thresholds allowed us to contrast MHW trends with and without the effect of long-term ocean warming (Oliver et al., 2021). The results imply that the underlying warming trend contributed to increase the number of MHW days in the Cantabrian coast by a 20% (Fig. 3.5 & Fig. 3.A.6). These outcomes are consistent with the

assessment of the impact of global warming on MHW incidence conducted by Laufkötter et al., (2020) and Marin, Feng, et al. (2021).

The contrast in the trends obtained with each MHW detection threshold for all MHW features (Fig. 3.4) suggests that their overall increase has its origin in the progressive ocean warming trend. It should be noted that the warming period to which the Bay of Biscay is currently subjected began in the 1970s (deCastro et al., 2009). The extended modelled series comprises most of it; nonetheless, a time series spanning the warming period thoroughly may have likely revealed a clearer increasing trend for MHW features such as i_{max} and i_{mean} (Fig. 3.4). The observed differences in the progression of the number of MHW days per decade calculated with each detection threshold also pointed towards the effect of the underlying sea warming trend (Fig. 3.5 & Fig. 3.A.6). The static threshold series followed a quite accentuated trend from the very beginning though it reached maximum steepness from the 2000s on, coinciding with an increase in the SST warming rate in central Cantabrian Sea (Voerman et al., 2013).

Since the 1970s, the N coast of Spain has been subjected to a global warming-associated increase in SST (deCastro et al., 2009), especially during summer, enhancing water column stratification (González-Gil et al., 2015, 2018); this trend parallels a decrease in the number of upwelling days and their intensity, especially towards the inner part of the Bay of Biscay (Gómez-Gesteira et al., 2011; Llope et al., 2006; Pérez et al., 2010). Taken together, these trends may lead to an enhanced warming of the upper ocean layer in the coming years, which could be particularly remarkable during summer months (Llope et al., 2006). Coastal upwelling can abate SST anomalies in coastal areas (Fewings & Brown, 2019; Gentemann et al., 2017) and provide thermal refugia to cold-affinity species (Lourenço et al., 2016; Seabra et al., 2019). Our findings support the understanding of upwelling systems as key factors buffering ocean warming nearshore and preventing the impact of threatening climate extremes.

Cold-temperate canopy-forming macroalgae are key components of Cantabrian coastal marine ecosystems, as they provide complex habitat for a wide range of associated flora and fauna (Martínez et al., 2015). Several authors have recently reported the abundance decrease, retreat and redistribution of numerous macroalgae communities and their associated biodiversity since the end of the XX century (Fernández, 2011; Viejo et al., 2011; Duarte et al., 2013; Nicastro et al., 2013; Fernández, 2016; Casado-Amezúa et al., 2019; Ramos et al., 2020). These shifts have generally been attributed to the general increase in SST in the Cantabrian Sea; indeed, ocean warming has a negative effect on seaweed species (Wernberg, Russell, Thomsen, et al., 2011).

Long-term changes in mean SST are the main driver of the observed trends in the occurrence of coastal MHWs globally (Frölicher & Laufkötter, 2018; Oliver et al., 2019). Considering the above-described trends in the Cantabrian Sea, this hints at an alarming scenario for the coming

years. Extreme temperature events tend to exert stronger, more immediate impacts than average gradual trends associated with ocean warming (Oliver et al., 2018; Sanz-Lázaro, 2016). In fact, MHWs have been accounted for remarkable impacts on macroalgae-dominated ecosystems around the world (Wernberg, Russell, Moore, et al., 2011; Wernberg et al., 2013; Smale & Wernberg, 2013; Reed et al., 2016; Wernberg & Straub, 2016; Wernberg et al., 2016; Arafeh-Dalmau et al., 2019). Extreme thermal stress derived from MHWs have well-documented effects on seaweeds (from resistance to altered physiological and ecological performance, disruption of ecosystem structure and regime shifts), although these may not be evident during, or immediately after SST peaks, but might rather have long time-lags (Straub et al., 2019). Overall, increasing temperatures and MHWs directly and indirectly alter the distribution and abundance of canopy-forming species. Thus, our findings highlight the high conservation value and the suitability of climate refugia associated with upwelling areas to safeguard seaweed diversity in the Cantabrian Sea.

The results in this study imply that, during the last decade, half of the MHW events detected along the Cantabrian coast occurred under the influence of the ocean warming trend. Future projections under different global warming scenarios predict an increase in the occurrence and intensity of MHWs in the coming years (Oliver et al., 2019). This urgently calls for a full risk assessment of the Cantabrian Sea marine organisms and ecosystems in order to encourage the elaboration of appropriate conservation and management strategies for a warmer future. The approach presented here might contribute to improve the monitoring of the impact of MHWs on marine coastal ecosystems, which remain key for human livelihood but are currently endangered under the threat of escalating global warming.

Appendix

3.A. Supporting figures and tables

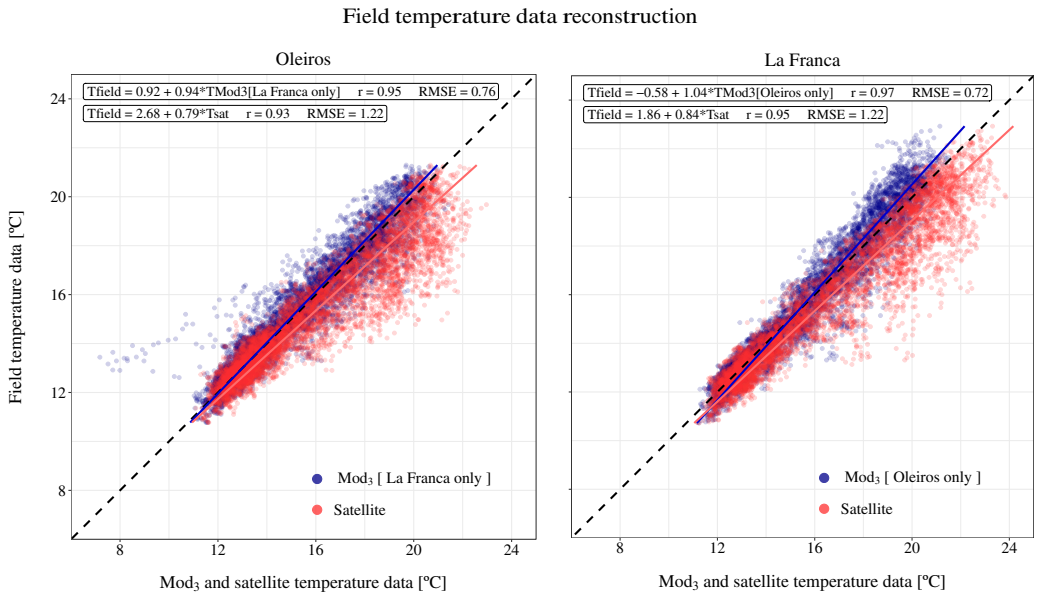

Figure 3.A.1. Assessment of the transferability of model Mod_3 based on the ability to predict field coastal temperatures from satellite measurements when trained with data from a different location. The left panel shows the improvement in predictions of temperatures at Oleiros based on Mod_3 using satellite, *bui* and *Qi* data from the closest pixel but parameters derived from fitting the model only using data from La Franca. The right panel shows the equivalent result when predicting field data at La Franca using a model trained with data from Oleiros. Each panel details the resulting linear regression (solid lines), Pearson correlation coefficients and RMSEs between field observations and model predictions (blue), and between observations and satellite retrievals (red). The black dashed line is the reference 1:1 line.

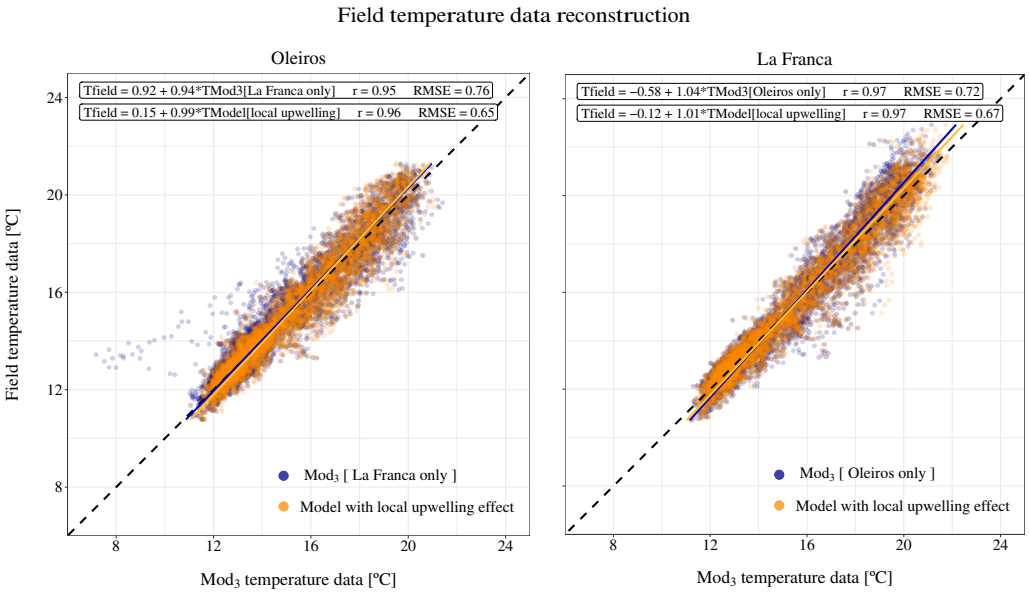

Figure 3.A.2. Assessment of the transferability of model Mod_3 based on the comparison with a model trained at both Oleiros and La Franca featuring a local effect of upwelling. As in Fig. 3.A.1, we focused on the ability to predict field coastal temperatures from satellite measurements, but now comparing Mod_3 (blue) with a model where the interaction between *bui* and *Qi* was allowed to vary between locations (orange). Both models were fit to all available data. Other conventions as in Figure 3.A.1.

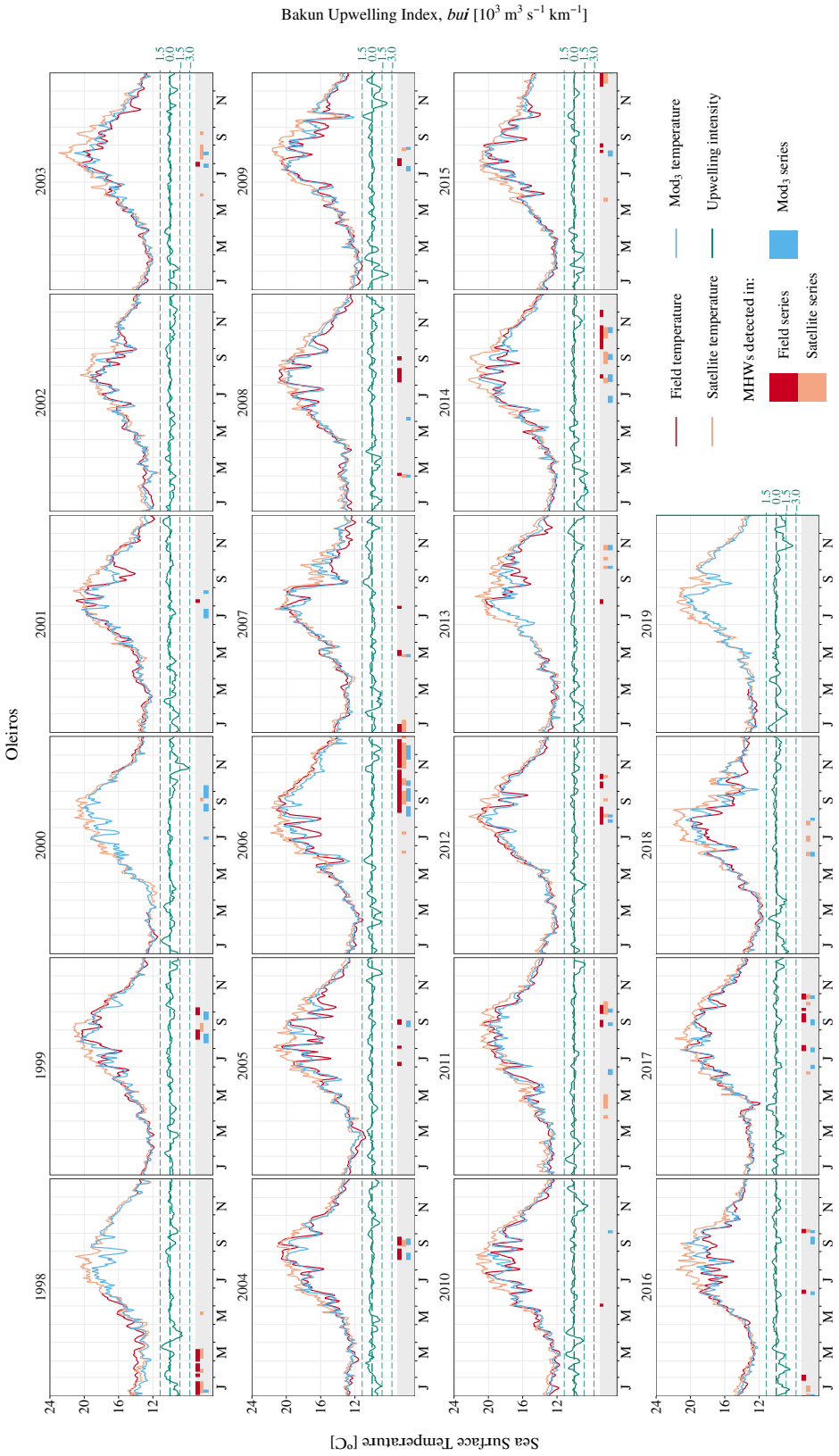

Figure 3.A.3. Seasonal sea temperature variations at Oleiros within 1998-2019. Colored bars in red (field), orange (satellite) and light blue (best selected model [Mod_3, Table 3.1]) show marine heatwave days detected with each temperature series.

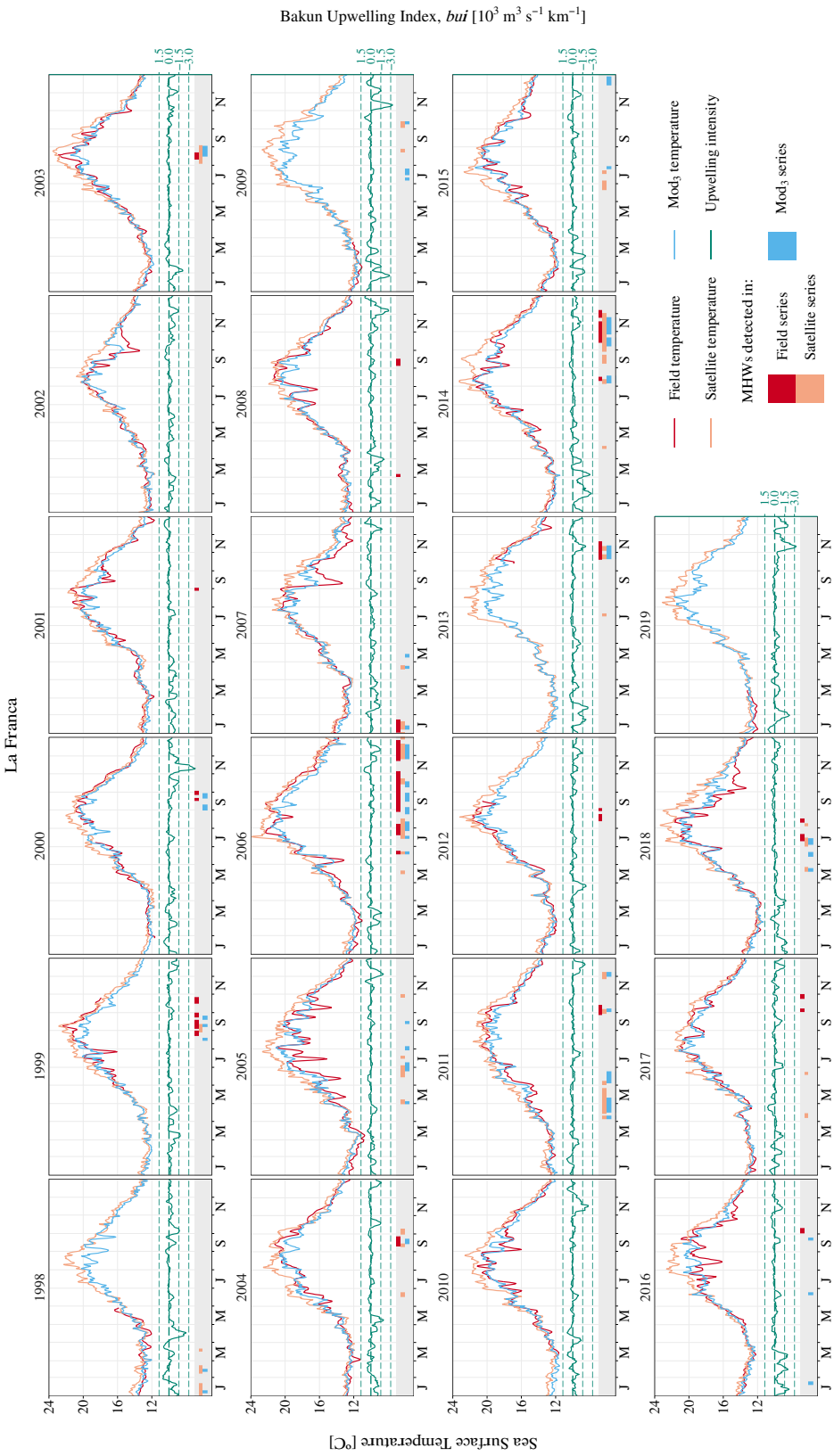

Figure 3.A.4. Seasonal sea temperature variations at La Franca within 1998-2019. Colored bars in red (field), orange (satellite) and light blue (best selected model [Mod_3, Table 3.1]) show marine heatwave days detected with each temperature series.

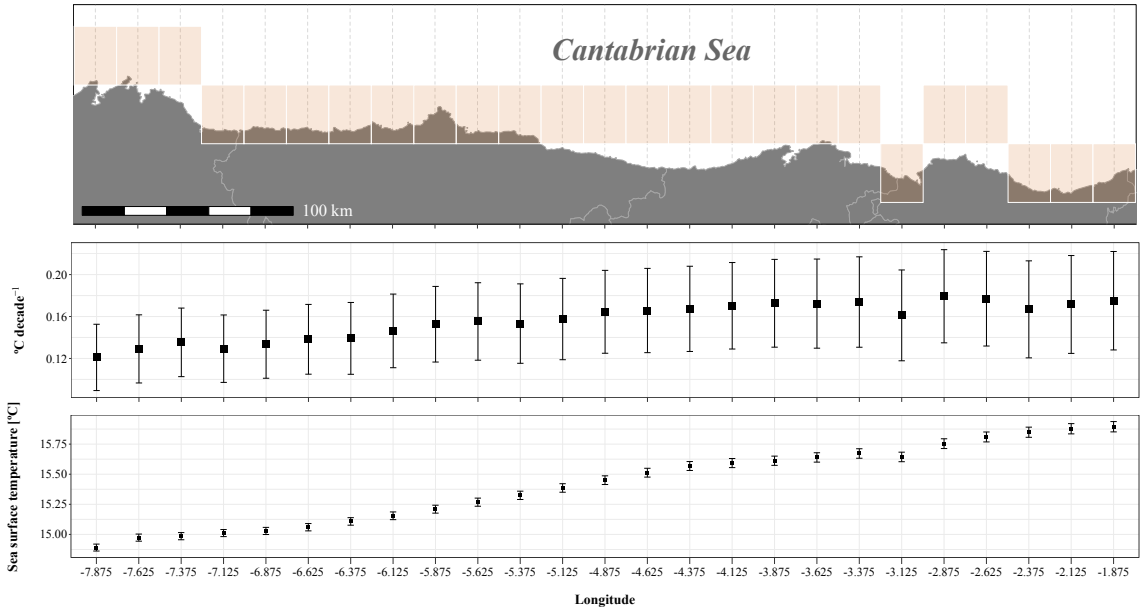

Figure 3.A.5. Sea surface temperature trend (*middle row*) and average sea surface temperatures (*bottom row*) within Sep. 1981 - Dec. 2019 at each locality examined with the extended modelled series (*top row*, salmon-colored rectangles). Error bars correspond to 95% confidence intervals.

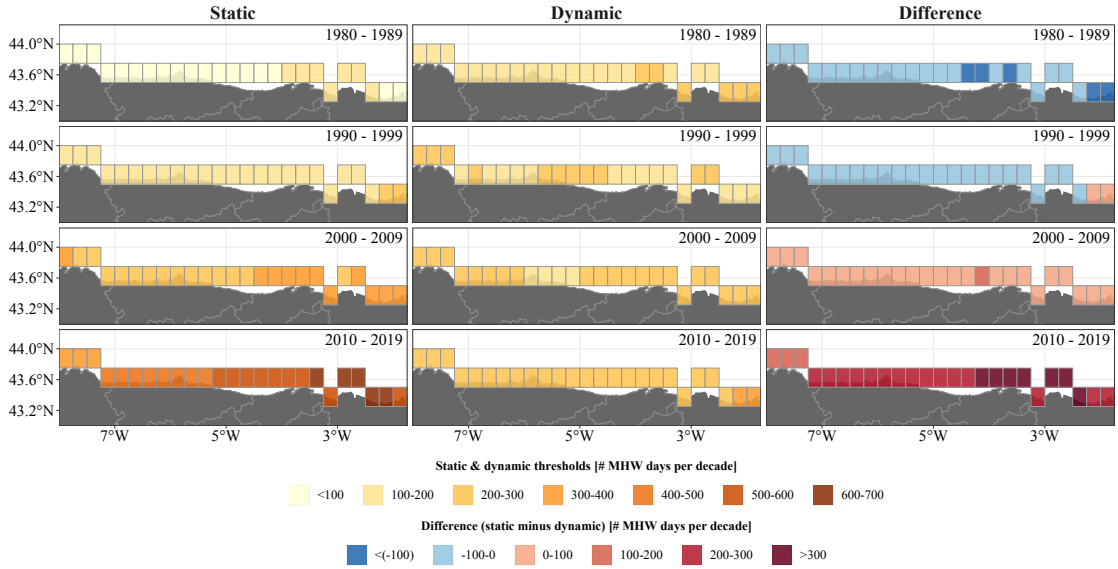

Figure 3.A.6. Average decadal number of marine heatwave days detected with the extended modelled temperature series along the coastal interface of the Cantabrian Sea (n=25). Note that we adjusted the estimates by the total number of days per decade to compensate lack of data in the early 1980s. Marine heatwaves are calculated using static (*first column*) *vs.* dynamic (*second column*) detection thresholds. *Third column:* difference in marine heatwave days between both approaches (static - dynamic).

Table 3.A.1. Annual trends in sea surface temperature (SST) within the Bay of Biscay according to different authors, databases and spatiotemporal scales.

Authors	Period	Area	Database	SST trend (°C dec^{-1})
Koutsikopoulos et al. (1998)	1972–1993	Global	Meteo-France	0.64
Gómez-Gesteira et al. (2008)	1985–2005	French Coast	AVHRR	0.27
		Cantabrian Coast	AVHRR	0.21
deCastro et al. (2009)	1985–2006	Global	AVHRR	0.30
	1974–2007	Global	ERSST	0.22
Costoya et al. (2015)	1982–2014	Global	AVHRR	0.26
González-Gil et al. (2018)	1981–2012	Global	OISST	0.30
Chust et al. (2022)	2003–2019	Global	NASA OBPG	0.11
This study	1981–2019	Cantabrian Coast	OISST	0.23
			Model reconstruction	0.16

Chapter 4

Divergent responses to warming and marine heatwaves in a small pelagic fish community

Abstract

Early life survival in marine fish is intricately linked to fluctuations in environmental conditions, a relationship that accentuates as climate change reshapes global oceans. This study explores the effects of environmental variability on a small pelagic fish community in the Bay of Biscay, NE Atlantic, focusing on four species: anchovy, mackerel, horse mackerel and sardine. These species have contrasting life history strategies and show divergent population trends, with record abundance levels of anchovy and a poleward expansion of mackerel accompanied by a steady decline in the abundance of horse mackerel and sardine. We examined changes in recruitment, population biomass, pre-recruitment survival and population growth in these species in relation to physical conditions, considering changes in upwelling, turbulence, and temperature, including marine heatwaves and cold-spells. We analyzed long-term trends and the impact of environmental variability on the early life survival of each species. Our analyses revealed an increase in sea surface temperature, an intensification of marine heatwaves and a weakening of cold-spells throughout the region over the last four decades. Coastal upwelling and turbulence affected the early survival of anchovy, mackerel and horse mackerel, but the effect varied depending on the region examined. Importantly, warmer waters and marine heatwaves were positively associated with mackerel survival and negatively with horse mackerel across the Bay – suggesting a potential link between increased mean and extreme temperatures and distributional and phenological shifts in the populations of both species. In contrast, marine cold-spells were detrimental to the survival of anchovy and mackerel in most regions of the Bay. No effects were observed on the early survival of sardine. Our study seeks to provide new insights into the environmental and ecological scenario currently emerging in temperate spawning regions, with the aim to devise sensible strategies that enhance the resilience of fish populations in a changing climate.

Keywords: Sea surface temperature, marine heatwaves, pelagic fish, population dynamics, life history, survival rate.

4.1. Introduction

Marine fisheries play a crucial role in the global food system, sustaining the livelihoods of millions while generating huge economic benefits (FAO, 2022). Alteration of the physics, chemistry and ecology of the global oceans due to human-induced climate change and mismanagement directly compromises the provision of these vital goods and services (Breitburg et al., 2018; Xiu et al., 2018; Tittensor et al., 2021; Cheng et al., 2023) and lies behind reported declines in marine ecosystems and their associated fish populations worldwide (IPBES, 2019; Sumaila & Tai, 2020).

The impact of environmental stressors on the abundance of fish populations is often channeled through the modulation of recruitment success (Myers, 1998; Minto et al., 2008). Survival until recruitment age depends on a variety of factors, amongst which the environmental and trophic interactions experienced during early life stages play a fundamental role, as over 90% of mortality happens soon after larvae absorb their yolk and begin feeding (Houde, 2008). Understanding how the environment shapes early life survival in fish populations is essential for gauging the potential effects of climate-driven shifts and to develop strategies to bolster climate readiness and marine fisheries resilience (Free et al., 2019; Bell et al., 2020).

Amongst the environmental factors that modulate recruitment success, temperature plays a pivotal role. Temperature governs metabolic and physiological processes that modulate spawning phenology and early development (Garrido et al., 2016; Kanamori et al., 2019; Alix et al., 2020). Ocean warming might alter these processes due to rising temperatures and through the increasing occurrence of marine heatwaves (MHWs, discrete and prolonged extreme warm water events; Hobday et al., 2016), which are projected to intensify in coming decades with direct consequences on fish populations and fisheries (Cheung et al., 2021; Payne, 2023). Conversely, marine cold-spells (MCSs, discrete and prolonged extreme cold-water events; Schlegel et al., 2021) are consistently becoming weaker and less frequent (Wang et al., 2022).

Another family of processes affecting recruitment success relate to wind-driven phenomena like upwelling and turbulent mixing, which operate in two main fronts. First, they moderate temperature extremes that can be potentially harmful for spawners and/or early life stages by promoting a more uniform thermal environment across the water column. Coastal upwelling lowers upper ocean temperatures by bringing deep, cool waters to the surface, and turbulence redistributes heat across the mixed layer, deepening it and reducing surface temperature gradients (Large et al., 1994; Varela et al., 2024). Second, they drive essential transportation patterns and nutrient dynamics that, following Bakun's triad hypothesis (Bakun, 1996), can influence recruitment success through three main mechanisms: enrichment of the food chain by regenerated nutrients in upwelled waters (Ware & Thomson, 1991), retention or drift of eggs and larvae in

suitable nursery areas taking advantage of seasonal cycles in offshore transport (Parrish et al., 1981), and concentration of food for larvae and subsequent development stages due to moderate turbulence (MacKenzie, 2000). These mechanisms infer a dome shape interaction between recruitment and upwelling/turbulence intensity, as successful recruitment hinges on the balance between enhanced feeding and calm conditions (see Cury & Roy, 1989). Future projections point towards enhanced land-sea atmospheric pressure gradients under global warming, which will likely alter wind regimes worldwide and consequently affect fish larval dispersal and survival in relation to coastal winds (García-Reyes et al., 2015; Bashevkin et al., 2020).

Large-scale shifts in the distribution and productivity of commercial fish species have been observed on both sides of the North Atlantic as a response to climate change (Barange et al., 2018). In the Northeast Atlantic, the European anchovy (*Engraulis encrasicolus*), Atlantic mackerel (*Scomber scombrus*), Atlantic horse mackerel (*Trachurus trachurus*) and European sardine (*Sardina pilchardus*) are among some of the most valuable pelagic fish species, providing substantial amounts of catch along their range of distribution (ICES, 2023a, 2023b). The four species spawn across the continental shelf of the Bay of Biscay and exhibit unique distributions and phenologies (Motos et al., 1996; Uriarte & Lucio, 2001; Abaunza et al., 2003). These species play a crucial role not only in sustaining the socio-economic framework of local fisheries but also in preserving balance within the marine ecosystems in the Bay (ICES, 2021a, 2021b; Corrales et al., 2022).

Over the past decades, the Bay of Biscay has experienced a rise in air and sea temperatures (Costoya et al., 2015; Chust et al., 2022), an increased frequency and intensity of MHWs (Izquierdo et al., 2022b; Simon et al., 2023) and elevated maximum wind speeds (Chust et al., 2022). The potential impact of temperature extremes such as MHWs and MCSs on pelagic fish species in the Bay of Biscay has not yet been examined. However, reported impacts on fish stocks around the world (Feng et al., 2021; Thompson et al., 2022) suggest that similar effects may be observed in the Bay of Biscay. In fact, some fish populations have started to respond to the former trends, particularly those associated with temperature (Erauskin-Extramiana et al., 2019; Véron et al., 2020; Chust et al., 2023), which raises concerns on the ecological implications and the adaptive strategies that fish populations may employ to cope with ocean warming, and how it will affect local fisheries.

Our study aims to shed light on the impact of shifting climate conditions on small pelagic fish amidst in the Bay of Biscay – which so far include alterations in migration and distribution patterns and changes in spawning phenology (Montero-Serra et al., 2015; Erauskin-Extramiana et al., 2019; Schickele et al., 2020; Chust et al., 2022, 2023). To achieve this, we rely on i) relevant oceanic environmental factors (alongshore upwelling, turbulence, average sea surface temperature and metrics characterizing marine heatwaves and cold-spells) and ii) indices of

recruitment and population abundance. To capture the interannual variability in the environmental conditions experienced by the four species during their early life stages, we restrict the environmental data spatially to the continental shelf and slope, and temporally to the specific spawning period of each species. Through this targeted approach, we assess long-term trends over the last four decades and examine the impact of environmental fluctuations on the early life survival of small pelagic fish in the Bay of Biscay. We anticipate varying responses on the latter based on species-specific spawning preferences and life history traits, though a consistent effect of temperature -either broadly or through discrete extreme events- is expected owing to the overarching ocean warming trend. Our results highlight the intricate interplay between the environment and fish populations and contribute valuable insights to their understanding in the Bay of Biscay, paving the way for informed decisions that foster resilience in the face of ongoing climate change.

4.2. Materials and methods

4.2.1. Study area

Located between 0-10ºW and 43–48ºN, the Bay of Biscay (NE Atlantic) is a gulf dominated by an extensive, central abyssal plain surrounded by three continental shelves (Fig. 4.1). The Cantabrian shelf is in the south and it is relatively narrow (up to 30 km) compared to the Aquitanian shelf and the Armorican shelf in the east, whose width increases with latitude (up to 150 km offshore the tip of Brittany; Lavín et al., 2006).

As a temperate sea, the Bay of Biscay exhibits a pronounced seasonal mixing and stratification of water masses. This pattern is modified over the shelf by upwelling and other transport-related processes, leading to substantial variation in primary production and phytoplankton biomass within the region (ICES, 2021a). Habitats further offshore are shaped by the influence of Atlantic waters, although circulation tends to be weak (Borja et al., 2019).

The Bay of Biscay primarily encompasses a pelagic ecosystem, particularly in low trophic levels in which the interactions between phytoplankton, zooplankton and forage fishes define the main trophic flows (Lavín et al., 2006).A significant portion of primary production ends up as detritus, sustaining suspension and deposit feeders and demersal fishes (Corrales et al., 2022).

4.2.2. Study species

The European anchovy is a small pelagic fish found from northern Europe to southwestern Africa (Whitehead et al., 1988). It reaches maturity within a year and forms large migratory schools that, in the Bay of Biscay, migrate to northern deeper waters in summer and to southern shallower waters in winter (Uriarte et al., 1996). Spawning occurs from March to August

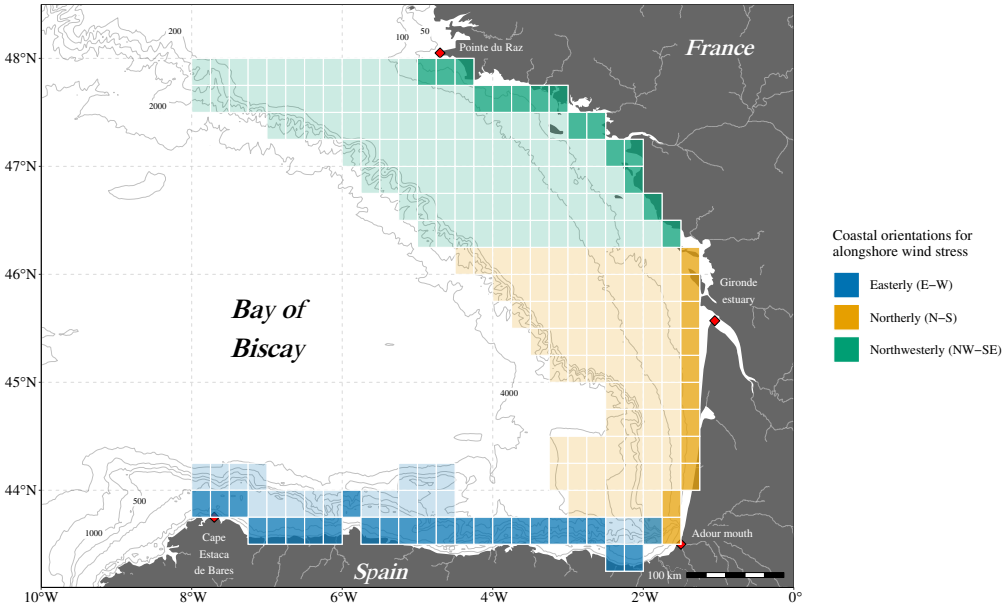

Figure 4.1. Map of the Bay of Biscay. Each 0.25° quadrangle (n = 240) corresponds to an aerial pixel location where we gathered sea surface temperature and wind vector data. Cape Estaca de Bares, the Adour River mouth, the Gironde estuary and Pointe du Raz delimit the Cantabrian (blue), Aquitanian (orange) and Armorican (green) shelves. Strongly colored cells indicate the pixels selected to calculate the Bakun Index, for which we considered the different orientations of the wind stress component, τ_a, along the coastline: easterly (E-W) from Cape Estaca de Bares to the Adour mouth (dark blue), northerly (N-S) from the Adour mouth to northern Gironde estuary (orange), and northwesterly (NW-SE) encompassing the stretch from this point to Pointe du Raz (green). Bathymetry data were extracted from the GEBCO 2023 Grid (GEBCO Compilation Group, 2023).

in three main spawning grounds: two near the Garonne and Adour-Bidasoa rivers (younger fish) and one along the shelf break (older fish), with additional centers scattered in the Cantabrian Sea (Lucio & Uriarte, 1990; Motos et al., 1996; Solá et al., 1990). However, environmental changes are projected to expand the anchovy spawning area in upcoming decades (Erauskin-Extramiana et al., 2019). In the Bay of Biscay, a serious population decline led to a fishery closure from 2005 to 2009, with a regulated reopening in 2010 under TAC limits (Andrés & Prellezo, 2012; Uriarte et al., 2023). The population rebounded back to sustainable levels, with a historical highest abundance estimate above 200×10^3 t in 2021 (ICES, 2021f), but rising concerns about declines in body size (Böens et al 2023; Taboada et al. 2024).

The Atlantic mackerel is a pelagic, migrating fish inhabiting the Northeast Atlantic, where it forms size-dependent schools that migrate seasonally between wintering grounds in the Norwegian and North Seas and spawning areas near the British Isles and the Bay of Biscay (Uriarte et al., 2001). The stock is divided into three spawning components: northern, western, and southern (ICES, 1996). Here we focus on the major, western component, which spawns from February to July along the European continental shelf margin, from the Bay of Biscay through the Celtic Sea and the Porcupine Bank to the Faroes Grounds (ICES, 2020). Spawning starts and

peaks in the southern Bay of Biscay in late winter and spring, where most of the reproductive effort concentrates (Chust et al., 2023). Over the last decades, the increasing abundance of mackerel has been accompanied by a poleward expansion attributed to ocean warming and increased prey availability (Olafsdottir et al 2019; Chust et al., 2023; dos Santos Schmidt et al., 2024), a trend expected to continue in the coming years (Bruges et al., 2016). The expansion triggered an international dispute in the fisheries (Hannesson, 2013; Østhagen et al., 2020), but the population has declined back from peak levels in 2013.

Atlantic horse mackerel is a long-lived species distributed along the East Atlantic, from northern and western Europe to West Africa, including the Mediterranean Sea (Smith-Vanith, 1986). It is divided into several stock units: North Sea, western, southern, and Mediterranean, with debate on an additional Saharo-Mauritanian stock (ICES, 2005; El Mghazli et al., 2022). Here we focus on the western stock, which is distributed from the Bay of Biscay to the Norwegian Sea along the western European margin. Horse mackerel migrates seasonally between these areas in the search of food-rich regions and to their spawning grounds along the continental shelf, exhibiting a certain degree of site fidelity (Abaunza et al., 2008; Chust et al., 2023). The Bay of Biscay concentrates a large fraction of horse mackerel spawning from March to August with a peak in May-June (Lucio & Martin, 1989). The size of the stock has declined steadily since the 1990s due to a decrease in production (ICES, 2022; 2023b), and it has even been listed as a vulnerable species by IUCN (Smith-Vaniz et al., 2015). Importantly, a 2021 stock reassessment led to a rebuilding plan aimed at recovery to safe biomass levels (ICES, 2021c), but subsequent revisions resulted in zero-catch recommendations for 2023 and 2024 (ICES, 2022; 2023b).

The European sardine is a widely distributed, small pelagic fish found from northern and western Europe to northwestern Africa (Parrish et al., 1989). In European waters it is divided into northern and southern stocks, with key spawning grounds in the English Channel and in the Bay of Biscay (ICES, 2021d; Coombs et al., 2005; Planque et al., 2007). Spawning grounds in the Bay show a nearly continuous geographical distribution across the shelf, except for a break at its southeast corner (Bernal et al., 2007). Spawning extends from autumn to spring, divided into two periods that reach peak activity in April and October (Véron et al., 2020). Sardine biomass and catches have declined steadily since the early 1980s and it is considered to be partially trapped in a low productivity regime (ICES 2022a). Future projections point at a decline in sardine populations due to ocean warming (Torralba & Besada, 2015), alongside worsening body condition and slower growth (Véron et al., 2020), raising concerns on their long-term sustainability.

4.2.3. Population indices

We focused on the dynamics of the four small fish species that dominate the pelagic habitat in the Bay of Biscay: European anchovy, Atlantic mackerel, Atlantic horse mackerel and

Table 4.1. Details on ICES stocks and life history traits of anchovy, mackerel, horse mackerel and sardine in the Bay of Biscay (FAO Subarea 27.8; see also Fig. 4.A.1 in the Appendix).

	European anchovy (*Engraulis encrasicolus*)[1]	Atlantic mackerel (*Scomber scombrus*)[2]	Atlantic horse mackerel (*Trachurus trachurus*)[3]	European sardine (*Sardina pilchardus*)[4]
Stock ID	ane.27.8	mac.27.nea	hom.27.2a4a5b6a7a-ce-k8 (W)	pil.27.8abd (N)
Time span	1987-2022	1980-2022	1983-2021	2002-2020
Egg hatching [h]	28-55	90-102	40-167	30-72
Maturity [y]	1	3	5	1
Longevity [years]	5	12	>20	6
Adult size [cm]	~15	~35-45	~25-35	~20
Fecundity [eggs/g]	200-600	1000	500-1500	400
Spawning period(s)	Mar-Aug	Mar-Jul	Mar-Aug	Apr-Jun, Oct-Dec
Spawning peak(s)	May-Jun	Apr	May-Jun	Apr, Oct
Spawning thermal niche	14-18ºC	9-16ºC	13-17ºC	13-17ºC

[1]Lucio & Uriarte (1990), Motos et al. (1996), Bernal et al. (2012); [2]Lockwood et al. (1977), Borja et al. (2002), Chust et al. (2023); [3]Pipe & Walker (1987), Abaunza et al. (2003), Chust et al. (2023); [4]Coombs et al. (2006), Garrido et al. (2016), Véron et al. (2020).

European sardine (ICES, 2021b). Table 4.1 provides key information on the selected ICES stocks for each species and their corresponding life history traits, while Figure 4.A.1 in the Appendix illustrates the spatial extent of each stock. Contrarily to the anchovy and sardine stocks, which are mainly confined to the Bay of Biscay, the stocks for mackerel and horse mackerel cover a much larger area due to their migratory behavior. Analyses of triennial egg surveys demonstrate that most the spawning activity of both species in the Northeast Atlantic occurs along the Cantabrian shelf, in the Bay of Biscay (Chust et al. 2023), which reinforces the significance of our regional focus. For sardine, we concentrated on the western stock, which covers the Armorican and Aquitanian shelves, as the southern stock only marginally extends into the Bay of Biscay (Díaz-Conde et al., 2017). As a result, our analyses for sardine focus exclusively on the two primary shelves and do not consider the Cantabrian shelf.

These four pelagic species differ on their life history strategies: anchovy and sardine are small, short-lived species with rapid growth and maturation and a fast population turnover, while mackerel and horse mackerel have a larger body size, slower growth and longer lifespans, with dominant cohorts and variable reproductive success that result in a slower replacement of mature individuals (Rochet, 2000). Different life history strategies reflect alternative adaptive solutions to cope with environmental variations. As Winemiller (2005) notes, life history strategies determine the demographic rates, population dynamics, and long-term viability of fish under exploitation. Thus, understanding these life history traits is crucial when evaluating how environmental factors influence fish populations, as short-lived species may react rapidly to

favorable or adverse conditions, while longer-lived species may buffer short-term impacts but face challenges over prolonged environmental shifts.

We gathered biomass estimates of the spawning stock (SSB) and age-1 cohorts of recruits (R) from stock assessment models informed by scientific, bottom-trawl, acoustic and egg surveys (ICES, 2021a, 2021b). We converted recruitment to biomass units multiplying their abundance by the mean body weight in the stock at age-1. Focusing on age-1 recruits allowed us to fully capture lagged effects of environmental forcing on the pre-recruitment survival index (PRSI), which we calculated as the natural logarithm of the ratio between R and SSB (Minto et al., 2008). PRSI is a proxy for early life survival, offering insights into how environmental factors influence the survival of recruits relative to the reproductive potential of the adult population. Additionally, we calculated the population growth rate (PGR; defined as $PGR_{t+1} = log_e\left(\frac{SSB_{t+1}}{SSB_t}\right)$, Sibly & Hone, 2002) to assess short and long term trends in adult fish component of the population and to frame the impact of recruitment fluctuations in the dynamics of the stock contribution.

Finally, to explore the degree of association among all the population indices, we estimated the cross-correlation between i) log-transformed R and SSB and ii) PRSI and PGR through Pearson correlation tests. We aligned PRSI and PGR taking into account the time lag due to the age of maturation of each species, which might differ from the age of recruitment (Table 4.1).

4.2.4. Environmental data

Early-life fish survival depends on multiple mechanisms, among which fluctuations in environmental forcing play a major role (Houde, 2008). Temperature affects the spawning activity and recruitment variability of anchovy, mackerel, horse mackerel and sardine in the Bay of Biscay (Pipe & Walker, 1987; Planque et al., 2007; Hughes et al., 2014). Previous work has revealed a positive effect of wind-induced upwelling upon anchovy recruitment in the Bay (Borja et al., 1996, 1998; Allain et al., 2001, 2007), which turned non-significant for mackerel and horse mackerel (Borja et al., 2002; Lavín et al., 2007). Borja et al. (1996, 1998, 2002) also found negative associations between wind induced turbulence and larval survival and recruitment in both anchovy and mackerel.

We gathered satellite and reanalysis data on surface temperature and ocean winds over the Bay of Biscay during the last four decades to assess the impact of environmental variability on early life survival. The analyses focused on spawning and early life stages. We masked the continental shelf and slope (Fig. 4.1), where most spawning and early life activity occurs, up to 2000 meters deep (Lavín et al., 2006; Ibaibarriaga et al., 2007). Then, we averaged data corresponding to the entire and peak spawning periods of each species (Table 4.1), which encompass the most vulnerable early life stages.

Bakun Index, alongshore upwelling and turbulence

Hourly ocean surface wind vectors between Jan. 1982 and Dec. 2022 were extracted from ERA5 0.25º reanalysis available at the Climate Data Store (CDS) of the Copernicus Climate Change Service (C3S) (Hersbach et al., 2020) and conveniently averaged into daily estimates.

We calculated wind stress (τ [N m^{-2}]) from neutral wind speed vectors at 10 m (U_{10} [m s^{-1}]) using the bulk formula; $\tau = \rho_{air} \cdot C_D \cdot U_{10} \cdot |U_{10}|$, where ρ_{air} is air density (taken as 1.223 kg m^{-3}) and C_D is a non-dimensional drag coefficient. C_D was estimated as a function of U_{10} based on Large et al. (1994):

$$10^3 C_D = \frac{2.70}{U_{10}} + 0.142 + 0.0764 U_{10}$$

We calculated Bakun (1973) Index (BI) $= TL = \frac{\tau_a L}{\rho_{sw} f}$ [m^3 s^{-1}], which is based on estimates of seaward Ekman transport (T [m^2 s^{-1}]) along a segment of coast of a given length (L = 1 m). To accurately capture the driving wind forces and acknowledge their localized nature, we estimated the Bakun Index based on wind speed data from the nearest pixels to the coast (Fig. 4.1).

Wind-induced upwelling in the Bay of Biscay is mainly produced by easterly winds along the Cantabrian coast, and northerly and northwesterly winds off southern Brittany (Lavín et al., 2006). Thus, we estimated the alongshore component of wind stress, τ_a, assuming different coastline orientations for each continental shelf: easterly for the Cantabrian shelf, northerly for the Aquitanian shelf and northwesterly for the Armorican shelf (Fig. 4.1). Seawater density, ρ_{sw}, was set to 1025 kg m^{-3}, and the Coriolis parameter, f (s^{-1}), was calculated following $\Omega = 2 \sin \varphi$, where Ω is the rotation rate of the Earth ($\Omega = 7.27 \cdot 10^{-5}$ s^{-1}) and φ is latitude. We applied a 5-day simple moving average on the resulting Bakun Index estimates to integrate the cumulated impact of high frequency wind variability on cross-shore transport (García-Reyes & Largier, 2010). Positive values correspond to the upwelling of deep waters and leads to surface cooling, whereas negative values correspond to downwelling, sinking and warming. To capture the net upwelling-downwelling annual balance, we took monthly means of daily Bakun Index estimates and added them for each year. Additionally, we derived the total annual alongshore upwelling (which we will refer to as Upwelling Index, UI) by taking monthly means of positive-only Bakun Index values and adding them for each year, as implemented in Borja et al. (1996).

Finally, we calculated wind-generated turbulence (*turb*) as the cube of wind stress (Bakun & Parrish, 1982). Annual estimates were computed by averaging daily turbulence values for each year.

Sea surface temperature

Sea surface temperature (SST) data were retrieved from the NOAA Optimum interpolation 0.25° daily sea surface temperature analysis (oiSST version 2, Jan. 1982–2022, see Reynolds et al., 2007; Banzon et al., 2016) and www.ncdc.noaa.gov/oisst for further details). To ensure temporal homogeneity (Reynolds & Chelton, 2010), we used the Advanced Very High-Resolution Radiometer (AVHRR-only) product from the Pathfinder Version 5 dataset (Casey et al., 2010). This dataset includes an optimal interpolation step to fill gaps and aggregate fine scale high resolution retrievals (~1 km) that effectively smooths original observations and avoids biases in measurements close to the land-sea interface.

Spawning thermal niche

We calculated the number of days per year in which SSTs fell within thermal spawning preferences of the European anchovy, Atlantic mackerel, Atlantic horse mackerel and European sardine during their respective spawning seasons (see Table 4.1). We classified each day based on temperature conditions falling within or outside the optimal spawning thermal niche of each species based on reanalyzed, daily satellite retrievals (Table 4.A.1 in the Appendix). This classification allowed us to identify conditions that could potentially be detrimental to the species.

Marine heatwaves (MHWs) and cold-spells (MCSs)

We identified extreme marine temperature events by analyzing SST data spanning the last four decades on the continental shelf of the Bay of Biscay. We followed Hobday et al. (2016) criteria, by which MHWs (MCSs) can be defined as periods warmer (colder) than the 90^{th} (10^{th}) percentile of the climatological observations at a given location lasting for at least 5 consecutive days and based on a 30-year historical baseline period - though a 10-year-long period provides acceptable results (Schlegel et al., 2019).

In line with the methodology outlined in Izquierdo et al. (2022b), we used a parametric Monte Carlo approach to estimate the 90th and 10th threshold climatologies for the detection of MHWs and MCSs, respectively. This approach was adopted as an alternative to the conventional 30-day moving window method to prevent potential directional lags and enhance accuracy. For the 1982-2022 SST series, we used a Generalized Additive Model (GAM) incorporating a constant seasonal cycle. We then generated 10,000 sets of model parameters by randomly selecting values from the estimated mean and covariance to simulate daily surrogate time series, which resulted in an unbiased dataset of 90th and 10th threshold estimates spanning our study period. To avoid minor fluctuations, we smoothed the obtained thresholds applying a 15-day central moving average.

To effectively assess and describe the occurrence of both MHWs and MCSs over time, we gathered the following metrics: the total number of events (n_{events}) and event days (n_{days}) per year,

as well as the maximum, mean and cumulative intensity (i_{max}, i_{mean} and i_{cum}, respectively) and duration (D) of each event - averaged per year. See (Hobday et al., 2016) for a comprehensive definition of these metrics.

4.2.5. Statistical analyses

We assessed long-term trends on environmental factors (Bakun Index, Upwelling Index, turbulence, SST, spawning thermal niche classes and MHW/MCS features) and population indices for anchovy, mackerel, horse mackerel and sardine (R, SSB, PRSI and PGR) over the past four decades across the Bay of Biscay. Then we used linear and GAM models to assess potential effects of environmental forcing on the PRSI of each species.

Long-term trends

We performed linear regression to assess temporal trends in SST, Bakun Index, Upwelling Index, turbulence and MHW/MCS metrics over the period 1982-2022 in the continental shelf of the Bay of Biscay. We analyzed annual trends, but also trends for averages and counts taken over the spawning period of each species. We used simple linear regression to assess trends in continuous variables (*e.g.* SST), and Poisson generalized linear models (GLMs; Gelman & Hill, 2006) to assess trends in counts of discrete events during some period of time (*e.g.* spawning thermal niche classes, MHW/MCS n_{events} and n_{days}). We performed standard residual checks and tests to assess model adequacy. In some cases, it was necessary to account for overdispersion using quasi-Poisson GLMs (Gelman & Hill, 2006).

To examine the overall change in the population indices extracted for each selected species within their respective time frames, we computed linear regression analyses on R, SSB, and PRSI and the arithmetic mean of PGR. We applied a logarithmic transformation on the SSB and R biomass data to stabilize variance.

PRSI variability and environmental forcing

We implemented both linear regression and GAM models to assess the effect of Bakun Index, Upwelling Index, turbulence, SST and MHW/MCS features on the PRSI of each of the selected fish species. Linear models provide a simple, first-order approach to assessing the effect of environmental covariates, while GAM models bring flexibility to accommodate potentially nonlinear responses.

Survival variability mostly arises from environmental conditions acting on early life stages; however, regulation through mechanisms dependent on population density can also play a role (Houde, 2008). Here, we follow the Ricker spawner-recruit model and assume PRSI to be

negatively correlated to SSB through a linear function (compensatory population dynamics, Minto et al., 2008). The resulting model takes the form:

$$PRSI = \beta_0 + \beta_1 SSB + \beta_2 X$$

where X represents the environmental variable of choice. To facilitate a direct comparison of the coefficient magnitudes, we standardized the regression inputs by dividing them by two standard deviations, following the recommendations in Gelman (2008). Note that the models cover different time periods depending on the length of the available datasets for each species (Table 4.1).

The models were computed to assess both Bay-wide and shelf-specific effects, considering the entire and peak spawning periods for each species to capture the full spectrum of environmental variability while focusing on the most critical periods for reproductive success.

4.3. Results

Long-term trend analyses on environmental variables unveiled a statistically significant rise in SST on the continental shelf of the Bay of Biscay, with an average warming rate of 0.27ºC per decade that was evident on an annual basis and during the spawning months of each species (Table 4.2; Fig. 4.2). Visualizing the decadal average maps for SST highlights the escalating trend (Fig. 4.A.2). No discernible trends were identified for the Bakun Index, Upwelling Index and turbulence, neither annually nor within the specific spawning seasons of each species.

The incidence and key features of MHWs and MCSs within 1982-2022 exhibited distinct and opposing patterns. First, there was a significant increase in the average annual count of MHWs and in the average number of MHW days per year (n_{events} and $n_{days,}$ ~58% and ~79% per decade, respectively); contrarily, an annual decrease in both variables was acknowledged for MCS (~-41% and ~-46% per decade, respectively) (Table 4.2; Fig. 4.3). Statistical significance for MHW and MCS n_{events} and n_{days} extended beyond an annual basis, persisting during the spawning seasons of all four species. To ease the interpretation of these contrasting trends, we displayed MHW and MCS n_{days} on a decadal scale through a map (Figs. 4.A.3 and 4.A.4) and on a parallel coordinates plot (Fig. 4.A.5). Second, the diverging pattern between MHW and MCS persisted when examining their key features. An annual increase was observed for MHWs i_{cum} (4.16ºC days per decade) and D (2.43 days per decade) as well as an annual weakening in MCS i_{cum} (2.77ºC days per decade) and D (-1.83 days per decade). These contrasting trends remained significant during the spawning seasons of all species. Consistent trends in MHW i_{max} and/or i_{mean} were observed during the spawning seasons of all species, though not annually; the same features displayed no significance for MCSs.

Analyses on the occurrence of optimal and non-optimal spawning SSTs for each species during their respective spawning seasons revealed an increasing frequency of SSTs exceeding their spawning thermal niche, as well as a decrease in SSTs falling below it (Table 4.3, Fig. 4.4). All species exhibited consistent trends. First, only mackerel demonstrated statistical significance in the occurrence of SSTs matching its spawning thermal niche - showing a declining trend over time. Second, a significant rise in the frequency of extremely hot SSTs (≥3ºC over niche) was observed for all species; consistent increases in the occurrence of hot (≤1.5ºC over niche) and very hot SSTs (1.5-3ºC over niche) were only acknowledged for sardine. Third, the frequency of

Table 4.2. Linear trends in environmental variables over the period 1982-2022 in the continental shelf of the Bay of Biscay. The tested variables include Bakun Index (BI), Upwelling Index (UI), wind turbulence (*turb*), sea surface temperature (SST), as well as marine heatwave and marine cold-spell total count of events (n_{events}) and event days (n_{days}) per year, average duration (D) and maximum, mean and cumulative intensity (i_{max}, i_{mean}, i_{cum}). Trends were estimated both for annually integrated metrics and for averages and counts taken over the spawning season of each species. The slope, standard error (SE) and proportion of variance explained (R^2) are shown for each variable. Significant effects (p-value < 0.05) are highlighted in bold. Variables displaying significant effects on all time spans are further highlighted in gray. Note that marine cold-spell i_{max}, i_{mean} and i_{cum} take negative values.

	Non-extreme				Marine heatwaves						Marine cold-spells					
Variable	BI	UI	*turb*	SST	n_{events}	n_{days}	i_{max}	i_{mean}	i_{cum}	D	n_{events}	n_{days}	i_{max}	i_{mean}	i_{cum}	D
Units decade^{-1}	10^3 m^3 s^{-1} km^{-1}	10^3 m^3 s^{-1} km^{-1}	m^3 s^{-3}	ºC	%	%	ºC	ºC	ºC days	Days	%	%	ºC	ºC	ºC days	Days
Annual (Jan-Dec)																
Slope	0.01	0.00	3.06	**0.27**	**57.65**	**78.87**	0.05	0.01	**4.16**	**2.44**	**-40.66**	**-46.09**	-0.01	-0.02	**2.77**	**-1.83**
SE	0.02	0.01	5.77	**0.03**	**10.48**	**13.80**	0.04	0.02	**1.22**	**0.66**	**10.70**	**11.06**	0.03	0.02	**0.94**	**0.49**
R^2	0.01	0.00	0.01	**0.61**	**0.45**	**0.38**	0.06	0.01	**0.24**	**0.27**	**0.56**	**0.46**	0.00	0.04	**0.19**	**0.27**
Anchovy & horse mackerel (Mar-Aug)																
Slope	0.03	0.01	0.47	**0.29**	**60.06**	**82.39**	**0.13**	**0.05**	**5.25**	**2.81**	**-38.69**	**-45.49**	0.04	0.00	**3.97**	**-2.28**
SE	0.02	0.01	5.88	**0.05**	**13.71**	**15.96**	**0.04**	**0.02**	**1.50**	**0.76**	**13.36**	**14.32**	0.04	0.02	**1.08**	**0.58**
R^2	0.07	0.03	0.00	**0.50**	**0.39**	**0.39**	**0.19**	**0.11**	**0.25**	**0.27**	**0.41**	**0.35**	0.03	0.00	**0.27**	**0.29**
Mackerel (Mar-Jul)																
Slope	0.03	0.01	-1.59	**0.30**	**60.46**	**83.71**	**0.14**	**0.06**	**5.54**	**2.92**	**-39.00**	**-44.72**	0.07	0.02	**3.74**	**-2.07**
SE	0.02	0.01	6.13	**0.05**	**15.25**	**17.66**	**0.05**	**0.03**	**1.70**	**0.86**	**14.59**	**15.24**	0.04	0.02	**1.34**	**0.72**
R^2	0.05	0.01	0.00	**0.52**	**0.35**	**0.36**	**0.17**	**0.11**	**0.23**	**0.24**	**0.40**	**0.34**	0.10	0.02	**0.18**	**0.19**
Sardine (Apr-Jun/Oct-Dec)																
Slope	0.02	0.00	0.99	**0.33**	**85.18**	**117.28**	**0.11**	0.04	**5.35**	**2.95**	**-41.90**	**-46.01**	0.02	-0.01	**2.99**	**-1.83**
SE	0.03	0.02	11.26	**0.04**	**15.50**	**17.78**	**0.05**	0.02	**1.54**	**0.82**	**15.36**	**15.67**	0.05	0.02	**1.28**	**0.64**
R^2	0.01	0.00	0.00	**0.59**	**0.46**	**0.40**	**0.15**	0.08	**0.25**	**0.26**	**0.46**	**0.34**	0.00	0.00	**0.13**	**0.18**

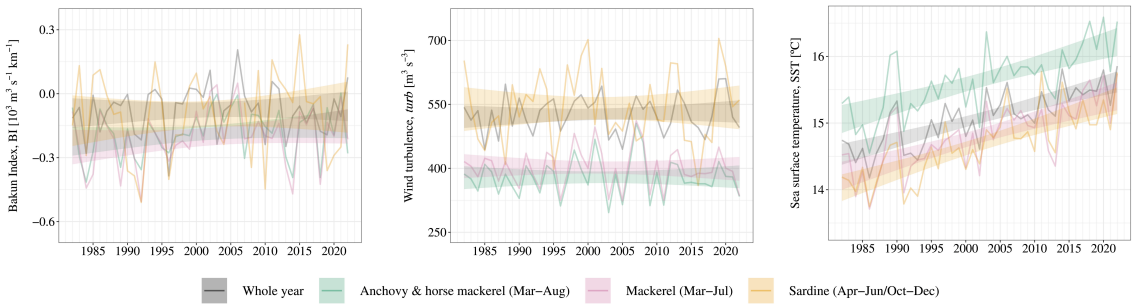

Figure 4.2. Average Bakun Index (BI), wind turbulence (*turb*) and sea surface temperature (SST) in the continental shelf of the Bay of Biscay within 1982-2022. Series represent annual estimates (grey) and seasonal estimates for the specific spawning seasons of different species (green, pink, orange). Shaded areas account for 95% confidence intervals of the estimated linear trends in each case.

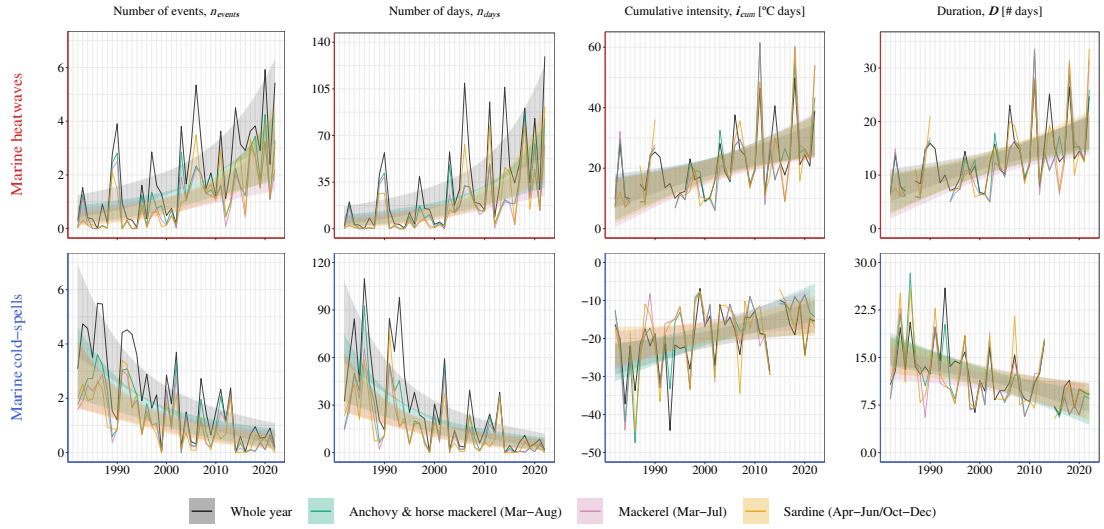

Figure 4.3. Annually averaged key metrics of marine heatwaves (top row) and marine cold-spells (bottom row) detected over the continental shelf of the Bay of Biscay over the period 1982-2022. Features with consistent trends on an annual basis are shown (see Table 4.2). The attributes and structure of this figure mirror those of Figure 4.2.

very cold (1.5-3ºC below niche) and extremely cold SSTs (≥3ºC below niche) showed consistent decreases for all species except mackerel; significant declines in the occurrence of cold SSTs (≤1.5ºC below niche) were only observed for mackerel and sardine. Figures 4.A.6-9 in the Appendix show decadal average maps of the frequency of SSTs within and below the spawning thermal niche of each species.

Different scenarios emerged for the populations of anchovy, mackerel, horse mackerel and sardine. First, there were significant and positive correlations between i) R and SSB for anchovy and mackerel and ii) PRSI and PGR for all species except sardine (Table 4.4). Second, long-term trend analyses revealed increases in R and SSB for anchovy and mackerel, yet these did not map

Table 4.3. Output summary of Poisson regression models analyzing long-term trends in the occurrence of sea surface temperatures falling within, above or below the spawning thermal niches of European anchovy, Atlantic mackerel, Atlantic horse mackerel and European sardine during their respective spawning seasons within 1982-2022 in the continental shelf of the Bay of Biscay. The slope and standard error (% decade^{-1}) are shown along with the proportion of variance explained (R^2, in between brackets). Significant trends (p-value < 0.05) are highlighted in bold.

	Extremely hot (≥3ºC over niche)	Very hot (1.5–3ºC over niche)	Hot (≤1.5ºC over niche)	Within niche	Cold (≤1.5ºC below niche)	Very cold (1.5–3ºC below niche)	Extremely cold (≥3ºC below niche)
Anchovy	**33.01 ± 3.96 (0.31)**	4.47 ± 3.06 (0.11)	1.45 ± 2.75 (0.01)	0.69 ± 1.8 (0.00)	3.85 ± 2.53 (0.03)	**-7.66 ± 2.28 (0.24)**	**-24.75 ± 4.03 (0.27)**
Mackerel	**20.60 ± 3.15 (0.34)**	2.61 ± 3.27 (0.03)	0.84 ± 3.10 (0.00)	**-3.79 ± 1.34 (0.29)**	**-33.14 ± 18.90 (0.10)**	-24.75 ± 201.99 (0.01)	0 (0)
H. mackerel	**18.73 ± 2.74 (0.30)**	1.97 ± 2.82 (0.03)	-0.03 ± 2.72 (0.00)	2.22 ± 1.79 (0.02)	-2.61 ± 2.22 (0.03)	**-18.55 ± 3.17 (0.32)**	**-31.64 ± 8.37 (0.18)**
Sardine	**67.32 ± 11.73 (0.30)**	**44.20 ± 5.08 (0.47)**	**18.04 ± 3.02 (0.46)**	1.97 ± 1.28 (0.05)	**-13.88 ± 2.21 (0.39)**	**-32.56 ± 4.90 (0.44)**	**-38.83 ± 21.13 (0.10)**

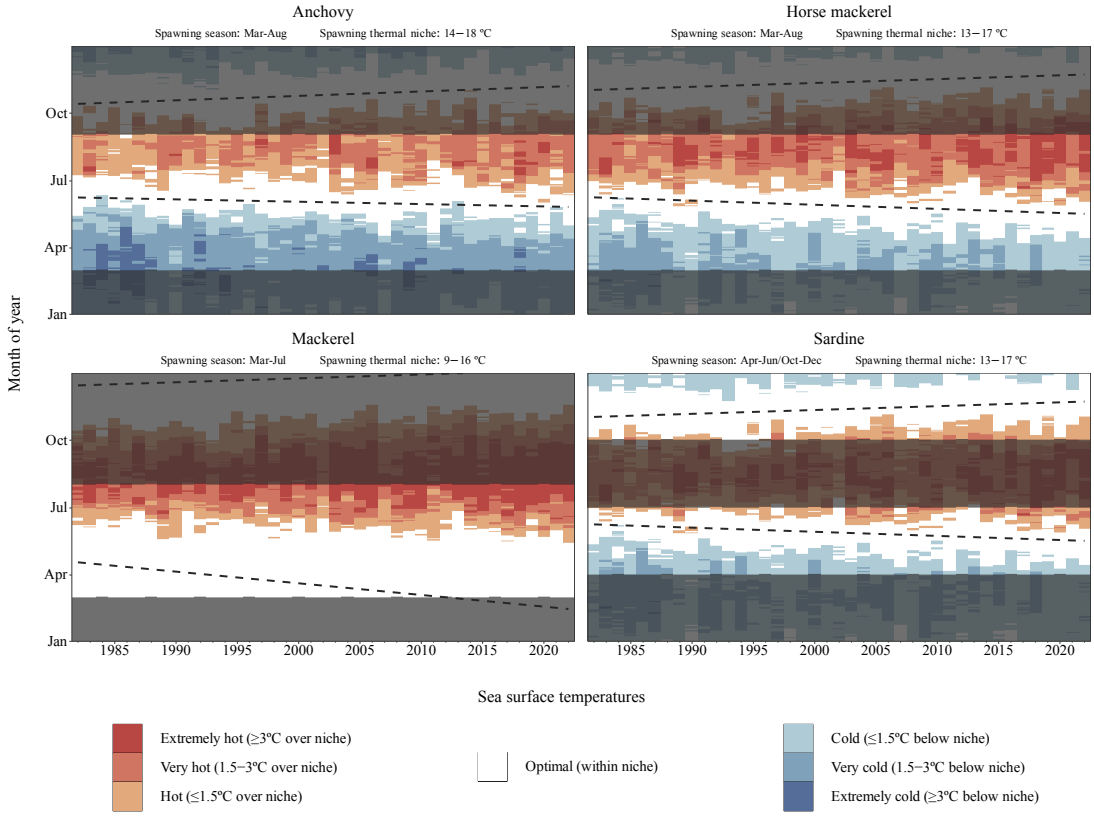

Figure 4.4. Hovmöller diagram depicting average daily sea surface temperatures in the continental shelf of the Bay of Biscay within 1982-2022, classified based on their proximity to the spawning thermal niche of each species. The shading highlights the spawning season of each species. Dashed lines indicate the progression of the estimated times of the year when temperatures approach the median of each species' spawning thermal niche. Note that this representation of averaged temperatures may obscure existing trends presented in Table 4.3.

Table 4.4. Pearson correlation coefficients of i) log-transformed recruitment and spawning stock biomass (R~SSB) and ii) pre-recruitment survival index and population growth rate (PRSI~PGR) for each examined species. Bold font is used to denote statistical significance (p-value < 0.05).

	Anchovy	Mackerel	Horse mackerel	Sardine
R~SSB	**0.39**	**0.35**	0.29	-0.31
PRSI~PGR	**0.95**	**0.66**	**0.49**	0.40

Table 4.5. Changes in the population indices extracted for European anchovy, Atlantic mackerel, Atlantic horse mackerel and European sardine in the Bay of Biscay within their respective time frames. Columns 1-3: outputs obtained from the linear regression models analyzing long-term trends in age-1 recruits (R), spawning stock biomass (SSB) and pre-recruitment survival index (PRSI). The slope and standard error (% decade^{-1}) are shown along with the proportion of variance explained (R^2, in between brackets), and significant trends (p-value < 0.05) are highlighted in bold. Column 4: arithmetic mean and standard error (% decade^{-1}) of population growth rate (PGR).

	Age-1 recruits (R)	Spawning Stock Biomass (SSB)	Pre-recruitment Survival Index (PRSI)	Population Growth Rate (PGR)
Anchovy (1987-2022)	23.89 ± 14.03 (0.07)	**38.48 ± 9.69 (0.27)**	-10.53 ± 13.51 (0.02)	52.14 ± 128.49
Mackerel (1980-2022)	**14.30 ± 3.52 (0.27)**	**9.79 ± 4.00 (0.12)**	4.10 ± 4.58 (0.02)	-0.82 ± 16.75
Horse mackerel (1982-2021)	**-19.18 ± 9.66 (0.13)**	**-44.32 ± 3.67 (0.88)**	**45.17 ± 9.49 (0.31)**	-28.27 ± 20.10
Sardine (2002-2020)	21.01 ± 18.58 (0.07)	**-38.53 ± 5.13 (0.85)**	**96.85 ± 20.85 (0.43)**	-31.22 ± 44.78

into positive PRSI trends, which instead remained almost constant (Fig. 4.5, Table 4.5). Conversely, while horse mackerel and sardine displayed contrasting patterns in R and overall negative trends in SSB, they both showed significant increases in PRSI. Lastly, average PGR estimates indicate the progressive increase to record abundance levels in anchovy, the decline of horse mackerel and sardine, but almost no change in mackerel, which is now slightly below 1980 abundance levels following the expansion and huge increase during the 2000s.

Linear regression and GAM models consistently identified the same environmental effects on the PRSI for anchovy, mackerel and horse mackerel, with only slight differences in the magnitude of the R^2 values. No environmental variable had a significant impact on sardine survival. Below, we discuss the results of the linear regression analyses (Table 4.6), reserving the output of GAM models to Table 4.A.2 in the Appendix.

Anchovy survival was linked to averaged conditions over its entire spawning period for upwelling (negatively in the Armorican shelf, positively in the Cantabrian shelf) and turbulence (negatively both on regional [Bay of Biscay] and shelf scales [Aquitanian shelf]). Mackerel appeared to benefit from warmer SSTs across most shelves and even from MHW incidence in the Armorican shelf; upwelling also exerted a positive effect on a regional scale. Finally, horse mackerel survival

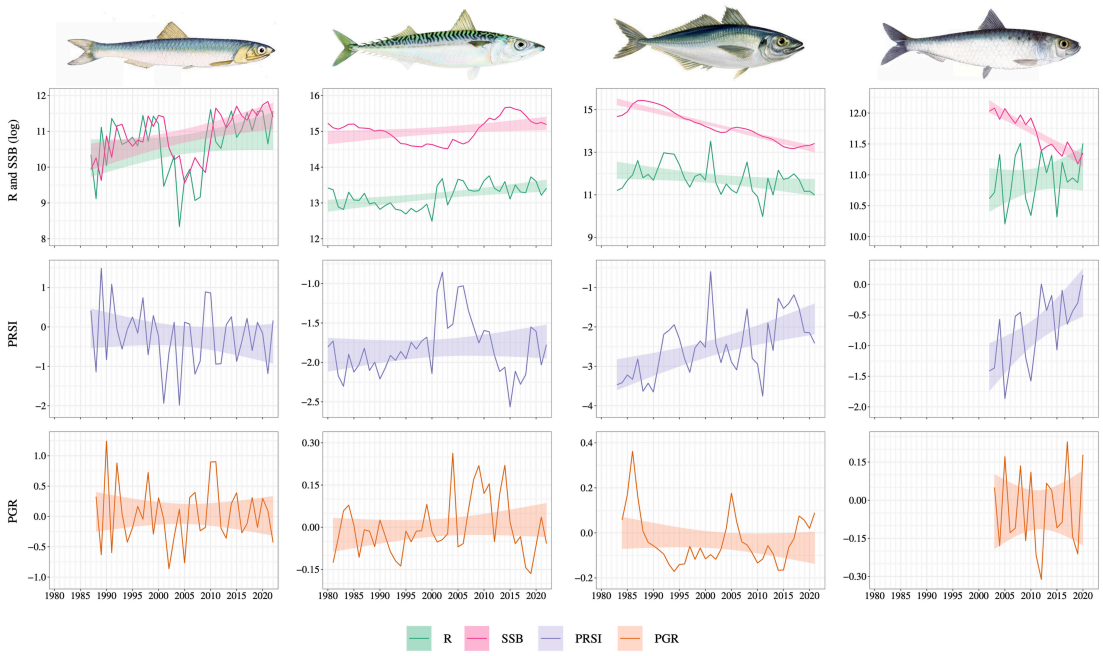

Figure 4.5. Evolution of log-transformed age-1 recruits and spawning stock biomass (R and SSB, respectively), pre-recruitment survival index (PRSI) and population growth rate (PGR) of -left to right- European anchovy, Atlantic mackerel, Atlantic horse mackerel and European sardine. Shaded areas account for 95% confidence intervals of the estimated linear trends in each case.

responded to upwelling (negatively in the Cantabrian shelf, positively in the Armorican shelf), turbulence (positively across all regions except the Cantabrian shelf) and MHW key features (negatively across most shelves [i_{max}, i_{mean}], if not all [i_{cum}, D]).

On the other hand, models considering only the peak spawning period revealed that negative association between anchovy survival and MCS i_{max} (all shelves) and i_{mean} (Cantabrian and Aquitanian). The effect of warmer temperatures continued to favor mackerel survival across the three shelves, as well as MHW incidence and maximum intensity; contrarily, MCS incidence hampered mackerel survival in the marginal shelves. Turbulence was also a significant negative influence on mackerel survival in the Cantabrian and Aquitanian shelves. Lastly, an overall negative effect of MCS mean intensity on horse mackerel survival was observed on a regional scale, but not on individual shelves.

Table 4.6. Output summary of the linear regression models testing the impact of environmental variables on the pre-recruitment survival index (PRSI) for European anchovy, Atlantic mackerel, Atlantic horse mackerel and European sardine during both their full and peak spawning periods. Variables tested include Bakun Index (BI), Upwelling Index (UI), wind turbulence (*turb*), sea surface temperature (SST) and key metrics of marine heatwaves (MHW) and cold-spells (MCS): number of events (n_{events}), event days (n_{days}), average duration (D), and intensity measures (i_{max}, i_{mean}, i_{cum}). Only statistically significant variables ($p < 0.05$) are shown, along with their region of influence: Bay of Biscay (BoB) or the Cantabrian (Cant), Aquitanian (Aquit), and Armorican (Arm) shelves. The slope, standard error (SE) and proportion of variance explained (R^2) are shown. For variables significant in more than one region with the same slope direction (positive/negative), only the strongest effect is presented. No significant trends were found for sardine. Full results are available in Tables 4.A.3-10 in the Appendix.

Species	Environmental variable	Region(s)	Slope ± SE	R^2
FULL SPAWNING PERIOD				
Anchovy	BI	Arm	-0.71 ± 0.23	0.32
	UI	Cant (+)	0.52 ± 0.24	0.23
		Arm (-)	-0.73 ± 0.22	0.34
	turb	BoB, Arm	-0.59 ± 0.24	0.26
Mackerel	UI	BoB	0.21 ± 0.09	0.41
	SST	BoB, Cant, Arm	0.21 ± 0.10	0.41
	MHW n_{events}	Arm	0.23 ± 0.10	0.42
Horse mackerel	BI	Cant (-)	-0.55 ± 0.19	0.45
		Arm (+)	0.48 ± 0.19	0.42
	UI	Cant	-0.54 ± 0.19	0.45
	turb	BoB, Aquit	0.59 ± 0.18	0.48
	MHW i_{max}	BoB, Aquit,	-0.67 ± 0.22	0.49
	MHW i_{mean}	BoB, Aquit,	-0.61 ± 0.21	0.48
	MHW i_{cum}	BoB, Cant, Aquit, Arm	-0.63 ± 0.21	0.47
	MHW D	BoB, Cant, Aquit, Arm	-0.62 ± 0.22	0.47
PEAK SPAWNING PERIOD				
Anchovy	MCS i_{max}	BoB, Cant, Aquit, Arm	-0.97 ± 0.34	0.32
	MCS i_{mean}	Cant, Aquit	-0.89 ± 0.35	0.28
Mackerel	*turb*	BoB, Cant, Aquit	-0.24 ± 0.09	0.43
	SST	BoB, Cant, Aquit, Arm	0.30 ± 0.09	0.49
	MHW n_{events}	BoB, Cant, Aquit, Arm	0.22 ± 0.10	0.41
	MHW n_{days}	BoB, Aquit, Arm	0.21 ± 0.10	0.41
	MHW i_{max}	Cant	0.32 ± 0.12	0.88
	MCS n_{events}	BoB, Cant, Arm	-0.27 ± 0.09	0.46
	MCS n_{days}	Cant	-0.22 ± 0.09	0.42
Horse mackerel	MCS i_{mean}	BoB	0.52 ± 0.22	0.36

4.4. Discussion

Our findings in the Bay of Biscay align with global warming trends and demonstrate an increase in sea surface temperatures and marine heatwave frequency and duration, as well as a decline in marine cold-spell occurrence and key features. We also found that divergent trends in the abundance of anchovy, sardine, mackerel and horse mackerel map to distinctive effects of environmental variables on their early life survival.

4.4.1. Long-term trends

Environmental variables

Analyses of long-term trends in environmental variables in the Bay of Biscay provide insights into the changing ocean dynamics across the continental shelf throughout the last decades.

Our results show no consistent trends in wind-driven upwelling and turbulence on the continental shelf of the Bay of Biscay. Alongshore upwelling is a complex process influenced by several factors, including wind patterns and ocean currents, which vary significantly from year to year (Simpson & Sharples, 2012). In the Bay of Biscay, wind-driven upwelling is highly seasonal (May-September), consisting of small-scale, short-lived events (Lavín et al., 2006). Similarly, wind turbulence is shaped by a fluctuating interplay of meteorological, oceanographic and topographic conditions (Simpson & Sharples, 2012). These variations may mask any underlying long-term trends, making it difficult to identify statistically significant changes in these wind-induced processes over time.

Warming rates across the Bay of Biscay continental shelf (~0.27ºC per decade for surface waters) align with trends reported in recent studies (~0.25ºC per decade; Costoya et al., 2015; Chust et al., 2022). Large-scale shifts in SST are identified as the primary driver behind MHWs and MCSs (Frölicher et al., 2018; Schlegel et al., 2021), with human-induced global warming increasing the likelihood of longer and more intense MHWs while reducing the frequency and severity of MCSs (Yao et al., 2022). Regional studies in the Bay of Biscay support these global trends, showing rising MHWs and declining MCS events in terms of frequency, intensity and duration (Izquierdo et al., 2022b; Simon et al., 2023). In the North Atlantic, MHWs are more frequent and intense during warmer months (Thoral et al., 2022), while MCSs primarily occur in winter, as rising temperatures decrease the likelihood of cold extremes (Schlegel et al., 2021). In the Bay of Biscay, these patterns are possibly enhanced by the prolonged warm season, which has reportedly increased the frequency of extreme hot SST days in spring and autumn (Costoya et al., 2015) and directly compromises local marine life.

Marine fish are often adapted to narrow thermal niches (Fry, 1971) and actively seek water temperatures that optimize their physiological performance while avoiding thermal stress (Calosi et al., 2008). Extreme temperature events can have more immediate and severe impacts on marine fish than long-term ocean warming, as they can quickly push SSTs beyond physiological tolerance thresholds critical for performance (Sanz-Lázaro, 2016; Dahlke et al., 2020). Importantly, the increasing(decreasing) frequency of extremely hot(cold) temperatures [over 3ºC above(below) spawning thermal niche] observed in this study suggests that the spawning environment in the Bay of Biscay is becoming less suitable for the fish species examined. For mackerel, progressive warming is already reducing the number of days with optimal SSTs for spawning, contributing to their northward population shift (Chust et al., 2023). As MHWs are projected to increase in frequency and intensity under future warming scenarios (Yao et al., 2022; Simon et al., 2023), temperature-driven shifts in fish distribution and phenology in the Bay of Biscay are becoming more likely (Asch et al., 2019; Jacox et al., 2020).

Spawning location and timing are critical for marine fish, as it is the primary strategy to ensure offspring survival from the egg to juvenile stage and their subsequent dispersal across diverse habitats, while minimizing predator exposure and maximizing access to food resources (Ciannelli et al., 2015). The pelagic species in this study, which provide no parental care, rely on selecting favorable spawning habitats to achieve reproductive success (Sargent & Gross, 1985), a choice increasingly compromised by persistent ocean warming and increasingly frequent MHWs. For example, a prolonged MHW in the Gulf of Alaska (2014-2016) reduced the thermal suitability of Pacific cod spawning grounds, resulting in low recruitment, reduced population biomass and the eventual closure of the fishery in 2020 (Laurel & Rogers, 2020). The degradation or loss of spawning habitats undermines their ability to support key life processes, ultimately affecting fish population viability and health (Chust et al., 2023).

Population indices

Our analyses reveal two main scenarios regarding the correlations between R~SSB and PRSI~PGR. The first scenario involves anchovy and mackerel, which show significant positive correlations, with R~SSB ranging from 0.3-0.4 and PRSI~PGR from 0.6-0.95. As expected in short lived species, recruitment contributes most variability in adult abundance, which consequently results in PRSI strongly influencing population growth – especially in the case of anchovy, where age-1 recruits make most of the population size (ICES, 2023a). The second scenario involves horse mackerel, the species with the longest lifespan, in which R and SSB seem unrelated and the correlation between PRSI and PGR is weak, and sardine, the species with the shortest time series, which shows no significant correlations. Unaccounted factors such as adult survival or depensatory effects may exert a stronger influence on the variability of the adult population and overall population growth in these species.

Anchovy populations in the Bay of Biscay have rebounded to record abundance levels following the collapse of 2005-10 (ICES, 2023a). The absence of a significant trend in anchovy R may relate to the recently reported decline in their size, which may have led to a decoupling between R biomass and the actual number of recruits (Böens et al 2023; ICES, 2023a; Taboada et al., 2024). On the other hand, the ability of mackerel to migrate and adapt to environmental changes has contributed to its poleward expansion and increased abundance along the Atlantic European margin (Trenkel et al., 2014; Chust et al., 2023). Although their abundance fell to levels seen in the 1980s between 2015 and 2020, recent agreements on mackerel quotas among most Coastal States (Northeast Atlantic Fisheries Commission) seem to have mitigated this decline (European Commission, 2023).

The observed declines in the SSB of horse mackerel and sardine are likely influenced by increased fishing mortality over the past decade (ICES 2023a, 2023b). At low population sizes, compensation mechanisms -the prevalent form of regulation in marine fish populations- are triggered to increase survival and maintain stability (Frank & Brickman, 2000). Generally, compensation works as follows: with reduced adult abundance, increased availability of food and habitat enhances growth and condition, which results in increased productivity through higher fecundity and improved recruitment, hence promoting survival (Nash et al., 2009). While both species show consistent increases in PRSI, trends in R differ. On the one hand, sardine parallels anchovy with a declining body length and weight over recent decades (Véron et al., 2020), which may be influencing trends in SSB and potentially masking an increase in recruit numbers – although they do not seem to be contributing to the adult population. On the other hand, horse mackerel increased PRSI likely emerges as a consequence of SSB decreasing at a faster pace than R, since the latter has not attained recovery beyond the 1982- and 2002-year classes (De Oliveira et al., 2010).

Marine fish have a strong inherent capacity to recover from low population sizes through compensation, making them highly resilient. However, evidence of collapsed populations failing to do so points at other mechanisms operating in these scenarios (Maroto & Moran, 2014). Contrary to compensation, depensation reduces survival at low population sizes through mechanisms like difficulty in finding mates, increased prey vulnerability, ongoing exploitation, decreased foraging efficiency or genetic drift (Liermann & Hilborn, 2001; Berec et al., 2007). Both horse mackerel and sardine populations have persistently remained below their respective precautionary reference points in recent years (ICES, 2023a, 2023b). Although their PRSIs are on the rise, identifying trends that may lead to population collapse is crucial for developing effective management and conservation strategies aimed at population recovery and long-term sustainability.

4.4.2. PRSI variability and environmental forcing

A key factor influencing the trajectory of fish stocks is their ability to survive early life stages and reach reproductive age. Survival is primarily determined by a combination of factors that operate from the early stages of eggs to juvenile development (Houde, 2016). These factors encompass mechanisms that are sensitive to population density fluctuations, such as competition among juveniles (density-dependent regulation), and mechanisms that impact populations regardless of their size, such as food availability, predation and environmental forcing (density-independent regulation), being the latter mechanism the most influential (Houde, 2008).

Wind-related processes, such as alongshore upwelling and turbulence, can either support or impede early life survival by affecting the distribution of eggs and larvae and food availability (MacKenzie, 2000). These processes are relatively localized, exhibiting intensities and impacts that vary across the Bay of Biscay as a response to the distinct wind patterns that generate them in each shelf (Lavín et al., 2006).

Alongshore upwelling was a significant source of variability in the early life survival of anchovy, mackerel and horse mackerel – though only when considering their respective full spawning seasons. This makes sense, as coastal upwelling off the Bay of Biscay typically begins in late spring and reaches its pinnacle during summer, outside of the peak spawning seasons for these species (Lavín et al., 2006). At optimal levels, it can boost early life survival through increased productivity and food availability, though enhanced offshore transport through stronger winds might increase egg and larval mortality (Wheeler et al., 2017). In the case of the anchovy, our findings align with literature: upwelling-favorable winds support survival in southern Bay of Biscay through enhanced primary production (Motos et al., 1996; Allain et al., 2007; Borja et al., 2008) but hamper over the Armorican shelf through detrimental seaward larval drift during summer months (Taboada & Anadón, 2015). However, alternative appeals (Irigoien et al., 2007) call for further research to clarify the anchovy recruitment process in the Bay. As for mackerel, significance of upwelling effects was observed only on a broad scale, likely due to the uniformity of upwelling conditions when averaged across the Bay – an observation supported by prior research suggesting that upwelling has minimal impact on mackerel recruitment variability in the Bay of Biscay (Borja et al., 2002). The peak spawning of mackerel in April occurs before coastal upwelling begins in late May (Lavín et al., 2006), which results in a calm environment that supports early larval development without significant offshore transport (Borja et al., 2002). Lastly, the contrasting responses of horse mackerel to upwelling may stem from their egg and larval distribution over the shelf break (Ibaibarriaga et al., 2007). On the one hand, upwelling in the Cantabrian shelf might lead to egg and larval drift towards less favorable conditions in the open sea due to its narrowness. On the other hand, upwelling in the Armorican shelf may reduce the extent of the *'cold pool*', a cold water mass that holds temperatures close to the lower thermal

threshold of horse mackerel (Pipe & Walker, 1987; Puillat et al., 2004), thus favoring early survival by raising temperatures and enhancing nutrient availability. However, further research is required to fully understand these mechanisms.

Turbulence mostly acts modulating encounter rates between predatory larvae and zooplankton prey, enhancing or hampering effective feeding (MacKenzie, 2000). Both anchovy and horse mackerel are sensitive to turbulence throughout their entire spawning seasons but not during their peak in May-June, when milder summer conditions may not generate the same intensity of water movement. The negative impact of turbulence on anchovy survival in the Armorican shelf may be linked to reduced food availability for larvae due to strong tidal currents (Puillat et al., 2004; Borja et al., 2008). Although we found no prior studies addressing the positive influence of turbulence on horse mackerel early life stages in the Bay of Biscay, it may be associated with increased dispersal to favorable areas and enhanced nutrient mixing (MacKenzie, 2000). Contrarily to these two species, mackerel survival is negatively affected by turbulence only in their peak spawning month, April. Borja et al. (2002) also found that turbulence does not impact mackerel survival throughout their spawning season, but they noted that strong turbulence in April—when spring transitions and interannual weather variability are pronounced—can significantly affect recruitment, which may explain our findings.

Temperature plays a fundamental role in shaping the ecological performance and survival of marine fishes by triggering physiological processes that are crucial for metabolism and development, especially for spawners and early life stages (Seibel & Drazen, 2007; Dahlke et al., 2020). Rising SSTs and increased MHW frequency and duration in the Bay of Biscay depict a changing scenario to which fish populations will respond according to their respective dynamics and life strategies. Here, we find that extreme temperature events, both MHWs and MCSs, primarily impact the early life survival of anchovy, mackerel and horse mackerel in their peak spawning periods.

According to Motos et al. (1996), anchovy reduce their spawning activity when the SST warming rate declines, and it ceases altogether when it becomes neutral or negative – which can explain the negative impact MCS intensity observed across all regions during their peak spawning season. As for mackerel and horse mackerel, temperature strongly influences spawning phenology, embryo development, and larval growth (Pipe & Walker, 1987; Abaunza et al., 2003; Mendiola et al., 2007; Rodríguez-Basalo et al., 2022). Despite their comparable spawning thermal ranges (Table 4.1), we acknowledge contrasting effects of temperature (either as SSTs or MHWs) on their survival. During their peak spawning period in April, mackerel seems to benefit from warmer SSTs and MHWs in all continental shelves; however, in the Aquitanian shelf, which experiences higher temperatures (Costoya et al., 2015; Izquierdo et al., 2022b), this effect fades when considering the full spawning season. This can be explained by considering that in April,

when conditions are cooler, MHWs may rise SSTs to optimal levels for mackerel spawning – but by early summer they may push SSTs beyond their niche, which possibly cancels their positive effect for the full spawning season in this shelf. Also in April, MCS incidence negatively affects mackerel survival in the Cantabrian and Armorican shelves but not in the Aquitanian shelf, where warmer conditions are likely to buffer their impact. As for horse mackerel, almost all MHW key features are detrimental on survival during their full spawning season across all shelves, especially in the Aquitanian, but not when they reach peak activity in May and June. This overall negative effect throughout the full season may arise from summer months, when MHWs are more frequent and intense (Thoral et al., 2022), but during early summer their influence might not be as relevant since horse mackerel has a relatively warm thermal range (13-17ºC). Importantly, the positive effect of MCS on horse mackerel survival for the entire Bay highlights a regional benefit that may not translate to specific shelves due to variations in local conditions. These findings, along with the increased occurrence of extremely hot SSTs (Fig. 4.4, Table 4.3), raises the risk of ocean temperatures exceeding critical metabolic, growth and reproductive thresholds that may compromise the survival of these fish populations (Jørgensen et al., 2022).

The absence of significant effects of environmental forcing on sardine early life survival may be attributed to factors such as its split spawning season, which occurs at two different times of the year, or the limited length of its data series (<20 years). Nevertheless, these observations highlight important areas where our approach could be refined by addressing several key considerations. On the one hand, while early life forms are the most vulnerable to environmental fluctuations, juveniles also represent an important stage where these changes can significantly impact survival, hence potentially contributing to overall variability in population dynamics. On the other hand, several aspects could be obscuring the observed effects of environmental forcing on survival. Complex interactions between environmental variables may mask joint influences - although addressing this would require longer time series or mechanistic models to avoid overfitting and bias. Factors beyond the scope of this study could also be playing a part. For example, the timing of the spring bloom of phytoplankton determines food availability during the critical period of larval development (Platt et al., 2003; Taboada & Anadón, 2015), modes of climate variability can prompt the occurrence of warmer temperatures and marine heatwaves (Holbrook et al., 2019; Izquierdo et al., 2022a) and fishing pressure can deplete adult abundance and lead to diminished recruitment (Houde, 2008). Lastly, while our model includes a linear effect with SSB to address its negative correlation with PRSI (as per the Ricker spawner-recruit model), it does not fully capture the complexity of density-dependent mechanisms, which may affect survival beyond environmental forces. While we acknowledge the limitations of our approach, this study provides reasonable evidence of environmental processes affecting the early life survival of anchovy, mackerel and horse mackerel in the Bay of Biscay. Our findings provide a valuable foundation

for understanding species-specific responses to the environment, reinforcing the importance of continued research to build on these insights.

Future projections point at different scenarios for anchovy, mackerel, horse mackerel and sardine fisheries in the Bay of Biscay under global warming. Rising ocean temperatures are inducing favorable feeding and spawning conditions in higher latitudes, which is leading to an earlier spawning of horse mackerel, as well as a poleward expansion of anchovy and mackerel (Chust et al., 2023; Petitgas et al., 2012; Erauskin-Extramiana et al., 2019). This expansion towards previously unoccupied areas suggests the latter species may be establishing in new habitats and undergoing significant changes in recruitment dynamics, which highlights the importance of examining the influence of environmental forcing in other parts of their distribution. Although these shifts could imply the potential emergence of new fishery opportunities, they may also decrease the likelihood of these species occurring in southern latitudes, as it has been predicted for anchovy for all regions located under 48ºN (Raybaud et al., 2017), thus affecting the Bay of Biscay. As for sardine, forecasts under different ocean warming scenarios point towards an ongoing decrease in SSB, irrespective of fishing pressure (Torralba & Besada, 2015).

Altogether, our observations align with the former predictions and hint at potential changes in small pelagic fisheries in the Bay of Biscay, particularly in a context of global climate change. Global warming is reshaping ocean dynamics around the world, and the upcoming increase in MHW frequency and severity worldwide is expected to contribute to amplified impacts on fisheries and fish populations. Understanding how fish populations respond to shifts in ocean conditions remains a persistent challenge that, in the current context of global climate change, leads to increased uncertainty on the sustained viability of marine food webs and the local fisheries that rely on them. This study aims to shed light on fluctuating fish populations amidst a changing ocean and calls for a continuous and vigilant management to secure their robust and sustainable development over the long term.

Appendix

4.A. Supporting figures and tables

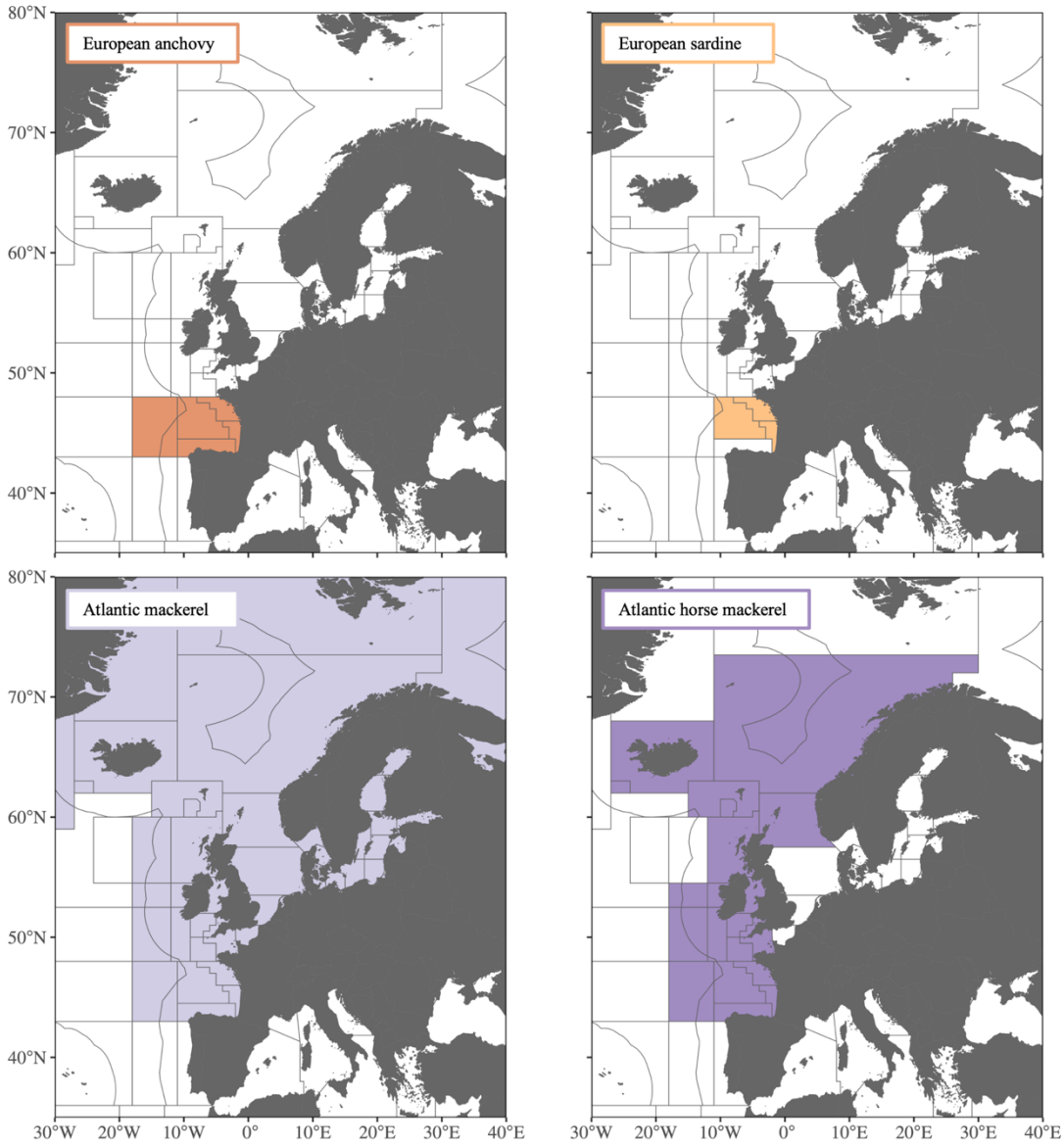

Figure 4.A.1. FAO Major Fishing Area 27 (Northeast Atlantic). Each map highlights the geographical coverage of the FAO subareas encompassing the ICES stocks selected for each individual species: European anchovy (top left; stock *ane.27.8*), Atlantic mackerel (bottom left; stock *mac.27.nea*), Atlantic horse mackerel (bottom right; stock *hom.27.2a4a5b6a7a-ce-k8*) and European sardine (top right; stock *pil.27.8abd*). See https://www.fao.org/fishery/en/area/27/en for further information on the subareas within the FAO Major Fishing Area 27.

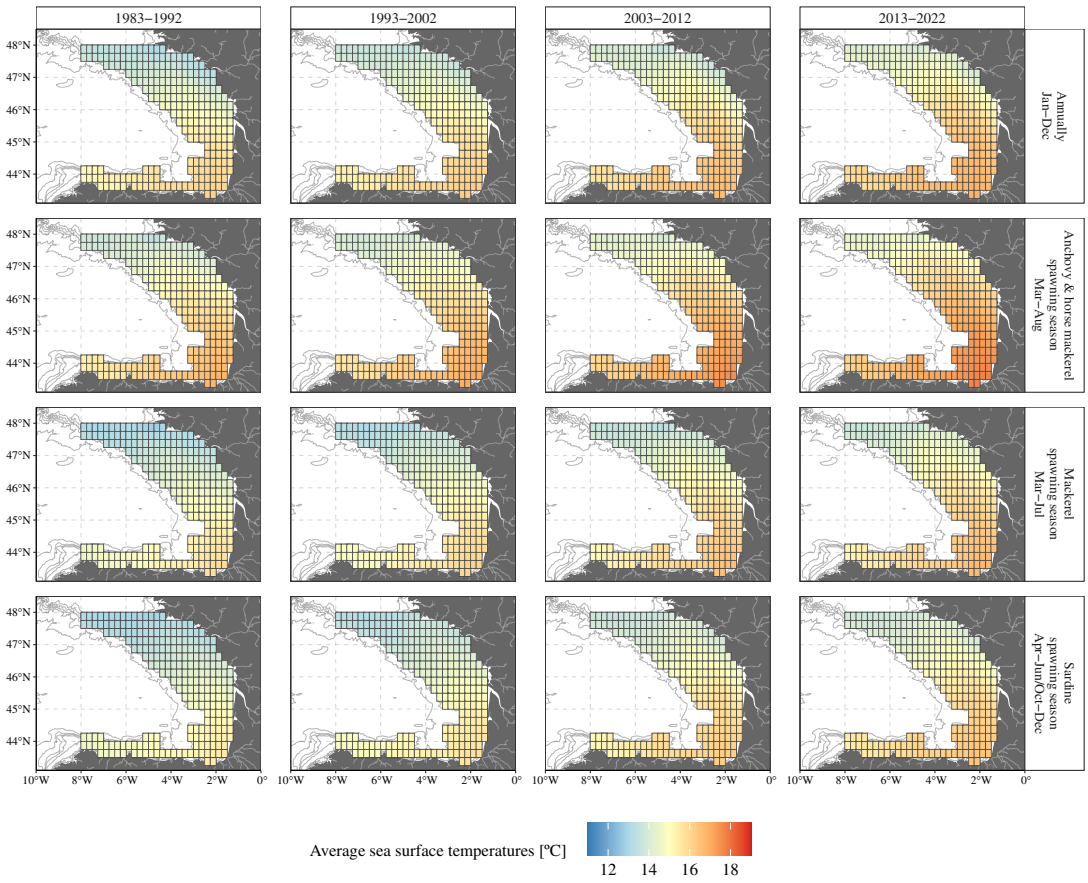

Figure 4.A.2. Average sea surface temperatures per decade along the continental shelf of the Bay of Biscay within 1983-2022. Each grid represents a 0.25º pixel (n = 240). Sea surface temperatures were averaged for entire years (1st row) as well as for the specific spawning seasons of different species (2nd, 3rd and 4th rows).

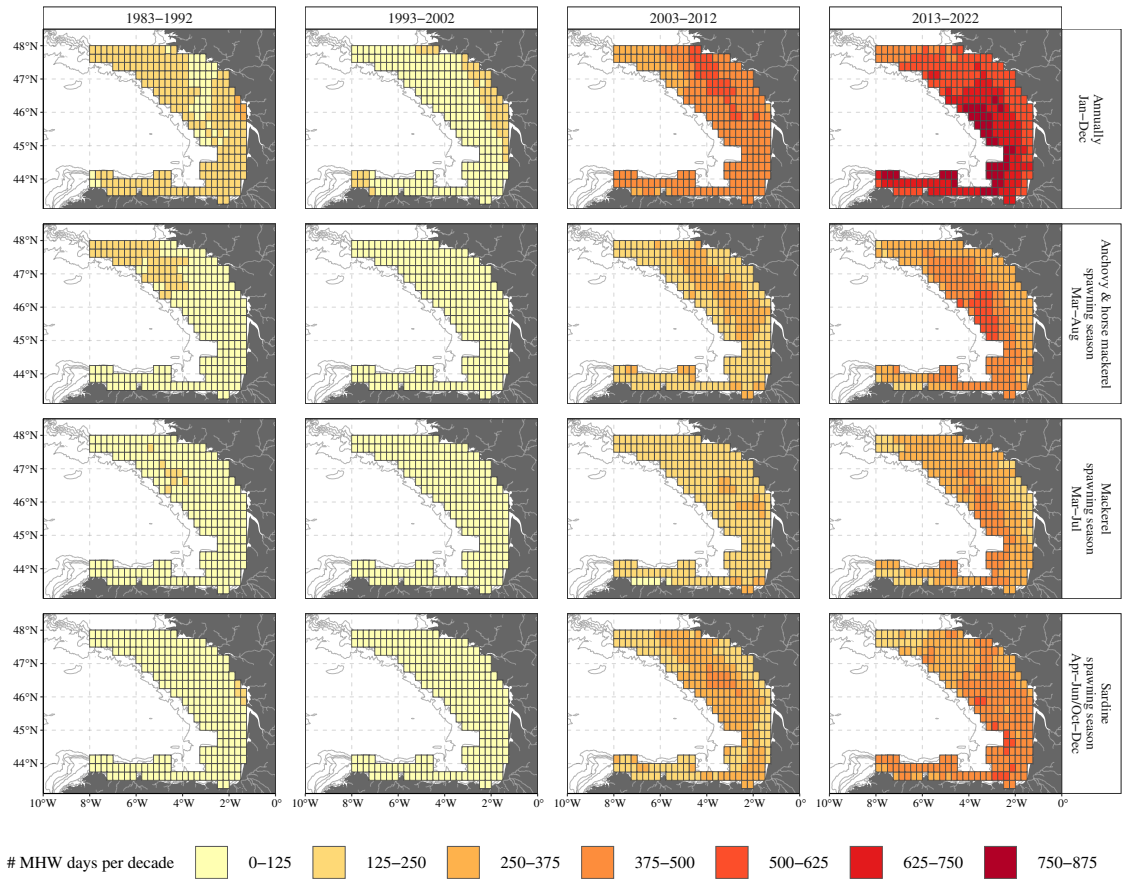

Figure 4.A.3. Average decadal number of marine heatwave (MHW) days detected along the continental shelf of the Bay of Biscay within 1983-2022. Each grid represents a 0.25º pixel (n = 240). The number of MHW days were averaged for entire years (1st row) as well as for the specific spawning seasons of different species (2nd, 3rd and 4th rows).

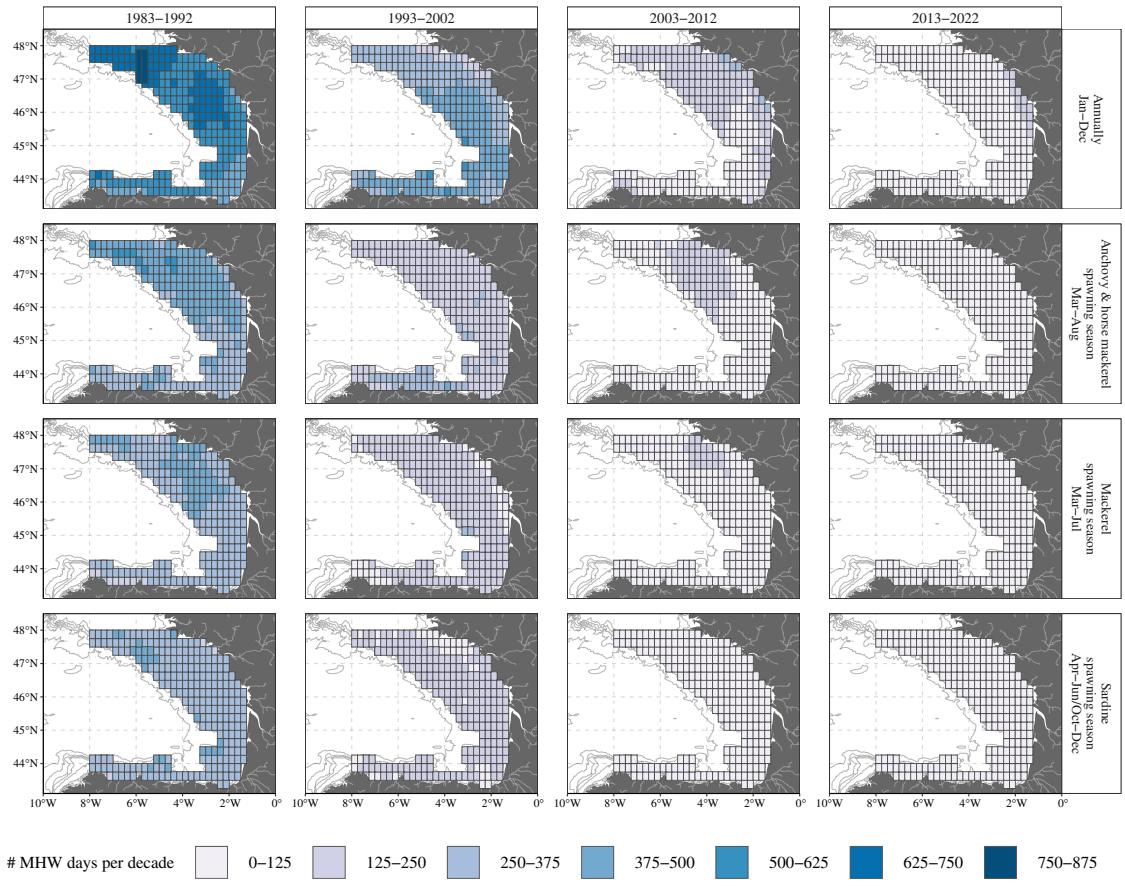

Figure 4.A.4. Average decadal number of marine cold-spell (MCS) days detected along the continental shelf of the Bay of Biscay within 1983-2022. Each grid represents a 0.25º pixel (n = 240). The number of MCS days were averaged for entire years (1st row) as well as for the specific spawning seasons of different species (2nd, 3rd and 4th rows).

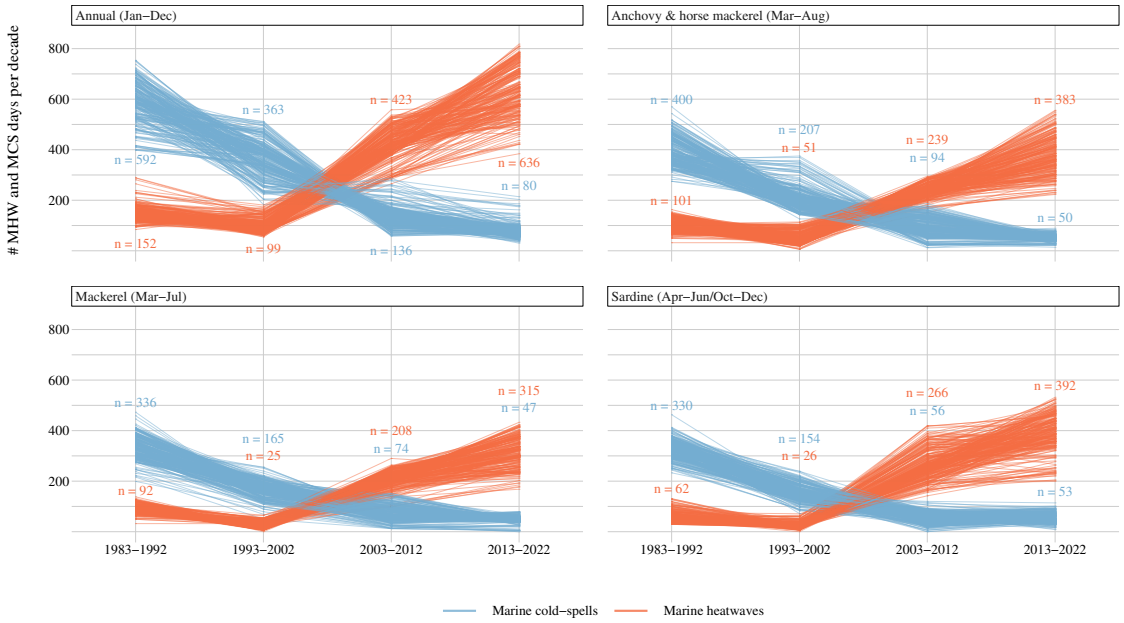

Figure 4.A.5. Progression of the number of marine heatwave (MHW) and marine cold-spell (MCS) days per decade detected along the continental shelf of the Bay of Biscay within 1983-2022. The number of MHW and MCS days were averaged for entire years (top left) as well as for the specific spawning seasons of different species (rest of the plots). Each line -for each color- corresponds to one of the 240 pixels examined. Numeric values indicate the average number of MHW and MCS days, respectively, for the entire Bay.

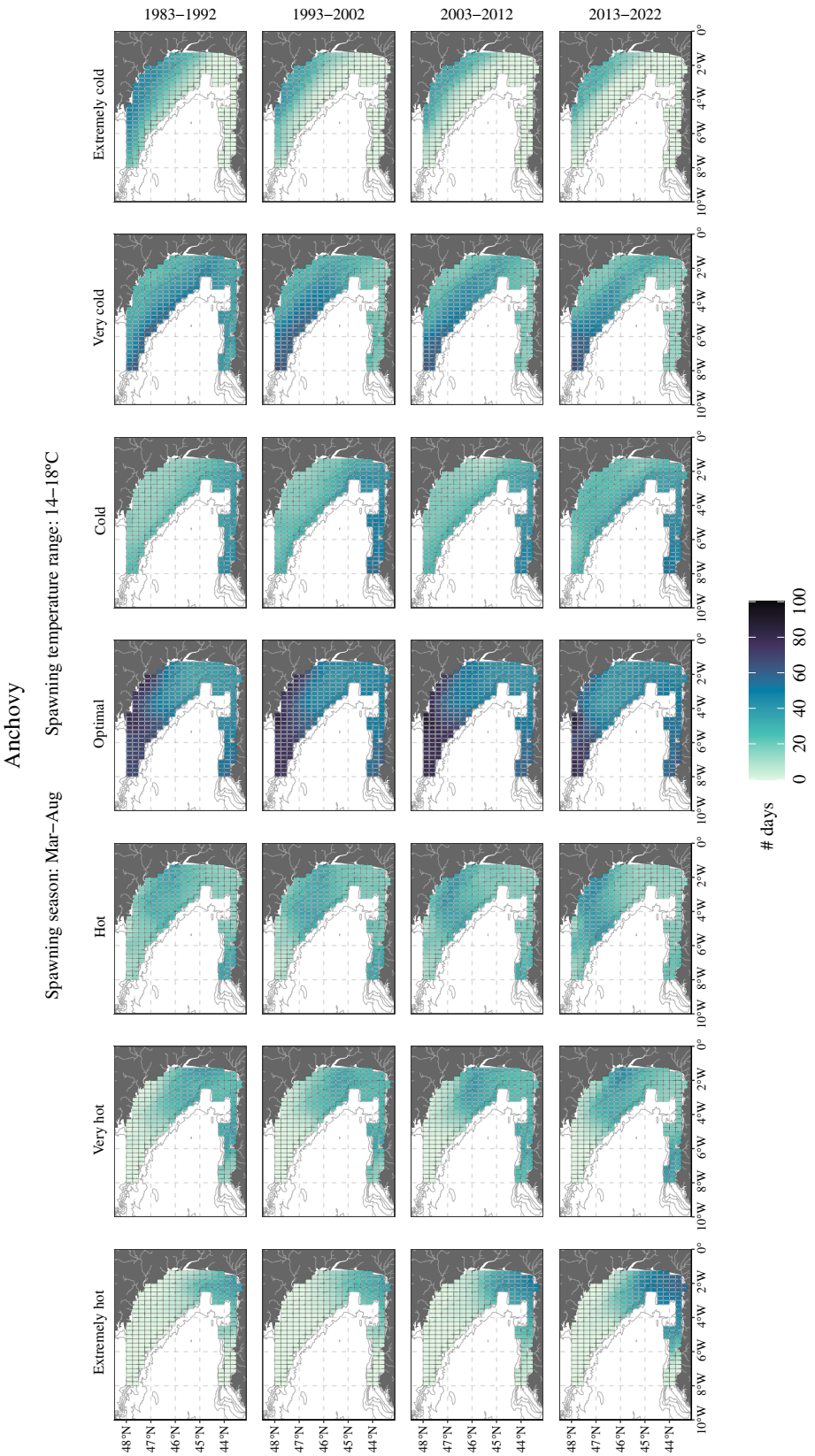

Figure 4.A.6. Decadal trends in the occurrence of optimal and non-optimal sea surface temperatures in the continental shelf of the Bay of Biscay within 1983-2022, categorized according to their proximity to the spawning thermal niche of the European anchovy.

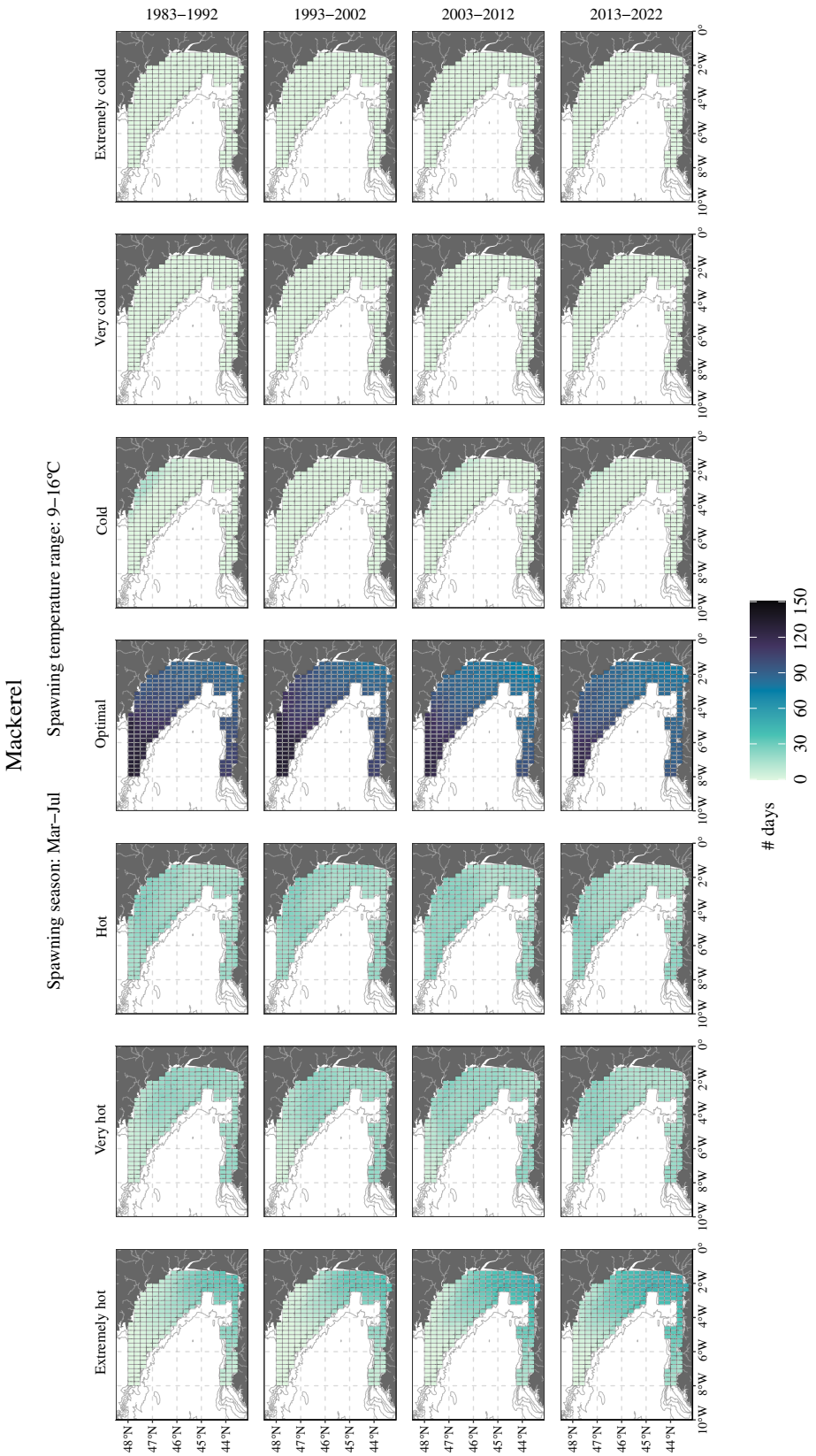

Figure 4.A.7. Decadal trends in the occurrence of optimal and non-optimal sea surface temperatures in the continental shelf of the Bay of Biscay within 1983-2022, categorized according to their proximity to the spawning thermal niche of the Atlantic mackerel.

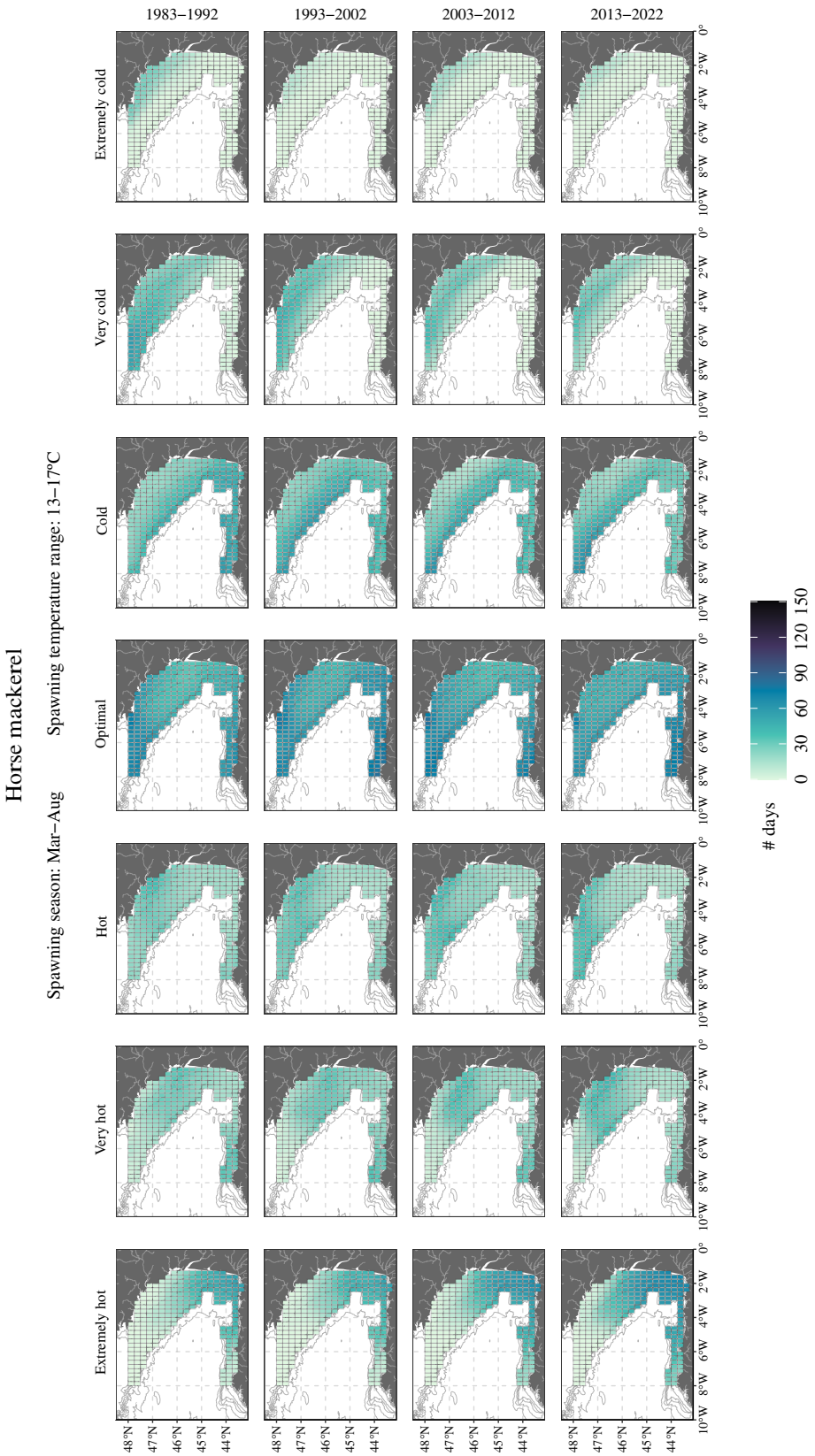

Figure 4.A.8. Decadal trends in the occurrence of optimal and non-optimal sea surface temperatures in the continental shelf of the Bay of Biscay within 1983-2022, categorized according to their proximity to the spawning thermal niche of the Atlantic horse mackerel.

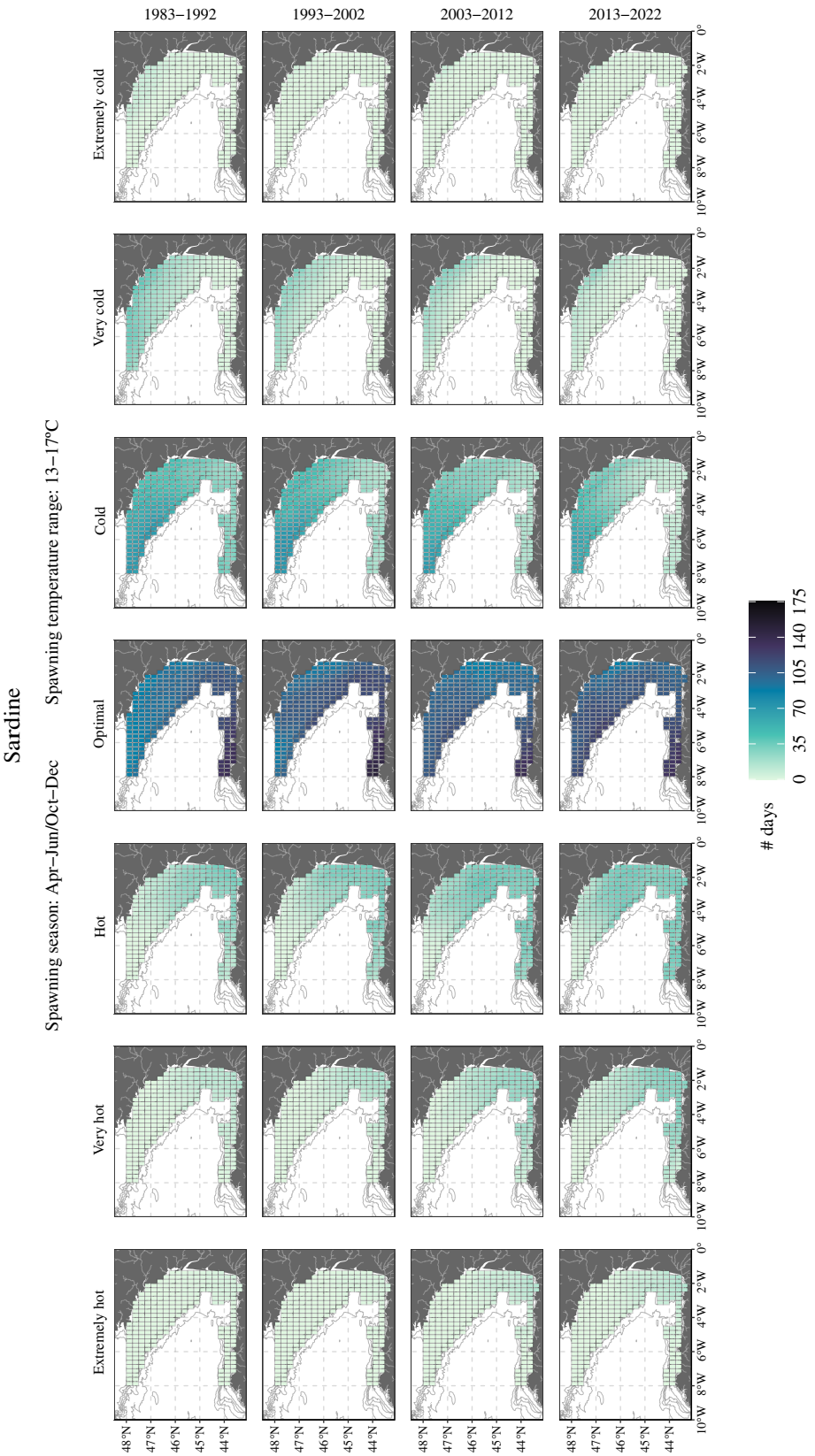

Figure 4.A.9. Decadal trends in the occurrence of optimal and non-optimal sea surface temperatures in the continental shelf of the Bay of Biscay within 1983-2022, categorized according to their proximity to the spawning thermal niche of the European sardine.

Table 4.A.1. Categorization of sea surface temperatures based on their proximity to the respective spawning thermal niches of European anchovy, Atlantic mackerel, Atlantic horse mackerel, and European sardine.

Sea surface temperature conditions	**Category**
Over 3ºC over niche	Extremely hot
From 1.5 to 3ºC over niche	Very hot
Up to 1.5ºC over niche	Hot
Within niche	Optimal
Up to 1.5ºC below niche	Cold
From 1.5 to 3ºC below niche	Very cold
Over 3ºC below niche	Extremely cold

Table 4.A.2. Output summary of the GAM model testing the impact of environmental variables on the pre-recruitment survival index (PRSI) for European anchovy, Atlantic mackerel, Atlantic horse mackerel and European sardine during both their full and peak spawning periods. Variables tested include Bakun Index (BI), Upwelling Index (UI), wind turbulence (*turb*), sea surface temperature (SST) and key metrics of marine heatwaves (MHW) and cold-spells (MCS): number of events (n_{events}), event days (n_{days}), average duration (D), and intensity measures (i_{max}, i_{mean}, i_{cum}). Only statistically significant variables ($p < 0.05$) are shown, along with their region of influence: Bay of Biscay (BoB) or the Cantabrian (Cant), Aquitanian (Aquit), and Armorican (Arm) shelves. The slope, standard error (SE) and proportion of variance explained (R^2) are shown. For variables significant in more than one region with the same slope direction (positive/negative), only the strongest effect is presented. No significant trends were found for sardine.

Species	Environmental variable	Region(s)	Slope ± SE	R^2
FULL SPAWNING PERIOD				
Anchovy	BI	Arm	-1.28 ± 0.39	0.30
	UI	Cant (+)	0.76 ± 0.35	0.18
		Arm (-)	-1.81 ± 0.55	0.29
	turb	BoB, Arm	-0.01 ± 0.00	0.17
Mackerel	UI	BoB	1.13 ± 0.50	0.38
	SST	BoB, Cant, Arm	0.22 ± 0.10	0.38
	MHW n_{events}	Arm	0.12 ± 0.05	0.39
Horse mackerel	BI	Cant (-)	-0.33 ± 0.11	0.42
		Arm (+)	0.82 ± 0.34	0.39
	UI	Cant	-0.77 ± 0.27	0.42
	turb	BoB, Aquit	0.01 ± 0.00	0.39
	MHW i_{max}	BoB, Aquit,	-0.86 ± 0.28	0.46
	MHW i_{mean}	BoB, Aquit,	-1.83 ± 0.62	0.44
	MHW i_{cum}	BoB, Cant, Aquit, Arm	-0.03 ± 0.01	0.44
	MHW D	BoB, Cant, Aquit, Arm	-0.06 ± 0.02	0.41
PEAK SPAWNING PERIOD				
Anchovy	MCS i_{max}	BoB, Cant, Aquit, Arm	-1.74 ± 0.62	0.66
	MCS i_{mean}	Cant, Aquit	-3.28 ± 1.30	0.64
Mackerel	*turb*	BoB, Cant, Aquit	0.00 ± 0.00	0.43
	SST	BoB, Cant, Aquit, Arm	0.28 ± 0.08	0.49
	MHW n_{events}	BoB, Cant, Aquit, Arm	0.01 ± 0.01	0.41
	MHW n_{days}	BoB, Aquit, Arm	0.21 ± 0.10	0.04
	MHW i_{max}	Cant	0.56 ± 0.21	0.98
	MCS n_{events}	BoB, Cant, Arm	-0.42 ± 0.14	0.46
	MCS n_{days}	Cant	-0.02 ± 0.01	0.42
Horse mackerel	MCS i_{mean}	BoB	1.51 ± 0.64	0.53

Table 4.A.3. Output summary of the linear regression models testing the influence of environmental variables on the pre-recruitment survival index (PRSI) of the European anchovy (*Engraulis encrasicolus*) during its full spawning season. The model follows the formula PRSI = $\beta_0 + \beta_1 SSB + \beta_2 X$, where SSB stands for spawning stock biomass and X represents the variable of choice. The model was computed for the entire Bay of Biscay, as well as for each of the three continental shelves: Cantabrian, Aquitanian and Armorican. The tested variables include Bakun Index (BI), Upwelling Index (UI), wind turbulence (*turb*) and sea surface temperature (SST), as well as marine heatwave (MHW) and marine cold-spell (MCS) total count of events (n_{events}) and event days (n_{days}) per year, average duration (D) and maximum, mean and cumulative intensity (i_{max}, i_{mean}, i_{cum}). Note that the three latter take negative values. The slope, standard error (SE), p-value and proportion of variance explained (R^2) are shown. Significant effects (p-value < 0.05) are highlighted in bold.

EUROPEAN ANCHOVY – FULL SPAWNING SEASON

	Non-extreme				Marine heatwaves						Marine cold-spells					
	BI	UI	*turb*	SST	n_{events}	n_{days}	i_{max}	i_{mean}	i_{cum}	D	n_{events}	n_{days}	i_{max}	i_{mean}	i_{cum}	D
Bay of Biscay																
Slope	-0.31	-0.45	**-0.51**	0.23	0.26	0.2	0.03	-0.14	0.02	0.08	-0.26	-0.11	-0.15	-0.17	-0.06	-0.01
SE	0.25	0.25	**0.24**	0.26	0.26	0.26	0.27	0.26	0.27	0.27	0.26	0.26	0.27	0.27	0.28	0.28
p-value	0.22	0.08	**0.04**	0.40	0.31	0.45	0.91	0.60	0.93	0.76	0.32	0.66	0.57	0.54	0.82	0.97
R^2	0.16	0.20	**0.22**	0.14	0.15	0.13	0.10	0.11	0.10	0.10	0.14	0.12	0.13	0.14	0.13	0.12
Cantabrian shelf																
Slope	0.42	**0.52**	-0.01	0.16	0.24	0.19	-0.11	-0.11	0.02	0.06	0.01	0.04	-0.43	-0.50	-0.28	0.23
SE	0.25	**0.24**	0.26	0.26	0.26	0.26	0.28	0.28	0.28	0.28	0.26	0.26	0.30	0.30	0.30	0.31
p-value	0.10	**0.04**	0.96	0.54	0.36	0.48	0.71	0.69	0.94	0.83	0.97	0.87	0.16	0.11	0.36	0.47
R^2	0.19	**0.23**	0.12	0.13	0.14	0.13	0.11	0.12	0.11	0.11	0.12	0.12	0.16	0.18	0.12	0.11
Aquitanian shelf																
Slope	-0.18	-0.11	-0.39	0.21	0.27	0.17	0.11	0.04	0.01	0.03	-0.23	-0.01	-0.49	-0.53	-0.31	0.22
SE	0.27	0.26	0.25	0.26	0.25	0.26	0.27	0.27	0.29	0.29	0.26	0.26	0.27	0.27	0.29	0.29
p-value	0.50	0.70	0.13	0.42	0.29	0.52	0.70	0.87	0.98	0.91	0.39	0.96	0.09	0.06	0.29	0.45
R^2	0.13	0.12	0.18	0.13	0.15	0.13	0.13	0.13	0.13	0.13	0.14	0.12	0.19	0.21	0.13	0.12
Armorican shelf																
Slope	**-0.71**	**-0.73**	**-0.59**	0.25	0.26	0.22	-0.06	-0.27	-0.01	0.07	-0.35	-0.24	0.04	0.03	0.28	-0.28
SE	**0.23**	**0.22**	**0.24**	0.26	0.25	0.26	0.27	0.26	0.27	0.27	0.25	0.26	0.28	0.28	0.28	0.28
p-value	**0.00**	**0.00**	**0.02**	0.34	0.32	0.39	0.82	0.31	0.97	0.79	0.18	0.35	0.89	0.92	0.33	0.33
R^2	**0.32**	**0.34**	**0.26**	0.14	0.14	0.14	0.10	0.13	0.10	0.10	0.17	0.14	0.14	0.14	0.16	0.16

Table 4.A.4. Output summary of the linear regression model testing the influence of environmental variables on the pre-recruitment survival index (PRSI) of the Atlantic mackerel (*Scomber scombrus*) during its full spawning season. Structure and attributes as in Table 4.A.3.

ATLANTIC MACKEREL – FULL SPAWNING SEASON

	Non-extreme				Marine heatwaves						Marine cold-spells					
	BI	UI	*turb*	SST	n_{events}	n_{days}	i_{max}	i_{mean}	i_{cum}	*D*	n_{events}	n_{days}	i_{max}	i_{mean}	i_{cum}	*D*
Bay of Biscay																
Slope	0.13	**0.21**	0.07	**0.20**	0.19	0.17	0.06	0.00	0.13	0.15	-0.16	-0.10	0.06	-0.03	0.05	-0.06
SE	0.10	**0.09**	0.10	**0.10**	0.10	0.10	0.11	0.11	0.11	0.11	0.10	0.10	0.11	0.11	0.11	0.11
p-value	0.19	**0.03**	0.51	**0.04**	0.06	0.10	0.56	0.97	0.23	0.18	0.11	0.30	0.62	0.78	0.65	0.56
R^2	0.36	**0.41**	0.34	**0.40**	0.39	0.38	0.36	0.35	0.38	0.38	0.38	0.35	0.32	0.32	0.32	0.33
Cantabrian shelf																
Slope	0.04	0.05	-0.01	**0.21**	0.15	0.17	0.10	0.05	0.17	0.15	-0.16	-0.08	0.17	0.16	0.06	-0.05
SE	0.10	0.10	0.10	**0.10**	0.10	0.10	0.13	0.13	0.12	0.13	0.10	0.10	0.12	0.12	0.12	0.12
p-value	0.71	0.61	0.92	**0.03**	0.14	0.10	0.43	0.68	0.19	0.23	0.11	0.41	0.17	0.19	0.63	0.68
R^2	0.33	0.34	0.33	**0.41**	0.37	0.38	0.39	0.38	0.41	0.40	0.38	0.34	0.26	0.26	0.22	0.21
Aquitanian shelf																
Slope	-0.07	0.04	-0.03	0.19	0.15	0.13	0.07	0.01	0.09	0.09	-0.14	-0.08	0.07	-0.02	0.06	-0.07
SE	0.10	0.10	0.10	0.10	0.10	0.10	0.11	0.11	0.11	0.11	0.10	0.10	0.12	0.13	0.12	0.12
p-value	0.50	0.67	0.77	0.06	0.14	0.20	0.55	0.94	0.44	0.44	0.17	0.43	0.56	0.88	0.62	0.55
R^2	0.34	0.33	0.33	0.39	0.37	0.36	0.38	0.38	0.39	0.39	0.36	0.34	0.31	0.31	0.31	0.31
Armorican shelf																
Slope	0.10	0.16	0.12	**0.21**	**0.23**	0.19	-0.02	-0.07	0.10	0.13	-0.16	-0.12	0.02	-0.08	0.04	-0.06
SE	0.10	0.10	0.10	**0.10**	**0.10**	0.10	0.11	0.11	0.11	0.11	0.10	0.10	0.12	0.11	0.11	0.11
p-value	0.32	0.11	0.23	**0.04**	**0.02**	0.07	0.89	0.52	0.36	0.23	0.10	0.22	0.87	0.52	0.73	0.58
R^2	0.35	0.37	0.36	**0.41**	**0.42**	0.39	0.34	0.35	0.36	0.37	0.38	0.36	0.31	0.32	0.31	0.32

Table 4.A.5. Output summary of the linear regression model testing the influence of environmental variables on the pre-recruitment survival index (PRSI) of the Atlantic horse mackerel (*Trachurus trachurus*) during its full spawning season. Structure and attributes as in Table 4.A.3.

ATLANTIC HORSE MACKEREL – FULL SPAWNING SEASON

	Non-extreme				Marine heatwaves						Marine cold-spells					
	BI	UI	*turb*	SST	n_{events}	n_{days}	i_{max}	i_{mean}	i_{cum}	*D*	n_{events}	n_{days}	i_{max}	i_{mean}	i_{cum}	*D*
Bay of Biscay																
Slope	-0.15	-0.03	**0.48**	-0.07	-0.28	-0.38	**-0.54**	**-0.44**	**-0.63**	**-0.62**	-0.08	-0.13	0.24	0.30	0.33	-0.27
SE	0.22	0.22	**0.19**	0.27	0.24	0.23	**0.22**	**0.21**	**0.21**	**0.22**	0.27	0.26	0.21	0.21	0.24	0.25
p-value	0.51	0.91	**0.02**	0.80	0.24	0.11	**0.02**	**0.04**	**0.01**	**0.01**	0.76	0.62	0.27	0.16	0.18	0.28
R^2	0.33	0.32	**0.43**	0.33	0.35	0.37	**0.44**	**0.41**	**0.47**	**0.47**	0.33	0.33	0.34	0.35	0.35	0.34
Cantabrian shelf																
Slope	**-0.55**	**-0.54**	0.33	-0.20	-0.30	-0.40	-0.24	-0.16	**-0.60**	**-0.60**	0.03	0.08	0.18	0.22	0.06	-0.02
SE	**0.19**	**0.19**	0.20	0.26	0.24	0.22	0.24	0.24	**0.22**	**0.22**	0.26	0.24	0.24	0.24	0.26	0.26
p-value	**0.01**	**0.01**	0.10	0.46	0.22	0.08	0.33	0.52	**0.01**	**0.01**	0.92	0.73	0.45	0.35	0.82	0.93
R^2	**0.45**	**0.45**	0.37	0.33	0.35	0.38	0.33	0.31	**0.45**	**0.45**	0.32	0.33	0.28	0.29	0.27	0.27
Aquitanian shelf																
Slope	0.05	0.01	**0.59**	-0.07	-0.25	-0.37	**-0.67**	**-0.61**	**-0.60**	**-0.55**	0.00	-0.12	0.25	0.37	0.32	-0.25
SE	0.21	0.21	**0.18**	0.26	0.23	0.23	**0.22**	**0.21**	**0.23**	**0.23**	0.27	0.25	0.23	0.22	0.24	0.25
p-value	0.79	0.94	**0.00**	0.80	0.28	0.11	**0.00**	**0.01**	**0.01**	**0.02**	0.99	0.65	0.28	0.11	0.20	0.33
R^2	0.33	0.32	**0.48**	0.33	0.35	0.37	**0.49**	**0.48**	**0.46**	**0.43**	0.32	0.33	0.32	0.35	0.33	0.31
Armorican shelf																
Slope	**0.48**	0.34	0.40	-0.02	-0.28	-0.34	-0.40	-0.34	**-0.53**	**-0.54**	-0.16	-0.20	0.32	0.22	0.38	-0.34
SE	**0.19**	0.20	0.20	0.26	0.23	0.23	0.22	0.22	**0.22**	**0.22**	0.25	0.25	0.22	0.22	0.24	0.25
p-value	**0.02**	0.12	0.05	0.95	0.24	0.14	0.08	0.13	**0.02**	**0.02**	0.53	0.43	0.16	0.32	0.13	0.18
R^2	**0.42**	0.37	0.39	0.32	0.35	0.36	0.38	0.37	**0.42**	**0.43**	0.33	0.34	0.35	0.33	0.36	0.35

Table 4.A.6. Output summary of the linear regression model testing the influence of environmental variables on the pre-recruitment survival index (PRSI) of the European sardine (*Sardina pilchardus*) during its full spawning season. Structure and attributes as in Table 4.A.3.

EUROPEAN SARDINE – FULL SPAWNING SEASON

	Non-extreme				Marine heatwaves						Marine cold-spells					
	BI	UI	*turb*	SST	n_{events}	n_{days}	i_{max}	i_{mean}	i_{cum}	*D*	n_{events}	n_{days}	i_{max}	i_{mean}	i_{cum}	*D*
Bay of Biscay																
Slope	-0.22	-0.22	-0.03	-0.03	-0.14	-0.09	0.13	0.15	0.06	0.02	0.12	0.10	-0.08	0.00	-0.25	0.24
SE	0.18	0.19	0.20	0.20	0.19	0.19	0.19	0.19	0.19	0.19	0.19	0.19	0.21	0.20	0.19	0.19
p-value	0.24	0.26	0.90	0.89	0.49	0.64	0.50	0.43	0.77	0.93	0.54	0.61	0.72	0.98	0.22	0.23
R^2	0.60	0.59	0.56	0.56	0.57	0.57	0.57	0.58	0.56	0.56	0.57	0.57	0.56	0.55	0.60	0.59
Cantabrian shelf																
Slope	-0.11	-0.19	-0.04	-0.14	-0.19	-0.22	0.03	0.01	-0.09	-0.15	0.13	0.07	-0.22	-0.17	-0.33	0.26
SE	0.20	0.20	0.19	0.20	0.19	0.19	0.20	0.21	0.21	0.21	0.19	0.19	0.23	0.23	0.21	0.23
p-value	0.58	0.36	0.86	0.48	0.35	0.28	0.88	0.96	0.68	0.49	0.50	0.71	0.35	0.49	0.15	0.27
R^2	0.57	0.58	0.56	0.57	0.58	0.59	0.53	0.53	0.53	0.54	0.57	0.56	0.63	0.62	0.67	0.64
Aquitanian shelf																
Slope	-0.22	-0.30	0.01	-0.05	-0.14	-0.11	0.07	0.09	-0.01	-0.04	0.09	0.11	-0.24	-0.17	-0.32	0.29
SE	0.19	0.18	0.20	0.20	0.19	0.19	0.20	0.20	0.19	0.19	0.19	0.19	0.22	0.22	0.20	0.20
p-value	0.28	0.12	0.96	0.81	0.49	0.59	0.72	0.66	0.97	0.83	0.64	0.58	0.29	0.46	0.12	0.17
R^2	0.59	0.62	0.56	0.56	0.57	0.57	0.56	0.57	0.56	0.56	0.57	0.57	0.57	0.55	0.61	0.59
Armorican shelf																
Slope	-0.11	-0.11	-0.04	0.05	-0.10	-0.02	0.15	0.18	0.13	0.11	0.13	0.10	0.20	0.31	-0.03	0.10
SE	0.20	0.19	0.19	0.20	0.19	0.19	0.19	0.19	0.19	0.19	0.19	0.19	0.21	0.19	0.22	0.21
p-value	0.60	0.58	0.84	0.82	0.60	0.91	0.43	0.34	0.50	0.58	0.50	0.63	0.36	0.14	0.91	0.65
R^2	0.57	0.57	0.56	0.56	0.57	0.56	0.58	0.59	0.57	0.57	0.57	0.57	0.62	0.66	0.58	0.59

Table 4.A.7. Output summary of the linear regression model testing the influence of environmental variables on the pre-recruitment survival index (PRSI) of the European anchovy (*Engraulis encrasicolus*) during its peak spawning season. Structure and attributes as in Table 4.A.3.

EUROPEAN ANCHOVY – PEAK SPAWNING SEASON

	Non-extreme				Marine heatwaves						Marine cold-spells					
	BI	UI	*turb*	SST	n_{events}	n_{days}	i_{max}	i_{mean}	i_{cum}	D	n_{events}	n_{days}	i_{max}	i_{mean}	i_{cum}	D
Bay of Biscay																
Slope	-0.37	-0.24	-0.02	-0.12	0.11	0.07	0.09	-0.06	0.06	0.06	0.01	0.10	**-0.63**	-0.55	-0.51	0.44
SE	0.25	0.26	0.26	0.26	0.26	0.26	0.30	0.30	0.30	0.30	0.26	0.26	**0.30**	0.30	0.34	0.35
p-value	0.15	0.35	0.95	0.65	0.68	0.78	0.77	0.84	0.84	0.84	0.97	0.69	**0.05**	0.08	0.15	0.23
R^2	0.17	0.14	0.12	0.12	0.12	0.12	0.09	0.08	0.08	0.08	0.12	0.12	**0.20**	0.17	0.13	0.11
Cantabrian shelf																
Slope	0.02	0.36	0.30	-0.05	0.07	0.04	0.02	-0.01	-0.03	-0.07	0.13	0.16	**-0.97**	**-0.89**	-0.57	0.50
SE	0.26	0.25	0.26	0.26	0.26	0.26	0.32	0.32	0.32	0.32	0.26	0.26	**0.34**	**0.35**	0.39	0.40
p-value	0.93	0.16	0.25	0.85	0.78	0.86	0.94	0.98	0.92	0.84	0.61	0.53	**0.01**	**0.02**	0.17	0.23
R^2	0.12	0.17	0.15	0.12	0.12	0.12	0.12	0.12	0.12	0.12	0.12	0.13	**0.32**	**0.28**	0.12	0.09
Aquitanian shelf																
Slope	-0.17	-0.31	0.11	-0.13	0.13	0.13	0.23	0.24	0.14	0.13	0.03	0.14	**-0.82**	**-0.81**	-0.69	0.64
SE	0.26	0.26	0.26	0.26	0.26	0.26	0.33	0.33	0.34	0.34	0.26	0.26	**0.31**	**0.31**	0.37	0.38
p-value	0.52	0.24	0.66	0.62	0.61	0.63	0.49	0.47	0.68	0.71	0.89	0.61	**0.01**	**0.01**	0.07	0.12
R^2	0.13	0.15	0.12	0.12	0.12	0.12	0.14	0.14	0.13	0.12	0.12	0.12	**0.28**	**0.28**	0.18	0.15
Armorican shelf																
Slope	-0.39	-0.38	-0.14	-0.13	0.09	0.03	0.05	-0.12	0.04	0.05	-0.05	0.05	**-0.67**	-0.63	-0.49	0.39
SE	0.25	0.25	0.26	0.26	0.26	0.26	0.30	0.31	0.31	0.31	0.26	0.26	**0.32**	0.32	0.37	0.38
p-value	0.12	0.13	0.58	0.63	0.72	0.91	0.87	0.71	0.90	0.88	0.84	0.85	**0.05**	0.06	0.20	0.32
R^2	0.18	0.18	0.13	0.12	0.12	0.12	0.08	0.09	0.08	0.08	0.12	0.12	**0.22**	0.21	0.13	0.11

Table 4.A.8. Output summary of the linear regression model testing the influence of environmental variables on the pre-recruitment survival index (PRSI) of the Atlantic mackerel (*Scomber scombrus*) during its peak spawning season. Structure and attributes as in Table 4.A.3.

ATLANTIC MACKEREL – PEAK SPAWNING SEASON

	Non-extreme				Marine heatwaves						Marine cold-spells					
	BI	UI	*turb*	SST	n_{events}	n_{days}	i_{max}	i_{mean}	i_{cum}	*D*	n_{events}	n_{days}	i_{max}	i_{mean}	i_{cum}	*D*
Bay of Biscay																
Slope	0.12	-0.16	**-0.21**	**0.28**	**0.22**	**0.21**	0.10	0.04	0.13	0.12	**-0.22**	-0.16	0.09	0.05	0.08	-0.09
SE	0.10	0.10	**0.10**	**0.09**	**0.10**	**0.10**	0.15	0.16	0.15	0.16	**0.09**	0.10	0.16	0.17	0.16	0.16
p-value	0.23	0.09	**0.04**	**0.00**	**0.03**	**0.03**	0.51	0.82	0.41	0.45	**0.02**	0.11	0.58	0.78	0.62	0.59
R^2	0.36	0.38	**0.41**	**0.47**	**0.41**	**0.41**	0.64	0.63	0.65	0.64	**0.42**	0.38	0.32	0.31	0.32	0.32
Cantabrian shelf																
Slope	0.09	-0.05	**-0.24**	**0.30**	**0.21**	**0.20**	**0.32**	0.18	0.23	0.21	**-0.27**	**-0.22**	0.11	0.06	0.11	-0.13
SE	0.10	0.10	**0.09**	**0.09**	**0.10**	**0.10**	**0.12**	0.15	0.14	0.14	**0.09**	**0.09**	0.14	0.14	0.14	0.14
p-value	0.36	0.61	**0.02**	**0.00**	**0.05**	**0.05**	**0.04**	0.28	0.15	0.20	**0.01**	**0.02**	0.44	0.68	0.44	0.37
R^2	0.35	0.34	**0.43**	**0.49**	**0.40**	**0.40**	**0.88**	0.79	0.82	0.80	**0.46**	**0.42**	0.33	0.31	0.34	0.35
Aquitanian shelf																
Slope	0.00	-0.13	**-0.22**	**0.28**	**0.22**	**0.21**	0.21	0.22	0.23	0.23	**-0.19**	-0.13	-0.02	-0.04	0.05	-0.05
SE	0.10	0.10	**0.10**	**0.09**	**0.10**	**0.10**	0.15	0.15	0.15	0.15	**0.09**	0.10	0.19	0.19	0.19	0.19
p-value	0.98	0.19	**0.03**	**0.01**	**0.04**	**0.04**	0.19	0.18	0.17	0.17	**0.05**	0.20	0.92	0.85	0.80	0.81
R^2	0.33	0.36	**0.41**	**0.46**	**0.40**	**0.41**	0.71	0.71	0.72	0.72	**0.39**	0.36	0.25	0.26	0.26	0.26
Armorican shelf																
Slope	-0.02	-0.08	-0.17	**0.27**	**0.22**	**0.20**	0.08	0.01	0.12	0.12	**-0.22**	-0.15	0.18	0.18	0.07	-0.08
SE	0.10	0.10	0.10	**0.09**	**0.10**	**0.10**	0.16	0.16	0.16	0.16	**0.09**	0.10	0.15	0.15	0.15	0.15
p-value	0.83	0.40	0.08	**0.01**	**0.03**	**0.04**	0.63	0.95	0.45	0.47	**0.02**	0.11	0.27	0.25	0.66	0.62
R^2	0.33	0.34	0.38	**0.46**	**0.41**	**0.40**	0.60	0.59	0.61	0.61	**0.42**	0.37	0.31	0.32	0.25	0.25

Table 4.A.9**.** Output summary of the linear regression model testing the influence of environmental variables on the pre-recruitment survival index (PRSI) of the Atlantic horse mackerel (*Trachurus trachurus*) during its peak spawning season. Structure and attributes as in Table 4.A.3.

ATLANTIC HORSE MACKEREL – PEAK SPAWNING SEASON

	Non-extreme				Marine heatwaves						Marine cold-spells					
	BI	UI	*turb*	SST	n_{events}	n_{days}	i_{max}	i_{mean}	i_{cum}	*D*	n_{events}	n_{days}	i_{max}	i_{mean}	i_{cum}	*D*
Bay of Biscay																
Slope	-0.13	-0.29	-0.14	0.00	-0.02	0.05	-0.02	-0.04	0.00	-0.02	-0.22	-0.25	0.45	**0.52**	0.38	-0.33
SE	0.21	0.20	0.21	0.24	0.22	0.22	0.26	0.25	0.26	0.26	0.22	0.22	0.23	**0.22**	0.24	0.25
p-value	0.54	0.16	0.51	0.99	0.94	0.83	0.94	0.89	0.99	0.93	0.34	0.25	0.07	**0.03**	0.13	0.19
R^2	0.33	0.36	0.33	0.32	0.32	0.33	0.35	0.35	0.35	0.35	0.34	0.35	0.32	**0.36**	0.30	0.28
Cantabrian shelf																
Slope	0.06	-0.17	-0.15	-0.12	-0.09	-0.01	0.09	0.06	-0.02	-0.03	0.05	-0.14	0.49	0.50	0.42	-0.36
SE	0.21	0.21	0.22	0.24	0.22	0.22	0.29	0.29	0.29	0.29	0.23	0.21	0.25	0.25	0.26	0.26
p-value	0.79	0.42	0.51	0.60	0.69	0.96	0.77	0.84	0.94	0.91	0.81	0.50	0.06	0.06	0.12	0.18
R^2	0.33	0.34	0.33	0.33	0.33	0.32	0.28	0.28	0.28	0.28	0.33	0.33	0.38	0.38	0.35	0.33
Aquitanian shelf																
Slope	-0.06	0.01	0.01	-0.02	0.00	0.03	-0.2	-0.26	0.00	0.01	-0.16	-0.26	0.40	0.44	0.47	-0.46
SE	0.21	0.21	0.21	0.24	0.22	0.22	0.29	0.28	0.29	0.28	0.22	0.22	0.25	0.25	0.25	0.26
p-value	0.78	0.95	0.96	0.92	1.00	0.88	0.50	0.36	0.99	0.99	0.47	0.24	0.12	0.09	0.07	0.09
R^2	0.33	0.32	0.32	0.32	0.32	0.32	0.34	0.35	0.33	0.33	0.33	0.35	0.31	0.33	0.33	0.33
Armorican shelf																
Slope	-0.20	-0.23	-0.2	0.07	0.00	0.08	0.09	0.13	0.01	-0.08	-0.31	-0.27	0.44	0.49	0.36	-0.30
SE	0.21	0.21	0.21	0.24	0.23	0.22	0.27	0.26	0.27	0.27	0.22	0.22	0.24	0.24	0.25	0.25
p-value	0.35	0.27	0.33	0.78	0.99	0.71	0.74	0.61	0.98	0.77	0.17	0.21	0.08	0.06	0.15	0.24
R^2	0.34	0.35	0.34	0.33	0.32	0.33	0.33	0.33	0.33	0.33	0.36	0.35	0.21	0.24	0.18	0.16

Table 4.A.10. Output summary of the linear regression model testing the influence of environmental variables on the pre-recruitment survival index (PRSI) of the European sardine (*Sardina pilchardus*) during its peak spawning season. Structure and attributes as in Table 4.A.3.

EUROPEAN SARDINE – PEAK SPAWNING SEASON

	Non-extreme				Marine heatwaves						Marine cold-spells					
	BI	UI	*turb*	SST	n_{events}	n_{days}	i_{max}	i_{mean}	i_{cum}	D	n_{events}	n_{days}	i_{max}	i_{mean}	i_{cum}	D
Bay of Biscay																
Slope	-0.22	-0.04	0.23	-0.01	0.00	0.07	0.12	0.05	0.15	0.14	0.34	0.30	0.08	0.08	-0.23	0.28
SE	0.18	0.19	0.18	0.20	0.20	0.19	0.19	0.20	0.19	0.19	0.17	0.18	0.27	0.27	0.26	0.26
p-value	0.24	0.82	0.22	0.95	0.99	0.73	0.53	0.80	0.45	0.48	0.06	0.11	0.79	0.78	0.40	0.31
R^2	0.60	0.56	0.60	0.56	0.56	0.56	0.57	0.56	0.58	0.57	0.65	0.63	0.49	0.50	0.53	0.54
Cantabrian shelf																
Slope	-0.30	-0.22	0.16	-0.01	-0.02	0.00	0.12	0.14	0.09	0.08	0.16	0.20	0.10	0.08	-0.22	0.31
SE	0.18	0.19	0.19	0.20	0.22	0.20	0.20	0.20	0.20	0.20	0.19	0.19	0.31	0.31	0.31	0.32
p-value	0.11	0.25	0.40	0.95	0.92	0.99	0.55	0.48	0.67	0.71	0.41	0.31	0.76	0.80	0.50	0.36
R^2	0.63	0.60	0.58	0.56	0.56	0.56	0.54	0.54	0.53	0.53	0.58	0.59	0.43	0.43	0.46	0.50
Aquitanian shelf																
Slope	0.06	-0.04	0.29	0.00	-0.04	0.07	0.29	0.19	0.26	0.24	0.18	0.21	-0.02	0.01	-0.24	0.25
SE	0.19	0.19	0.18	0.20	0.21	0.19	0.20	0.20	0.20	0.21	0.19	0.19	0.29	0.29	0.27	0.27
p-value	0.77	0.84	0.13	0.99	0.86	0.74	0.18	0.37	0.23	0.27	0.34	0.27	0.96	0.98	0.41	0.38
R^2	0.56	0.56	0.62	0.56	0.56	0.56	0.65	0.62	0.64	0.63	0.59	0.59	0.69	0.69	0.72	0.72
Armorican shelf																
Slope	0.15	0.11	0.20	-0.03	0.03	0.09	0.24	0.11	0.29	0.27	0.36	0.36	-0.28	-0.19	-0.24	0.24
SE	0.19	0.19	0.19	0.20	0.19	0.19	0.16	0.17	0.16	0.16	0.17	0.17	0.40	0.41	0.32	0.32
p-value	0.45	0.59	0.30	0.89	0.90	0.65	0.17	0.55	0.09	0.11	0.06	0.06	0.52	0.67	0.50	0.49
R^2	0.58	0.57	0.59	0.56	0.56	0.57	0.75	0.72	0.77	0.76	0.66	0.65	0.64	0.61	0.64	0.65

Chapter 5

Discussion and conclusions

The results presented in the previous chapters offer valuable insights into the incidence and duration of marine heatwaves in the Bay of Biscay in recent decades. As the spatiotemporal scope of the research broadens in each chapter, three pivotal facets of marine heatwave exploration are progressively addressed: characterization, detectability, and impact assessment. Marine heatwave analyses in central Cantabrian Sea showed no significant trends in occurrence or duration, yet a positive correlation with the positive phase of the East Atlantic pattern and a potential association with populations shifts of habitat-founding macroalgae was acknowledged (Chapter 2). Coast-level monitoring of marine heatwaves was improved through our downscaling approach, which allowed to hindcast their incidence over a more widespread spatiotemporal extent and revealed a consistent six-fold increase across northern Spain throughout the last four decades, largely attributable to ocean warming (Chapter 3). This pattern persisted across the entire Bay of Biscay continental shelf with longer and more frequent marine heatwaves which, along with increasing sea surface temperatures, were shown to have divergent effects on the early life survival of mackerel and horse mackerel (Chapter 4).

This study dedicates significant attention to estimating long-term trends in sea surface temperatures and marine heatwave key features, among other environmental variables of interest. In all three chapters sea surface temperatures displayed significant rises that align with mean warming patterns observed in the Bay of Biscay (~0.10 - 0.25ºC per decade depending on the timescale, Chust et al., 2022). In contrast, marine heatwave trends only showed consistency over broad temporal scales (*i.e.*, 40 years) with overall increases in frequency (~75-80% MHW days per decade) and duration (2.5-3 days per decade) that mirror global patterns (Yao et al., 2022). While mean ocean warming has been identified as the main driver of marine heatwave occurrence worldwide (Oliver, 2019), atmospheric modes of climate variability are also a powerful source of above-average temperatures across vast oceanic regions (Holbrook et al., 2019). The influence of the East Atlantic pattern in prompting temperature extremes was acknowledged in Chapter 2 through a strong association with marine heatwave incidence in the Cantabrian Sea. While this pattern accounts for approximately 25% of sea surface temperature variability in the Bay of Biscay, the North Atlantic Oscillation also exerts substantial influence in the region (Borja et al., 2019), which can make its potential contribution to marine heatwave occurrence worth exploring in upcoming research. Although uncertainties persist regarding future projections of sea surface temperature and marine heatwave trends in the Bay of Biscay, global scale predictions (Oliver et

al., 2019; Cheng et al., 2022) and the increased frequency and endurance of the positive phase of the East Atlantic pattern in the past decade (see NOAA Climate Prediction Center, 2024) strongly indicate that the temperature-related processes examined in this study will likely persist in the coming years.

The ecological and socioeconomic effects stemming from increased ocean warming and marine heatwave incidence are primarily conspicuous in coastal areas (Smith et al., 2021). These regions, recognized as some of the most dynamic and productive on our planet, serve as critical interfaces where diverse ecosystems thrive and interact, what makes them exceptionally sensitive to climatic stressors (He & Silliman, 2019). Accurate temperature assessments in coastal areas are essential for developing management strategies to protect valuable marine ecosystems from the impacts of mean and extreme temperature trends (Melet et al., 2020). Acquiring them, however, remains challenging. On the one hand, remotely-sensed estimates are often biased by the influence of land and local processes, which skew the detection of small-scale variability and extremes (Woo & Park, 2020). On the other hand, *in situ* measurements have limited spatial coverage and usually require significant human effort for deployment, maintenance and collection. In fact, the unavailability of spatiotemporally longer, more comprehensive *in situ* temperature records in Chapter 2 prevented a more thorough trend analysis in sea surface temperature and marine heatwaves in the coast of central Cantabrian Sea. This conundrum led to the development of the downscaling method presented in Chapter 3. By reconciling field and satellite estimates in a regression model that includes the effect of alongshore upwelling and seasonal stratification, this method achieves to reliably reproduce nearshore sea surface temperatures over an extended spatiotemporal scope. The reconstructed temperature series enabled an improved detection of marine heatwaves along the entire Cantabrian coast over the last four decades, which holds potential for more precise predictions of their impacts and for conservation efforts to be more effectively targeted and timed.

Building on the success of this methodology in hindcasting marine heatwave incidence across the coast of northern Spain, several key strategies can be pursued for further refinement. First, the model could benefit from using temperature estimates derived from newly developed field and satellite products with heightened resolutions, particularly those with validated skill in coastal regions (Koutantou et al., 2023). Second, the inclusion of additional variables like river discharge or anthropogenic factors, contingent upon the distinctive features of the surveyed area, may enhance the ability of the model to reliably reproduce nearshore temperature conditions. Lastly, integrating sea surface temperature outputs from global climate model simulations (CMIP6, Kim et al., 2020) could be useful to accurately assess present and future trends in coastal temperatures under different global warming scenarios (*i.e.*, Representative Concentration Pathways 4.5 and 8.5). Collectively, these adjustments have the potential to improve the applicability and

robustness of our downscaling methodology, assuming it remains relevant. Recent advances in technology and modeling, particularly through the combination of data derived from satellites with measurements from UUV (unmanned underwater vehicles), have significantly improved the accuracy and resolution of remotely-sensed sea surface temperature estimates, which hold great promise in coastal areas (Vazquez-Cuervo et al., 2023). It is reasonable to expect these advancements to continue to evolve in the coming years, potentially reducing the need for methodologies such as the one presented here. In the interim, research efforts aimed at the precise detection of marine heatwaves remain key for enhancing our ability to assess and mitigate their impacts as we navigate a warming world.

Large marine ecosystems worldwide are projected to experience a widespread increase of marine heatwaves, which poses a grave threat to resident organisms – even if they were to adapt fully to the mean ocean warming trend (Guo et al., 2022). This implies that we should expect substantial disruptions in marine biodiversity across these valuable regions in the foreseeable future, including the Bay of Biscay. These may manifest through distribution range shifts, mass mortality events, alterations in food webs or extensive restructuring of ecosystems, among other well-documented environmental repercussions (Smith et al., 2023). The ecological effects derived from marine heatwave incidence in the Bay of Biscay remain an area yet to be investigated. This work contributes to filling the gap by examining marine heatwave impacts on two key marine communities: habitat-forming macroalgae (Chapter 2) and small pelagic fish (Chapter 4).

Macroalgae are critical components of marine ecosystems as they constitute the underpinning of the food web, provide essential habitats for a myriad of species and actively contribute to carbon sequestration (Krause-Jensen & Duarte, 2016; James & Whitfield, 2023). In recent decades, marine heatwaves have been reported to play a significant role in the decline of coastal foundation species globally, including macroalgae (Smith et al., 2024), which can trigger cascading effects that can lead to biodiversity loss and, ultimately, ecosystem disruption (Macreadie et al., 2017). For the last 50 years, cold-temperate macroalgae populations in southern Bay of Biscay have undergone a progressive retreat that has been paralleled by the expansion of warm-affinity non-indigenous species, a phenomenon that has been largely attributed to ocean warming (Fernández, 2016; Casado-Amezúa et al., 2019; Arriaga et al., 2023). While long-term temperature increases may induce sublethal stress in macroalgae physiology, prolonged exposure to above-average temperatures can surpass critical thermal thresholds, resulting in population attrition and ultimately triggering local extinctions and range contractions (Straub et al., 2019). Indeed, a potential correlation between the incidence of coastal marine heatwaves and documented shifts in macroalgae populations at a local level is inferred in Chapter 2. The lack of year-to-year abundance records for the selected macroalgae species prevented empirical validation of this association, as only disappearance data for specific periods have been recorded. Nonetheless, the

implications on ecosystem functioning may be significant, particularly within the context of projected reduced energy flows from low trophic levels (Ullah et al., 2018; Bindoff et al., 2019). One way to address this would be to annually monitor macroalgae populations in the region, which could yield crucial data to assess trends, validate correlations with marine heatwave occurrence, and advance research in this and related fields. Implementing citizen science programs to collect observational data from diverse geographic areas could alleviate the considerable human effort involved in this task (Herrero et al., 2023). Though preliminary, these findings emphasize the need for further research to elucidate how marine heatwaves are affecting macroalgae communities in the region, so that informed conservation and management efforts can be guided to counter their impacts.

Small pelagic fish, on the other hand, play vital roles across two critical fronts: ecological and commercial. Ecologically, they are integral to the pelagic food web as key energy transfer nodes that link and regulate production in both high and low trophic levels (Ruzicka et al., 2024). Commercially, they hold significant value as they represent a substantial percentage of the fisheries catch and contribute significantly to economic income, food security, and industry support through fishmeal and fish oil production (FAO, 2022). The sustained provision of these essential goods and services is currently compromised by overfishing and climate change, which lie behind reported declines in marine fish populations worldwide (IPBES, 2019a; IPCC, 2023). In this context, marine heatwaves emerge as powerful agents of change able to drive contrasting responses on fish communities depending on their life histories and sensitivity to environmental conditions (Cavole et al., 2016; Wernberg et al., 2016; Freedman et al., 2020; Ziegler et al., 2023). This impact variability is evident in the Bay of Biscay, where warmer sea surface temperatures and increased marine heatwave incidence do not affect the early life survival of anchovy and sardine but display contrasting effects on mackerel and horse mackerel, favoring the former and hampering the latter (Chapter 4). Global pelagic fauna is expected to redistribute as ocean warming intensifies, with species shifting polewards at the cooler edges of their ranges and contracting at their warmer boundaries (Ariza et al., 2022). Recent reports indicate that anchovy, mackerel, horse mackerel, and a diverse array of fish species inherent to lower latitudes in the NE Atlantic have been following this pattern (Gordó-Vilaseca et al., 2023), which suggests a diminishing likelihood of their presence in the Bay of Biscay over time. This scenario underscores the need for climate-adaptive management reforms to address these shifts and prevent potential fisheries conflict (Free et al., 2020; Mendenhall et al., 2020).

As rising temperatures and marine heatwaves continue to drive shifts in macroalgae and small pelagic fish populations, potential alterations in ecosystem function and services are imminent. Efforts to mitigate these trends are underway, including the EU Horizon projects FutureMARES and MaCoBioS, which aim to advance marine biodiversity research and ecosystem resilience

under climate change (FutureMARES, 2024; MaCoBioS, 2024), the attempts from the Pelagic Advisory Council to implement a horse mackerel fishery rebuilding plan (ICES, 2021e), and recent agreements on mackerel quotas by the Northeast Atlantic Fisheries Commission (European Commission, 2023). While these initiatives show promise, they would benefit from increased support as there are important next steps yet to fulfill, such as expanding conservation and restoration efforts to additional species and regions, renewing the rebuilding plan for horse mackerel, and reaching a consensus on mackerel stock sharing. Providing protection to marine ecosystems and enhancing the connectivity between them can aid in the restoration and preservation of affected areas (Fontoura et al., 2022), whereas implementing management strategies that align with scientific advice and respond to changing environmental conditions is essential (*i.e.* zero catch recommendations for western horse mackerel were issued in the last two years but were ultimately dismissed, see ICES, 2023). A coordinated and comprehensive approach is necessary to address the current and upcoming challenges of a planet undergoing climate change. Meeting the 1.5ºC global warming target is paramount to avoid critical scenarios, but the long-term endurance and sustainability of marine systems can only be secured if this goal is accompanied by actions that promote resilience and adaptation (Trebilco et al., 2022).

The cornerstone of sustainable ocean management is research, as it provides the knowledge and evidence needed to make informed decisions, implement effective conservation measures, and ensure the long-term health and resilience of global oceans. In this sense, monitoring marine heatwave incidence in the Bay of Biscay and understanding how they affect the biodiversity and functioning of local marine ecosystems is crucial for the preservation of ecological balance and the sustenance of livelihoods and economic activities reliant on its resources. Here, we present three main contributions: an analysis of marine heatwave trends over the past four decades, an improved methodology for detecting them at the coast level, and a deeper understanding of their influence and impacts on two significant marine communities in the region. Our endeavor is that this study will not only shed light on the effects of marine heatwaves in the Bay of Biscay, but also inspire research, conservation and policymaking efforts on the field to work towards a more sustainable future for the marine and human communities inhabiting it.

5.1. Conclusions

- The likelihood of marine heatwave occurrence in the central Cantabrian Sea associates with the positive phase of the East Atlantic pattern, supporting the prevailing role of large-scale climate modes as key drivers of these events.

- The incidence of marine heatwaves along the coast of the central Cantabrian Sea may link to population shifts of habitat-forming macroalgae species documented in literature.

- Coastal upwelling limits sea surface temperature monitoring at two coastal locations in the central Cantabrian Sea and prompts large biases between field and satellite records, especially during spring and summer.

- A downscaling approach based on regression modeling achieves to reconcile *in situ* and satellite temperature estimates by accounting for the effect of alongshore upwelling and air-sea heat fluxes. This method allows to predict an improved temperature series that i) reliably reproduces near-shore sea surface temperatures, ii) retains the spatiotemporal resolution of the satellite and iii) improves the detection of coastal marine heatwaves.

- Trend analyses based on static and dynamic detection thresholds indicate a significant impact of long-term ocean warming on the six-fold increase in marine heatwave incidence along the coast of southern Bay of Biscay over the last four decades.

- The incidence of marine heatwaves across the southern Bay of Biscay parallels the gradient in sea surface temperature, being more frequent towards the inner part of the Bay.

- The frequency and duration of extreme temperature events in the continental shelf of the Bay of Biscay over the past four decades aligns with global patterns: increasing for marine heatwaves, decreasing for marine cold-spells.

- Ocean warming and marine heatwaves are leading to a growing frequency of exceptionally high sea surface temperatures that exceed the spawning thermal niche of small pelagic fish, as well as a decline in the availability of optimal spawning temperatures for mackerel.

- The influence of environmental forcing on the early life survival of small pelagic fish in the continental shelf of the Bay of Biscay is closely tied to life history strategy. During their spawning period, wind-related processes have distinct effects on anchovy, mackerel, and horse mackerel depending on the region examined, whereas warmer waters and marine heatwaves favor mackerel and compromise horse mackerel across most, if not all regions in the Bay.

- Marine heatwave research conducted at local and regional scales remains crucial for acquiring detailed insights that are often overlooked by global analyses. When integrated into a broader framework, this smaller-scale knowledge facilitates a comprehensive understanding of marine heatwave trends and their impacts across various regions and ecosystems worldwide. Only through this holistic approach can we effectively guide targeted conservation and management strategies in a world facing climate change.

5.2. Conclusiones

- La probabilidad de ocurrencia de olas de calor marinas en el Mar Cantábrico central se asocia con la fase positiva del patrón del Atlántico Este, lo que respalda el papel predominante de los modos climáticos a gran escala como impulsores clave de estos eventos.
- La incidencia de olas de calor marinas a lo largo de la costa del Mar Cantábrico central puede estar relacionada con cambios poblacionales de especies de macroalgas formadoras de hábitat documentados en literatura reciente.
- El afloramiento costero limita el monitoreo de la temperatura superficial del mar en dos ubicaciones costeras en el Mar Cantábrico central y provoca grandes sesgos entre los registros de campo y satélite, especialmente durante la primavera y el verano.
- Un enfoque de reducción de escala basado en modelos de regresión consigue reconciliar estimaciones de temperatura *in situ* y satelitales al tener en cuenta el efecto del afloramiento costero y los flujos de calor aire-mar. Este método permite predecir una serie de temperatura mejorada que i) reproduce de manera fiable las temperaturas superficiales del mar cerca de la costa, ii) conserva la resolución espaciotemporal del satélite y iii) mejora la detección de olas de calor marinas costeras.
- Los análisis de tendencias basados en umbrales de detección estática y dinámica indican un impacto significativo del calentamiento oceánico a largo plazo en la sextuplicación de la incidencia de olas de calor marinas a lo largo de la costa sur del Golfo de Vizcaya en las últimas cuatro décadas.
- La incidencia de olas de calor marinas en el sur del Golfo de Vizcaya se correlaciona con el gradiente de temperatura superficial del mar, siendo más frecuentes hacia el interior del golfo.
- La frecuencia y duración de eventos extremos de temperatura en la plataforma continental del Golfo de Vizcaya en las últimas cuatro décadas se alinea con los patrones globales: aumento de olas de calor marinas, disminución de olas de frío marinas.
- El calentamiento de los océanos y las olas de calor marinas están provocando una frecuencia cada vez mayor de temperaturas superficiales del mar excepcionalmente altas que exceden el nicho térmico de desove de los pequeños peces pelágicos, así como una disminución en la disponibilidad de temperaturas óptimas de desove para la caballa.
- La influencia del forzamiento ambiental en la supervivencia temprana de pequeños peces pelágicos en la plataforma continental del Golfo de Vizcaya está estrechamente ligada a la estrategia de historia vital. En su periodo de desove, los procesos relacionados con el viento tienen efectos distintos sobre la anchoa, la caballa y el chicharro dependiendo de la región

examinada, mientras que las aguas más cálidas y las olas de calor marinas favorecen a la caballa y comprometen al chicharro en la mayoría de las regiones del Golfo, si no en todas.

- La investigación sobre olas de calor marinas realizada a escala local y regional sigue siendo crucial para adquirir conocimientos detallados que a menudo pasan desapercibidos en los análisis globales. Cuando se integra en un marco más amplio, este conocimiento a menor escala facilita una comprensión integral de las tendencias de las olas de calor marinas y sus impactos en diversas regiones y ecosistemas de todo el mundo. Sólo a través de este enfoque holístico podremos guiar eficazmente estrategias específicas de conservación y gestión en un mundo que enfrenta el cambio climático.

Bibliography

Abaunza, P., Gordo, L., Karlou-Riga, C., Murta, A., Eltink, A. T. G. W., García Santamaría, M. T., Zimmermann, C., Hammer, C., Lucio, P., Iversen, S. A., Molloy, J., & Gallo, E. (2003). Growth and reproduction of horse mackerel, Trachurus trachurus (carangidae). *Reviews in Fish Biology and Fisheries*, *13*(1), 27–61. https://doi.org/10.1023/A:1026334532390

Abaunza, P., Murta, A. G., Campbell, N., Cimmaruta, R., Comesaña, A. S., Dahle, G., García Santamaría, M. T., Gordo, L. S., Iversen, S. A., MacKenzie, K., Magoulas, A., Mattiucci, S., Molloy, J., Nascetti, G., Pinto, A. L., Quinta, R., Ramos, P., Sanjuan, A., Santos, A. T., … Zimmermann, C. (2008). Stock identity of horse mackerel (Trachurus trachurus) in the Northeast Atlantic and Mediterranean Sea: Integrating the results from different stock identification approaches. *Fisheries Research, 89*(2), 196–209. https://doi.org/10.1016/j.fishres.2007.09.022

Alix, M., Kjesbu, O. S., & Anderson, K. C. (2020). From gametogenesis to spawning: How climate-driven warming affects teleost reproductive biology. *Journal of Fish Biology*, *97*(3), 607–632. https://doi.org/10.1111/jfb.14439

Allain, G., Petitgas, P., & Lazure, P. (2001). The influence of mesoscale ocean processes on anchovy (Engraulis encrasicolus) recruitment in the Bay of Biscay estimated with a three-dimensional hydrodynamic mode. *Fisheries Oceanography*, *10*(2), 151–163. https://doi.org/10.1046/j.1365-2419.2001.00164.x

Allain, G., Petitgas, P., & Lazure, P. (2007). The influence of environment and spawning distribution on the survival of anchovy (Engraulis encrasicolus) larvae in the Bay of Biscay (NE Atlantic) investigated by biophysical simulations. *Fisheries Oceanography*, *16*(6), 506–514. https://doi.org/10.1111/j.1365-2419.2007.00442.x

Allouche, O., Tsoar, A., & Kadmon, R. (2006). Assessing the accuracy of species distribution models: Prevalence, kappa and the true skill statistic (TSS). *Journal of Applied Ecology*, *43*(6), 1223–1232. https://doi.org/10.1111/j.1365-2664.2006.01214.x

Anadón, R., & Niell, F. X. (1981). *Distribución longitudinal de macrofitos en la costa asturiana (N de España)*. https://digital.csic.es/handle/10261/89117

Andrés, M., & Prellezo, R. (2012). Measuring the adaptability of fleet segments to a fishing ban: The case of the Bay of Biscay anchovy fishery. *Aquatic Living Resources, 25*(3), Article 3. https://doi.org/10.1051/alr/2012018

Arafeh-Dalmau, N., Montaño-Moctezuma, G., Martínez, J. A., Beas-Luna, R., Schoeman, D. S., & Torres-Moye, G. (2019). Extreme Marine Heatwaves Alter Kelp Forest Community Near Its Equatorward Distribution Limit. *Frontiers in Marine Science*, *6*. https://www.frontiersin.org/articles/10.3389/fmars.2019.00499

Ariza, A., Lengaigne, M., Menkes, C., Lebourges-Dhaussy, A., Receveur, A., Gorgues, T., Habasque, J., Gutiérrez, M., Maury, O., & Bertrand, A. (2022). Global decline of pelagic fauna in a warmer ocean. *Nature Climate Change*, *12*(10), 928–934. https://doi.org/10.1038/s41558-022-01479-2

Arriaga, O., Wawrzynkowski, P., Ibáñez, H., Muguerza, N., Díez, I., Pérez-Ruzafa, I., Gorostiaga, J. M., Quintano, E., & Becerro, M. A. (2023). Short-term response of macroalgal communities to ocean warming in the Southern Bay of Biscay. *Marine Environmental Research*, *190*, 106098. https://doi.org/10.1016/j.marenvres.2023.106098

Asch, R. G., Stock, C. A., & Sarmiento, J. L. (2019). Climate change impacts on mismatches between phytoplankton blooms and fish spawning phenology. *Global Change Biology*, *25*(8), 2544–2559. https://doi.org/10.1111/gcb.14650

Bakun, A. (1973). Coastal upwelling indices, west coast of North America, 1946-71. *NOAA Technical Report NMFS SSRF*, *671*. https://repository.library.noaa.gov/view/noaa/9041

Bakun, A. (1996). *Patterns in the Ocean: Ocean Processes and Marine Population Dynamics*. California Sea Grant College System, National Oceanic and Atmospheric Administration.

Bakun, A., & Parrish, R. (1982). Turbulence, transport, and pelagic fish in the California and Peru current systems. *California Cooperative Oceanic Fisheries Investigations*, *23*, 99–112.

Banzon, V., Smith, T. M., Chin, T. M., Liu, C., & Hankins, W. (2016). A long-term record of blended satellite and in situ sea-surface temperature for climate monitoring, modeling and environmental studies. *Earth System Science Data*, *8*(1), 165–176. https://doi.org/10.5194/essd-8-165-2016

Barange, M., Bahri, T., Beveridge, M., Cochrane, K., Funge-Smith, S., & Poulain, F. (Eds.). (2018). Impacts of Climate Change on Fisheries and Aquaculture. Synthesis of Current Knowledge, Adaptation, and Mitigation Options. *FAO Fisheries and Aquaculture Technical Paper*, *627*, 628 pp.

Barbier, E. B. (2017). Marine ecosystem services. *Current Biology*, *27*(11), R507–R510. https://doi.org/10.1016/j.cub.2017.03.020

Barkhordarian, A., Nielsen, D. M., & Baehr, J. (2022). Recent marine heatwaves in the North Pacific warming pool can be attributed to rising atmospheric levels of greenhouse gases. *Communications Earth & Environment*, *3*(1), 1–12. https://doi.org/10.1038/s43247-022-00461-2

Barnston, A. G., & Livezey, R. E. (1987). Classification, Seasonality and Persistence of Low-Frequency Atmospheric Circulation Patterns. *Monthly Weather Review*, *115*(6), 1083–1126. https://doi.org/10.1175/1520-0493(1987)115<1083:CSAPOL>2.0.CO;2

Barrett, T., Dowle, M., Srinivasan, A., Gorecki, J., Chirico, M., Hocking, T., Stetsenko, P., Short, T., Lianoglou, S., Antonyan, E., Bonsch, M., Parsonage, H., Ritchie, S., Ren, K., Tan, X., Saporta, R., Seiskari, O., Dong, X., Lang, M., … Czekanski, M. (2021). data.table: Extension of 'data.frame'. *R Package Version 1.14.0.* https://cran.r-project.org/web/packages/data.table/index.html

Bashevkin, S. M., Dibble, C. D., Dunn, R. P., Hollarsmith, J. A., Ng, G., Satterthwaite, E. V., & Morgan, S. G. (2020). Larval dispersal in a changing ocean with an emphasis on upwelling regions. *Ecosphere*, *11*(1), e03015. https://doi.org/10.1002/ecs2.3015

Beare, D. J., & Reid, D. G. (2002). Investigating spatio-temporal change in spawning activity by Atlantic mackerel between 1977 and 1998 using generalized additive models. *ICES Journal of Marine Science*, *59*(4), 711–724. https://doi.org/10.1006/jmsc.2002.1207

Bell, R. J., Odell, J., Kirchner, G., & Lomonico, S. (2020). Actions to Promote and Achieve Climate-Ready Fisheries: Summary of Current Practice. *Marine and Coastal Fisheries*, *12*(3), 166–190. https://doi.org/10.1002/mcf2.10112

Benthuysen, J. A., Oliver, E. C. J., Chen, K., & Wernberg, T. (2020). Editorial: Advances in Understanding Marine Heatwaves and Their Impacts. *Frontiers in Marine Science*, *7*. https://www.frontiersin.org/articles/10.3389/fmars.2020.00147

Benthuysen, J. A., Smith, G. A., Spillman, C. M., & Steinberg, C. R. (2021). Subseasonal prediction of the 2020 Great Barrier Reef and Coral Sea marine heatwave. *Environmental Research Letters*, *16*(12), 124050. https://doi.org/10.1088/1748-9326/ac3aa1

Berec, L., Angulo, E., & Courchamp, F. (2007). Multiple Allee effects and population management. *Trends in Ecology & Evolution*, *22*(4), 185–191. https://doi.org/10.1016/j.tree.2006.12.002

Bernal, M., Jiménez, M. P., & Duarte, J. (2012). Anchovy egg development in the Gulf of Cádiz and its comparison with development rates in the Bay of Biscay. *Fisheries Research*, *117–118*, 112–120. https://doi.org/10.1016/j.fishres.2011.04.010

Bernal, M., Stratoudakis, Y., Coombs, S., Angelico, M. M., de Lanzós, A. L., Porteiro, C., Sagarminaga, Y., Santos, M., Uriarte, A., Cunha, E., Valdés, L., & Borchers, D. (2007). Sardine spawning off the European Atlantic coast: Characterization of and spatio-temporal variability in spawning habitat. *Progress in Oceanography, 74*(2), 210–227. https://doi.org/10.1016/j.pocean.2007.04.018

Bindoff, N. L., Cheung, W. W. L., Kairo, J. G., Arístegui, J., Guinder, V. A., Hallberg, R., Hilmi, N., Jiao, N., Karim, M. S., Levin, L., O'Donoghue, S., Purca Cuicapusa, S. R., Rinkevich, B., Suga, T., Tagliabue, A., & Williamson, P. (2019). Changing Ocean, Marine Ecosystems, and Dependent Communities. In *IPCC Special Report on the Ocean and Cryosphere in a Changing Climate* (pp. 447–587). https://www.ipcc.ch/srocc/chapter/chapter-5/

Boëns, A., Ernande, B., Petitgas, P., & Lebigre, C. (2023). Different mechanisms underpin the decline in growth of anchovies and sardines of the Bay of Biscay. *Evolutionary Applications*, *16*(8), 1393–1411. https://doi.org/10.1111/eva.13564

Bolker, B., R Development Core Team, & Giné-Vázquez, I. (2020). bbmle: Tools for General Maximum Likelihood Estimation. *R Package Version 1.0.23.1.* https://cran.r-project.org/web/packages/bbmle/

Borja, A., Amouroux, D., Anschutz, P., Gómez-Gesteira, M., Uyarra, M. C., & Valdés, L. (2019). Chapter 5—The Bay of Biscay. In C. Sheppard (Ed.), *World Seas: An Environmental Evaluation (Second Edition)* (pp. 113–152). Academic Press. https://doi.org/10.1016/B978-0-12-805068-2.00006-1

Borja, A., Chust, G., Fontán, A., Garmendia, J. M., & Uyarra, M. C. (2018). Long-term decline of the canopy-forming algae *Gelidium corneum*, associated to extreme wave events and reduced sunlight hours, in the southeastern Bay of Biscay. *Estuarine, Coastal and Shelf Science*, *205*, 152–160. https://doi.org/10.1016/j.ecss.2018.03.016

Borja, A., Fontán, A., & Muxika, I. (2013). Interactions between climatic variables and human pressures upon a macroalgae population: Implications for management. *Ocean & Coastal Management*, *76*, 85–95. https://doi.org/10.1016/j.ocecoaman.2013.02.023

Borja, A., Fontán, A., Sáenz, J., & Valencia, V. (2008). Climate, oceanography, and recruitment: The case of the Bay of Biscay anchovy (Engraulis encrasicolus). *Fisheries Oceanography*, *17*(6), 477–493. https://doi.org/10.1111/j.1365-2419.2008.00494.x

Borja, A., Uriarte, A., & Egaña, J. (2002). Environmental factors and recruitment of mackerel, Scomber scombrus L. 1758, along the north-east Atlantic coasts of Europe. *Fisheries Oceanography*, *11*(2), 116–127. https://doi.org/10.1046/j.1365-2419.2002.00190.x

Borja, A., Uriarte, A., Egaña, J., Motos, L., & Valencia, V. (1998). Relationships between anchovy (Engraulis encrasicolus) recruitment and environment in the Bay of Biscay (1967–1996). *Fisheries Oceanography*, *7*(3–4), 375–380. https://doi.org/10.1046/j.1365-2419.1998.00064.x

Borja, A., Uriarte, A., Valencia, V., & Motos, L. (1996). Relationships between anchovy (Engraulis encrasicolus) recruitment and environment in the Bay of Biscay. *Scientia Marina*, *60*, 179–192.

Botas, J. A., Fernandez, E., Bode, A., & Anadon, R. (1990). A persistent upwelling off the Central Cantabrian Coast (Bay of Biscay). *Estuarine, Coastal and Shelf Science*, *30*(2), 185–199. https://doi.org/10.1016/0272-7714(90)90063-W

Breitburg, D., Levin, L. A., Oschlies, A., Grégoire, M., Chavez, F. P., Conley, D. J., Garçon, V., Gilbert, D., Gutiérrez, D., Isensee, K., Jacinto, G. S., Limburg, K. E., Montes, I., Naqvi, S. W. A., Pitcher, G. C., Rabalais, N. N., Roman, M. R., Rose, K. A., Seibel, B. A., … Zhang, J. (2018). Declining oxygen in the global ocean and coastal waters. *Science*, *359*(6371), eaam7240. https://doi.org/10.1126/science.aam7240

Bruge, A., Alvarez, P., Fontán, A., Cotano, U., & Chust, G. (2016). Thermal Niche Tracking and Future Distribution of Atlantic Mackerel Spawning in Response to Ocean Warming. *Frontiers in Marine Science*, *3*. https://www.frontiersin.org/articles/10.3389/fmars.2016.00086

Burnham, K. P., & Anderson, D. R. (Eds.). (2002). *Model Selection and Multimodel Inference*. Springer. https://doi.org/10.1007/b97636

Calosi, P., Bilton, D. T., & Spicer, J. I. (2008). Thermal tolerance, acclimatory capacity and vulnerability to global climate change. *Biology Letters*, *4*(1), 99–102. https://doi.org/10.1098/rsbl.2007.0408

Campitelli, E. (2021). metR: Tools for Easier Analysis of Meteorological Fields. *R Package Version 0.10.0*. https://github.com/eliocamp/metR

Casado-Amezúa, P., Araújo, R., Bárbara, I., Bermejo, R., Borja, Á., Díez, I., Fernández, C., Gorostiaga, J. M., Guinda, X., Hernández, I., Juanes, J. A., Peña, V., Peteiro, C., Puente, A., Quintana, I., Tuya, F., Viejo, R. M., Altamirano, M., Gallardo, T., & Martínez, B. (2019). Distributional shifts of canopy-forming seaweeds from the Atlantic coast of Southern Europe. *Biodiversity and Conservation*, *28*(5), 1151–1172. https://doi.org/10.1007/s10531-019-01716-9

Casey, K. S., Brandon, T. B., Cornillon, P., & Evans, R. (2010). The Past, Present, and Future of the AVHRR Pathfinder SST Program. In V. Barale, J. F. R. Gower, & L. Alberotanza (Eds.), *Oceanography from Space: Revisited* (pp. 273–287). Springer Netherlands. https://doi.org/10.1007/978-90-481-8681-5_16

Cavole, L., Demko, A., Diner, R., Giddings, A., Koester, I., Pagniello, C., Paulsen, M.-L., Ramirez-Valdez, A., Schwenck, S., Yen, N., Zill, M., & Franks, P. (2016). Biological Impacts of the 2013–2015 Warm-Water Anomaly in the Northeast Pacific: Winners, Losers, and the Future. *Oceanography*, *29*(2). https://doi.org/10.5670/oceanog.2016.32

Chang, W. (2014). extrafont: Tools for Using Fonts. *R Package Version 0.17*. https://cran.r-project.org/web/packages/extrafont/index.html

Cheng, L., Abraham, J., Trenberth, K. E., Fasullo, J., Boyer, T., Mann, M. E., Zhu, J., Wang, F., Locarnini, R., Li, Y., Zhang, B., Yu, F., Wan, L., Chen, X., Feng, L., Song, X., Liu, Y., Reseghetti, F., Simoncelli, S., … Li, G. (2023). Another Year of Record Heat for the Oceans. *Advances in Atmospheric Sciences*, *40*(6), 963–974. https://doi.org/10.1007/s00376-023-2385-2

Cheung, W. W. L., Frölicher, T. L., Lam, V. W. Y., Oyinlola, M. A., Reygondeau, G., Sumaila, U. R., Tai, T. C., Teh, L. C. L., & Wabnitz, C. C. C. (2021). Marine high temperature extremes amplify the impacts of climate change on fish and fisheries. *Science Advances*, *7*(40), eabh0895. https://doi.org/10.1126/sciadv.abh0895

Chiriaco, M., Bastin, S., Yiou, P., Haeffelin, M., Dupont, J.-C., & Stéfanon, M. (2014). European heatwave in July 2006: Observations and modeling showing how local processes amplify conducive large-scale conditions. *Geophysical Research Letters*, *41*(15), 5644–5652. https://doi.org/10.1002/2014GL060205

Chiswell, S. M. (2022). Global Trends in Marine Heatwaves and Cold Spells: The Impacts of Fixed Versus Changing Baselines. *Journal of Geophysical Research: Oceans*, *127*(10), e2022JC018757. https://doi.org/10.1029/2022JC018757

Chust, G., González, M., Fontán, A., Revilla, M., Alvarez, P., Santos, M., Cotano, U., Chifflet, M., Borja, A., Muxika, I., Sagarminaga, Y., Caballero, A., de Santiago, I., Epelde, I., Liria, P., Ibaibarriaga, L., Garnier, R., Franco, J., Villarino, E., … Uriarte, A. (2022). Climate regime shifts and biodiversity redistribution in the Bay of Biscay. *Science of The Total Environment*, *803*, 149622. https://doi.org/10.1016/j.scitotenv.2021.149622

Chust, G., Taboada, F. G., Alvarez, P., & Ibaibarriaga, L. (2023). Species acclimatization pathways: Latitudinal shifts and timing adjustments to track ocean warming. *Ecological Indicators*, *146*, 109752. https://doi.org/10.1016/j.ecolind.2022.109752

Ciannelli, L., Bailey, K., & Olsen, E. M. (2015). Evolutionary and ecological constraints of fish spawning habitats. *ICES Journal of Marine Science*, *72*(2), 285–296. https://doi.org/10.1093/icesjms/fsu145

Clarke, A. (2017). *Principles of Thermal Ecology: Temperature, Energy, and Life*. Oxford University Press. https://doi.org/10.1093/oso/9780199551668.001.0001

Collins, M., Sutherland, M., Bouwer, L., Cheong, S.-M., Frölicher, T., Jacot Des Combes, H., Koll Roxy, M., Losada, I., McInnes, K., Ratter, B., Rivera-Arriaga, E., Susanto, R. D., Swingedouw, D., & Tibig, L. (2019). Extremes, Abrupt Changes and Managing Risks. In *Special Report on the Ocean and Cryosphere in a Changing Climate* (Cambridge University Press, pp. 589–655). https://doi.org/10.1017/9781009157964.008

Coombs, S. H., Halliday, N. C., Southward, A. J., & Hawkins, S. J. (2005). Distribution and abundance of sardine (sardina pilchardus) eggs in the english channel from continuous plankton recorder sampling, 1958–1980. *Journal of the Marine Biological Association of the United Kingdom, 85*(5), 1243–1247. https://doi.org/10.1017/S0025315405012385

Coombs, S. H., Smyth, T. J., Conway, D. V. P., Halliday, N. C., Bernal, M., Stratoudakis, Y., & Alvarez, P. (2006). Spawning season and temperature relationships for sardine (Sardina pilchardus) in the eastern North Atlantic. *Journal of the Marine Biological Association of the United Kingdom*, *86*(5), 1245–1252. https://doi.org/10.1017/S0025315406014251

Corrales, X., Preciado, I., Gascuel, D., Lopez de Gamiz-Zearra, A., Hernvann, P.-Y., Mugerza, E., Louzao, M., Velasco, F., Doray, M., López-López, L., Carrera, P., Cotano, U., & Andonegi, E. (2022). Structure and functioning of the Bay of Biscay ecosystem: A trophic modelling approach. *Estuarine, Coastal and Shelf Science*, *264*, 107658. https://doi.org/10.1016/j.ecss.2021.107658

Costanza, R., de Groot, R., Sutton, P., van der Ploeg, S., Anderson, S. J., Kubiszewski, I., Farber, S., & Turner, R. K. (2014). Changes in the global value of ecosystem services. *Global Environmental Change*, *26*, 152–158. https://doi.org/10.1016/j.gloenvcha.2014.04.002

Costello, M. J., Tsai, P., Wong, P. S., Cheung, A. K. L., Basher, Z., & Chaudhary, C. (2017). Marine biogeographic realms and species endemicity. *Nature Communications*, *8*(1), 1057. https://doi.org/10.1038/s41467-017-01121-2

Costoya, X., deCastro, M., Gómez-Gesteira, M., & Santos, F. (2015). Changes in sea surface temperature seasonality in the Bay of Biscay over the last decades (1982–2014). *Journal of Marine Systems*, *150*, 91–101. https://doi.org/10.1016/j.jmarsys.2015.06.002

Cury, P., & Roy, C. (1989). Optimal Environmental Window and Pelagic Fish Recruitment Success in Upwelling Areas. *Canadian Journal of Fisheries and Aquatic Sciences*, *46*(4), 670–680. https://doi.org/10.1139/f89-086

Dahlke, F. T., Wohlrab, S., Butzin, M., & Pörtner, H.-O. (2020). Thermal bottlenecks in the life cycle define climate vulnerability of fish. *Science*, *369*(6499), 65–70. https://doi.org/10.1126/science.aaz3658

De Oliveira, J. A. A., Darby, C. D., & Roel, B. A. (2010). A linked separable–ADAPT VPA assessment model for western horse mackerel (Trachurus trachurus), accounting for realized fecundity as a function of fish weight. *ICES Journal of Marine Science*, *67*(5), 916–930. https://doi.org/10.1093/icesjms/fsp290

deCastro, M., Gómez-Gesteira, M., Álvarez, I., & Crespo, A. J. C. (2011). Atmospheric modes influence on Iberian Poleward Current variability. *Continental Shelf Research*, *31*(5), 425–432. https://doi.org/10.1016/j.csr.2010.03.004

deCastro, M., Gómez-Gesteira, M., Alvarez, I., & Gesteira, J. L. G. (2009). Present warming within the context of cooling–warming cycles observed since 1854 in the Bay of Biscay. *Continental Shelf Research*, *29*(8), 1053–1059. https://doi.org/10.1016/j.csr.2008.11.016

deCastro, M., Gómez-Gesteira, M., Costoya, X., & Santos, F. (2014). Upwelling influence on the number of extreme hot SST days along the Canary upwelling ecosystem. *Journal of Geophysical Research: Oceans*, *119*(5), 3029–3040. https://doi.org/10.1002/2013JC009745

deCastro, M., Gómez-Gesteira, M., Lorenzo, M. N., Alvarez, I., & Crespo, A. J. C. (2008). Influence of atmospheric modes on coastal upwelling along the western coast of the Iberian Peninsula, 1985 to 2005. *Climate Research*, *36*(2), 169–179.

Denny, M. W., Hunt, L. J. H., Miller, L. P., & Harley, C. D. G. (2009). On the prediction of extreme ecological events. *Ecological Monographs*, *79*(3), 397–421. https://doi.org/10.1890/08-0579.1

Des, M., Martínez, B., deCastro, M., Viejo, R. M., Sousa, M. C., & Gómez-Gesteira, M. (2020). The impact of climate change on the geographical distribution of habitat-forming macroalgae in the Rías Baixas. *Marine Environmental Research*, *161*, 105074. https://doi.org/10.1016/j.marenvres.2020.105074

Deser, C., Alexander, M. A., Xie, S.-P., & Phillips, A. S. (2010). Sea Surface Temperature Variability: Patterns and Mechanisms. *Annual Review of Marine Science*, *2*(1), 115–143. https://doi.org/10.1146/annurev-marine-120408-151453

Di Lorenzo, E., & Mantua, N. (2016). Multi-year persistence of the 2014/15 North Pacific marine heatwave. *Nature Climate Change*, *6*(11), 1042–1047. https://doi.org/10.1038/nclimate3082

Díaz-Conde, M. P., Carrera, P., Angélico, M. M., Uriarte, A., Nunes, C., Marques, V., Silva, A., Pérez-Pérez, J. R., & Riveiro, I. (2017). Report of the Benchmark Workshop on Pelagic Stocks (WKPELA). *ICES CM 2017/ACOM:35*, 278 pp.

dos Santos Schmidt, T. C., Slotte, A., Olafsdottir, A. H., Nøttestad, L., Jansen, T., Jacobsen, J. A., Bjarnason, S., Lusseau, S. M., Ono, K., Hølleland, S., Thorsen, A., Sandø, A. B., & Kjesbu, O. S. (2024). Poleward spawning of Atlantic mackerel (Scomber scombrus) is facilitated by ocean warming but triggered by energetic constraints. *ICES Journal of Marine Science*, *81*(3), 600–615. https://doi.org/10.1093/icesjms/fsad098

Duarte, C. M. (2017). Reviews and syntheses: Hidden forests, the role of vegetated coastal habitats in the ocean carbon budget. *Biogeosciences*, *14*(2), 301–310. https://doi.org/10.5194/bg-14-301-2017

Duarte, C. M., Agusti, S., Barbier, E., Britten, G. L., Castilla, J. C., Gattuso, J.-P., Fulweiler, R. W., Hughes, T. P., Knowlton, N., Lovelock, C. E., Lotze, H. K., Predragovic, M., Poloczanska, E., Roberts, C., & Worm, B. (2020). Rebuilding marine life. *Nature*, *580*(7801), Article 7801. https://doi.org/10.1038/s41586-020-2146-7

Duarte, L., Viejo, R. M., Martínez, B., deCastro, M., Gómez-Gesteira, M., & Gallardo, T. (2013). Recent and historical range shifts of two canopy-forming seaweeds in North Spain and the link with trends in sea surface temperature. *Acta Oecologica*, *51*, 1–10. https://doi.org/10.1016/j.actao.2013.05.002

Dunnington, D., Thorne, B., & Hernangómez, D. (2021). ggspatial: Spatial Data Framework for ggplot2. *R Package Version 1.1.5.* https://cran.r-project.org/web/packages/ggspatial/index.html

El Mghazli, H., Znari, M., & Mounir, A. (2022). Stock Discrimination in the Horse Mackerel Trachurus trachurus (Teleostei: Carangidae) off the Moroccan Atlantic Coastal Waters using a Morphometric-Meristic Analysis. Thalassas: *An International Journal of Marine Sciences, 38*(1), 171–181. https://doi.org/10.1007/s41208-021-00372-7

Erauskin-Extramiana, M., Alvarez, P., Arrizabalaga, H., Ibaibarriaga, L., Uriarte, A., Cotano, U., Santos, M., Ferrer, L., Cabré, A., Irigoien, X., & Chust, G. (2019). Historical trends and future distribution of anchovy spawning in the Bay of Biscay. *Deep Sea Research Part II: Topical Studies in Oceanography*, *159*, 169–182. https://doi.org/10.1016/j.dsr2.2018.07.007

European Commission. (2023, December). *Northern agreements*. Oceans and Fisheries. https://oceans-and-fisheries.ec.europa.eu/fisheries/international-agreements/northern-agreements_en

FAO. (2022). *The State of World Fisheries and Aquaculture 2022: Towards Blue Transformation*. FAO. https://doi.org/10.4060/cc0461en

Feng, M., Caputi, N., Chandrapavan, A., Chen, M., Hart, A., & Kangas, M. (2021). Multi-year marine cold-spells off the west coast of Australia and effects on fisheries. *Journal of Marine Systems*, *214*, 103473. https://doi.org/10.1016/j.jmarsys.2020.103473

Fernández, C. (2011). The retreat of large brown seaweeds on the north coast of Spain: The case of Saccorhiza polyschides. *European Journal of Phycology*, *46*(4), 352–360. https://doi.org/10.1080/09670262.2011.617840

Fernández, C. (2016). Current status and multidecadal biogeographical changes in rocky intertidal algal assemblages: The northern Spanish coast. *Estuarine, Coastal and Shelf Science*, *171*, 35–40. https://doi.org/10.1016/j.ecss.2016.01.026

Fernández, C., & Anadón, R. (2008). La cornisa Cantábrica: Un escenario de cambios de distribución de comunidades intermareales. *ALGAS, Boletín Informativo de La Sociedad Española de Ficología*, *39*, 30–32.

Fewings, M. R., & Brown, K. S. (2019). Regional Structure in the Marine Heat Wave of Summer 2015 Off the Western United States. *Frontiers in Marine Science*, *6*. https://www.frontiersin.org/articles/10.3389/fmars.2019.00564

Fontoura, L., D'Agata, S., Gamoyo, M., Barneche, D. R., Luiz, O. J., Madin, E. M. P., Eggertsen, L., & Maina, J. M. (2022). Protecting connectivity promotes successful biodiversity and fisheries conservation. *Science*, *375*(6578), 336–340. https://doi.org/10.1126/science.abg4351

Fox-Kemper, B., Hewitt, H. T., Xiao, C., Aðalgeirsdóttir, G. G., Drijfhout, S. S., Edwards, T. L., Golledge, N. R., Hemer, M., Kopp, R. E., Krinner, G., Mix, A., Notz, D., Nowicki, S., Nurhati, I. S., Ruiz, L., Sallée, J.-B., Slangen, A. B. A., & Yu, Y. (2021). Ocean, Cryosphere and Sea Level Change. In *Climate Change 2021 – The Physical Science Basis: Working Group I Contribution to the Sixth Assessment Report of the Intergovernmental Panel on Climate Change* (pp. 1211–1362). Cambridge University Press. https://doi.org/10.1017/9781009157896.011

Franco, J. N., Tuya, F., Bertocci, I., Rodríguez, L., Martínez, B., Sousa-Pinto, I., & Arenas, F. (2018). The 'golden kelp' Laminaria ochroleuca under global change: Integrating multiple eco-physiological responses with species distribution models. *Journal of Ecology*, *106*(1), 47–58. https://doi.org/10.1111/1365-2745.12810

Frank, K. T., & Brickman, D. (2000). Allee effects and compensatory population dynamics within a stock complex. *Canadian Journal of Fisheries and Aquatic Sciences*, *57*(3), 513–517. https://doi.org/10.1139/f00-024

Free, C. M., Mangin, T., Molinos, J. G., Ojea, E., Burden, M., Costello, C., & Gaines, S. D. (2020). Realistic fisheries management reforms could mitigate the impacts of climate change in most countries. *PLOS ONE*, *15*(3), e0224347. https://doi.org/10.1371/journal.pone.0224347

Free, C. M., Thorson, J. T., Pinsky, M. L., Oken, K. L., Wiedenmann, J., & Jensen, O. P. (2019). Impacts of historical warming on marine fisheries production. *Science*, *363*(6430), 979–983. https://doi.org/10.1126/science.aau1758

Freedman, R. M., Brown, J. A., Caldow, C., & Caselle, J. E. (2020). Marine protected areas do not prevent marine heatwave-induced fish community structure changes in a temperate transition zone. *Scientific Reports*, *10*(1), 21081. https://doi.org/10.1038/s41598-020-77885-3

Frías, M. D., Fernández, J., Sáenz, J., & Rodríguez-Puebla, C. (2005). Operational predictability of monthly average maximum temperature over the Iberian Peninsula using DEMETER simulations and downscaling. *Tellus A*, *57*(3), 448–463. https://doi.org/10.1111/j.1600-0870.2005.00105.x

Frölicher, T. L. (2019). Chapter 5—Extreme climatic events in the ocean. In A. M. Cisneros-Montemayor, W. W. L. Cheung, & Y. Ota (Eds.), *Predicting Future Oceans* (pp. 53–60). Elsevier. https://doi.org/10.1016/B978-0-12-817945-1.00005-8

Frölicher, T. L., & Laufkötter, C. (2018). Emerging risks from marine heat waves. *Nature Communications*, *9*(1), Article 1. https://doi.org/10.1038/s41467-018-03163-6

Frölicher, T. L., Fischer, E. M., & Gruber, N. (2018). Marine heatwaves under global warming. *Nature*, *560*(7718), Article 7718. https://doi.org/10.1038/s41586-018-0383-9

Fry, F. E. J. (1971). The Effect of Environmental Factors on the Physiology of Fish. In W. S. Hoar & D. J. Randall (Eds.), *Fish Physiology* (Vol. 6, pp. 1–98). Academic Press. https://doi.org/10.1016/S1546-5098(08)60146-6

FutureMARES (2024). *HOME*. FutureMARES. https://www.futuremares.eu/

Gaitán, C. F. (2016). Effects of variance adjustment techniques and time-invariant transfer functions on heat wave duration indices and other metrics derived from downscaled time-series. Study case: Montreal, Canada. *Natural Hazards*, *83*(3), 1661–1681. https://doi.org/10.1007/s11069-016-2381-2

Gaitán, C. F., Hsieh, W. W., Cannon, A. J., & Gachon, P. (2014). Evaluation of Linear and Non-Linear Downscaling Methods in Terms of Daily Variability and Climate Indices: Surface Temperature in Southern Ontario and Quebec, Canada. *Atmosphere-Ocean*, *52*(3), 211–221. https://doi.org/10.1080/07055900.2013.857639

García-Reyes, M., & Largier, J. (2010). Observations of increased wind-driven coastal upwelling off central California. *Journal of Geophysical Research: Oceans*, *115*(C4). https://doi.org/10.1029/2009JC005576

García-Reyes, M., Sydeman, W. J., Schoeman, D. S., Rykaczewski, R. R., Black, B. A., Smit, A. J., & Bograd, S. J. (2015). Under Pressure: Climate Change, Upwelling, and Eastern Boundary Upwelling Ecosystems. *Frontiers in Marine Science*, *2*. https://www.frontiersin.org/articles/10.3389/fmars.2015.00109

Garcia-Soto, C., Pingree, R. D., & Valdés, L. (2002). Navidad development in the southern Bay of Biscay: Climate change and swoddy structure from remote sensing and in situ measurements. *Journal of Geophysical Research: Oceans*, *107*(C8), 28-1-28–29. https://doi.org/10.1029/2001JC001012

Garrido, S., Cristóvão, A., Caldeira, C., Ben-Hamadou, R., Baylina, N., Batista, H., Saiz, E., Peck, M. A., Ré, P., & Santos, A. M. P. (2016). Effect of temperature on the growth, survival, development and foraging behaviour of Sardina pilchardus larvae. *Marine Ecology Progress Series*, *559*, 131–145. https://doi.org/10.3354/meps11881

GEBCO Compilation Group. (2021). *GEBCO 2021 Grid* [dataset]. https://doi.org/10.5285/c6612cbe-50b3-0cff-e053-6c86abc09f8f

GEBCO Compilation Group. (2023). *GEBCO 2023 Grid* [dataset]. https://doi.org/doi:10.5285/f98b053b-0cbc-6c23-e053-6c86abc0af7b

Gelman, A. (2008). Scaling regression inputs by dividing by two standard deviations. *Statistics in Medicine*, *27*(15), 2865–2873. https://doi.org/10.1002/sim.3107

Gelman, A., & Hill, J. (2006). *Data Analysis Using Regression and Multilevel/Hierarchical Models*. Cambridge: Cambridge University Press. https://doi.org/10.1017/CBO9780511790942

Gentemann, C. L., Fewings, M. R., & García-Reyes, M. (2017). Satellite sea surface temperatures along the West Coast of the United States during the 2014–2016 northeast Pacific marine heat wave. *Geophysical Research Letters*, *44*(1), 312–319. https://doi.org/10.1002/2016GL071039

Gil, J., Valdés, L., Moral, M., Sánchez, R., & Garcia-Soto, C. (2002). Mesoscale variability in a high-resolution grid in the Cantabrian Sea (southern Bay of Biscay), May 1995. *Deep Sea Research Part I: Oceanographic Research Papers*, *49*(9), 1591–1607. https://doi.org/10.1016/S0967-0637(02)00041-9

Gómez-Gesteira, M., deCastro, M., Alvarez, I., & Gómez-Gesteira, J. L. (2008). Coastal sea surface temperature warming trend along the continental part of the Atlantic Arc (1985–2005). *Journal of Geophysical Research: Oceans*, *113*(C4). https://doi.org/10.1029/2007JC004315

Gómez-Gesteira, M., Gimeno, L., deCastro, M., Lorenzo, M. N., Alvarez, I., Nieto, R., Taboada, J. J., Crespo, A. J. C., Ramos, A. M., Iglesias, I., Gómez-Gesteira, J. L., Santo, F. E., Barriopedro, D., & Trigo, I. F. (2011). The state of climate in NW Iberia. *Climate Research*, *48*(2–3), 109–144. https://doi.org/10.3354/cr00967

González-Gil, R., González Taboada, F., Cáceres, C., Largier, J. L., & Anadón, R. (2018). Winter-mixing preconditioning of the spring phytoplankton bloom in the Bay of Biscay. *Limnology and Oceanography*, *63*(3), 1264–1282. https://doi.org/10.1002/lno.10769

González-Gil, R., Taboada, F. G., Höfer, J., & Anadón, R. (2015). Winter mixing and coastal upwelling drive long-term changes in zooplankton in the Bay of Biscay (1993–2010). *Journal of Plankton Research*, *37*(2), 337–351. https://doi.org/10.1093/plankt/fbv001

Gordó-Vilaseca, C., Stephenson, F., Coll, M., Lavin, C., & Costello, M. J. (2023). Three decades of increasing fish biodiversity across the northeast Atlantic and the Arctic Ocean. *Proceedings of the National Academy of Sciences*, *120*(4), e2120869120. https://doi.org/10.1073/pnas.2120869120

Grolemund, G., & Wickham, H. (2011). Dates and Times Made Easy with lubridate. *Journal of Statistical Software*, *40*, 1–25. https://doi.org/10.18637/jss.v040.i03

Gruber, N., Bakker, D. C. E., DeVries, T., Gregor, L., Hauck, J., Landschützer, P., McKinley, G. A., & Müller, J. D. (2023). Trends and variability in the ocean carbon sink. *Nature Reviews Earth & Environment*, *4*(2), 119–134. https://doi.org/10.1038/s43017-022-00381-x

Gulev, S. K., Thorne, P. W., Ahn, J., Dentener, F. J., Domingues, C. M., Gerland, S., Gong, D., Kaufman, D. S., Nnamchi, H. C., Quaas, J., Rivera, J. A., Sathyendranath, S., Smith, S. L., Trewin, B., von Schuckmann, K., & Vose, R. S. (2021). Changing State of the Climate System. In *Climate Change 2021- The Physical Science Basis: Contribution of Working Group I to the Sixth Assessment Report of the Intergovernmental Panel on Climate Change* (Cambridge University Press, pp. 287–422). https://doi.org/10.1017/9781009157896.004

Guo, X., Gao, Y., Zhang, S., Wu, L., Chang, P., Cai, W., Zscheischler, J., Leung, L. R., Small, J., Danabasoglu, G., Thompson, L., & Gao, H. (2022). Threat by marine heatwaves to adaptive large marine ecosystems in an eddy-resolving model. *Nature Climate Change*, *12*(2), 179–186. https://doi.org/10.1038/s41558-021-01266-5

Haas, B., Mackay, M., Novaglio, C., Fullbrook, L., Murunga, M., Sbrocchi, C., McDonald, J., McCormack, P. C., Alexander, K., Fudge, M., Goldsworthy, L., Boschetti, F., Dutton, I., Dutra, L., McGee, J., Rousseau, Y., Spain, E., Stephenson, R., Vince, J., … Haward, M. (2022). The future of ocean governance. *Reviews in Fish Biology and Fisheries*, *32*(1), 253–270. https://doi.org/10.1007/s11160-020-09631-x

Hannesson, R. (2013). Sharing the Northeast Atlantic mackerel. *ICES Journal of Marine Science*, *70*(2), 259–269. https://doi.org/10.1093/icesjms/fss134

Harris, V., Edwards, M., & Olhede, S. C. (2014). Multidecadal Atlantic climate variability and its impact on marine pelagic communities. *Journal of Marine Systems*, *133*, 55–69. https://doi.org/10.1016/j.jmarsys.2013.07.001

Hastie, T., & Tibshirani, R. (1986). Generalized Additive Models. *Statistical Science*, *1*(3), 297–310. https://doi.org/10.1214/ss/1177013604

He, Q., & Silliman, B. R. (2019). Climate Change, Human Impacts, and Coastal Ecosystems in the Anthropocene. *Current Biology*, *29*(19), R1021–R1035. https://doi.org/10.1016/j.cub.2019.08.042

Hernangómez, D. (2021). mapSpain: Administrative Boundaries of Spain. *R Package Version 0.2.3.* https://cran.r-project.org/web/packages/mapSpain/index.html

Herrero, J. J., Simes, D. C., Abecasis, R., Relvas, P., Garel, E., Ventura Martins, P., & Santos, R. (2023). Monitoring invasive macroalgae in southern Portugal: Drivers and citizen science contribution. *Frontiers in Environmental Science, 11*. https://doi.org/10.3389/fenvs.2023.1324600

Hersbach, H., Bell, B., Berrisford, P., Hirahara, S., Horányi, A., Muñoz-Sabater, J., Nicolas, J., Peubey, C., Radu, R., Schepers, D., Simmons, A., Soci, C., Abdalla, S., Abellan, X., Balsamo, G., Bechtold, P., Biavati, G., Bidlot, J., Bonavita, M., … Thépaut, J.-N. (2020). The ERA5 global reanalysis. *Quarterly Journal of the Royal Meteorological Society*, *146*(730), 1999–2049. https://doi.org/10.1002/qj.3803

Hirsch, A. L., Ridder, N. N., Perkins-Kirkpatrick, S. E., & Ukkola, A. (2021). CMIP6 MultiModel Evaluation of Present-Day Heatwave Attributes. *Geophysical Research Letters*, *48*(22), e2021GL095161. https://doi.org/10.1029/2021GL095161

Hobday, A. J., Alexander, L. V., Perkins, S. E., Smale, D. A., Straub, S. C., Oliver, E. C. J., Benthuysen, J. A., Burrows, M. T., Donat, M. G., Feng, M., Holbrook, N. J., Moore, P. J., Scannell, H. A., Sen Gupta, A., & Wernberg, T. (2016). A hierarchical approach to defining marine heatwaves. *Progress in Oceanography*, *141*, 227–238. https://doi.org/10.1016/j.pocean.2015.12.014

Hobday, A. J., Burrows, M. T., Filbee-Dexter, K., Holbrook, N. J., Sen Gupta, A., Smale, D. A., Smith, K. E., Thomsen, M. S., & Wernberg, T. (2023). With the arrival of El Niño, prepare for stronger marine heatwaves. *Nature*, *621*(7977), 38–41. https://doi.org/10.1038/d41586-023-02730-2

Hoegh-Guldberg, O., Northrop, E., & Lubchenco, J. (2019). The ocean is key to achieving climate and societal goals. *Science*, *365*(6460), 1372–1374. https://doi.org/10.1126/science.aaz4390

Holbrook, N. J., Scannell, H. A., Sen Gupta, A., Benthuysen, J. A., Feng, M., Oliver, E. C. J., Alexander, L. V., Burrows, M. T., Donat, M. G., Hobday, A. J., Moore, P. J., Perkins-Kirkpatrick, S. E., Smale, D. A., Straub, S. C., & Wernberg, T. (2019). A global assessment of marine heatwaves and their drivers. *Nature Communications*, *10*(1), Article 1. https://doi.org/10.1038/s41467-019-10206-z

Houde, E. D. (2008). Emerging from Hjort's Shadow. *Journal of Northwest Atlantic Fishery Science*, *41*, 53–70. https://doi.org/10.2960/J.v41.m634

Houde, E. D. (2016). Recruitment Variability. In *Fish Reproductive Biology* (pp. 98–187). John Wiley & Sons, Ltd. https://doi.org/10.1002/9781118752739.ch3

Hughes, K. M., Dransfeld, L., & Johnson, M. P. (2014). Changes in the spatial distribution of spawning activity by north-east Atlantic mackerel in warming seas: 1977–2010. *Marine Biology*, *161*(11), 2563–2576. https://doi.org/10.1007/s00227-014-2528-1

Ibaibarriaga, L., Irigoien, X., Santos, M., Motos, L., Fives, J. M., Franco, C., Lago De Lanzós, A., Acevedo, S., Bernal, M., Bez, N., Eltink, G., Farinha, A., Hammer, C., Iversen, S. A., Milligan, S. P., & Reid, D. G. (2007). Egg and larval distributions of seven fish species in north-east Atlantic waters. *Fisheries Oceanography*, *16*(3), 284–293. https://doi.org/10.1111/j.1365-2419.2007.00430.x

ICES. (1996). Report of the Working Group on the Assessment of Mackerel, Horse Mackerel, Sardine and Anchovy (WGMHSA). *ICES CM 1996/Assess:7*, 340pp.

ICES. (2005). Report of the Working Group on the Assessment of Mackerel, Horse Mackerel, Sardine and Anchovy (WGMHSA). *ICES CM 2005/ACFM:08*, 477pp.

ICES. (2020). *Working Group on Widely Distributed Stocks (WGWIDE)* [Report]. ICES Scientific Reports. https://doi.org/10.17895/ices.pub.7475

ICES. (2021a). *Bay of Biscay and the Iberian Coast ecoregion – Ecosystem Overview* [Report]. ICES Advice: Ecosystem Overviews. https://doi.org/10.17895/ices.advice.9436

ICES. (2021b). *Bay of Biscay and the Iberian Coast ecoregion – Fisheries overview* [Report]. ICES Advice: Fisheries Overviews. https://doi.org/10.17895/ices.advice.9100

ICES. (2021c). EU request to ICES on the assessment of a new rebuilding plan for western horse mackerel (Trachurus trachurus) in ICES Subarea 8 and divisions 2.a, 4.a, 5.b, 6.a, 7.a–c, and 7.e–k. *ICES Advice: Special Requests*. https://doi.org/10.17895/ices.advice.8039

ICES. (2021d). Stock Annex: Southern Sardine stock Annex (Divisions 8.c and 9.a). *ICES Stock Annexes*. https://doi.org/10.17895/ices.pub.18623345.v1

ICES. (2021e). *The Workshop for the review of the assessment of a new rebuilding plan for Western Horse Mackerel (WKWHMRP)* [Report]. ICES Scientific Reports. https://doi.org/10.17895/ices.pub.8023

ICES. (2021f). *Working Group on Southern Horse Mackerel, Anchovy and Sardine (WGHANSA)* [Report]. ICES Scientific Reports. https://doi.org/10.17895/ices.pub.8138

ICES. (2022). *Working Group on Widely Distributed Stocks (WGWIDE)* [Report]. ICES Scientific Reports. https://doi.org/10.17895/ices.pub.21088804.v1

ICES. (2023a). *Working Group on Southern Horse Mackerel, Anchovy and Sardine (WGHANSA)* [Report]. ICES Scientific Reports. https://doi.org/10.17895/ices.pub.23507922.v1

ICES. (2023b). *Working Group on Widely Distributed Stocks (WGWIDE)* [Report]. ICES Scientific Reports. https://doi.org/10.17895/ices.pub.24025482.v1

IPBES. (2019a). *Global assessment report on biodiversity and ecosystem services of the Intergovernmental Science-Policy Platform on Biodiversity and Ecosystem Services*. Zenodo. https://doi.org/10.5281/zenodo.6417333

IPBES. (2019b). *Summary for policymakers of the global assessment report on biodiversity and ecosystem services*. Zenodo. https://doi.org/10.5281/zenodo.3553579

IPCC. (2023). Climate Change 2023: Synthesis Report. Contribution of Working Groups I, II and III to the Sixth Assessment Report of the Intergovernmental Panel on Climate Change. *IPCC, Geneva, Switzerland*, 35–115. https://doi.org/10.59327/IPCC/AR6-9789291691647

Irigoien, X., Fiksen, Ø., Cotano, U., Uriarte, A., Alvarez, P., Arrizabalaga, H., Boyra, G., Santos, M., Sagarminaga, Y., Otheguy, P., Etxebeste, E., Zarauz, L., Artetxe, I., & Motos, L. (2007). Could Biscay Bay Anchovy recruit through a spatial loophole? *Progress in Oceanography*, *74*(2), 132–148. https://doi.org/10.1016/j.pocean.2007.04.011

Izquierdo, P., Rico, J. M., Taboada, F. G., González-Gil, R., & Arrontes, J. (2022a). Characterization of marine heatwaves in the Cantabrian Sea, SW Bay of Biscay. *Estuarine, Coastal and Shelf Science*, *274*, 107923. https://doi.org/10.1016/j.ecss.2022.107923

Izquierdo, P., Taboada, F. G., González-Gil, R., Arrontes, J., & Rico, J. M. (2022b). Alongshore upwelling modulates the intensity of marine heatwaves in a temperate coastal sea. *Science of The Total Environment*, *835*, 155478. https://doi.org/10.1016/j.scitotenv.2022.155478

Jacox, M. G., Alexander, M. A., Bograd, S. J., & Scott, J. D. (2020). Thermal displacement by marine heatwaves. *Nature*, *584*(7819), Article 7819. https://doi.org/10.1038/s41586-020-2534-z

James, N. C., & Whitfield, A. K. (2023). The role of macroalgae as nursery areas for fish species within coastal seascapes. *Cambridge Prisms: Coastal Futures*, *1*, e3. https://doi.org/10.1017/cft.2022.3

Jørgensen, L. B., Ørsted, M., Malte, H., Wang, T., & Overgaard, J. (2022). Extreme escalation of heat failure rates in ectotherms with global warming. *Nature*, *611*(7934), Article 7934. https://doi.org/10.1038/s41586-022-05334-4

Kajtar, J. B., Holbrook, N. J., & Hernaman, V. (2021). A catalogue of marine heatwave metrics and trends for the Australian region. *Journal of Southern Hemisphere Earth Systems Science*, *71*(3), 284–302. https://doi.org/10.1071/ES21014

Kanamori, Y., Takasuka, A., Nishijima, S., & Okamura, H. (2019). Climate change shifts the spawning ground northward and extends the spawning period of chub mackerel in the western North Pacific. *Marine Ecology Progress Series*, *624*, 155–166. https://doi.org/10.3354/meps13037

Kim, Y.-H., Min, S.-K., Zhang, X., Sillmann, J., & Sandstad, M. (2020). Evaluation of the CMIP6 multi-model ensemble for climate extreme indices. *Weather and Climate Extremes*, *29*, 100269. https://doi.org/10.1016/j.wace.2020.100269

Koutantou, K., Brunner, P., & Vazquez-Cuervo, J. (2023). Validation of NASA Sea Surface Temperature Satellite Products Using Saildrone Data. *Remote Sensing*, *15*(9), Article 9. https://doi.org/10.3390/rs15092277

Koutsikopoulos, C., Beillois, P., Leroy, C., & Taillefer, F. (1998). Temporal trends and spatial structures of the sea surface temperature in the Bay of Biscay. *Oceanologica Acta*, *21*(2), 335–344. https://doi.org/10.1016/S0399-1784(98)80020-0

Krause-Jensen, D., & Duarte, C. M. (2016). Substantial role of macroalgae in marine carbon sequestration. *Nature Geoscience*, *9*(10), 737–742. https://doi.org/10.1038/ngeo2790

Kuhn, M. (2008). Building Predictive Models in R Using the caret Package. *Journal of Statistical Software*, *28*, 1–26. https://doi.org/10.18637/jss.v028.i05

Kwiatkowski, L., Torres, O., Bopp, L., Aumont, O., Chamberlain, M., Christian, J. R., Dunne, J. P., Gehlen, M., Ilyina, T., John, J. G., Lenton, A., Li, H., Lovenduski, N. S., Orr, J. C., Palmieri, J., Santana-Falcón, Y., Schwinger, J., Séférian, R., Stock, C. A., … Ziehn, T. (2020). Twenty-first century ocean warming, acidification, deoxygenation, and upper-ocean nutrient and primary production decline from CMIP6 model projections. *Biogeosciences*, *17*(13), 3439–3470. https://doi.org/10.5194/bg-17-3439-2020

Large, W. G., McWilliams, J. C., & Doney, S. C. (1994). Oceanic vertical mixing: A review and a model with a nonlocal boundary layer parameterization. *Reviews of Geophysics*, *32*(4), 363–403. https://doi.org/10.1029/94RG01872

Laufkötter, C., Zscheischler, J., & Frölicher, T. L. (2020). High-impact marine heatwaves attributable to human-induced global warming. *Science*, *369*(6511), 1621–1625. https://doi.org/10.1126/science.aba0690

Laurel, B. J., & Rogers, L. A. (2020). Loss of spawning habitat and prerecruits of Pacific cod during a Gulf of Alaska heatwave. *Canadian Journal of Fisheries and Aquatic Sciences*, *77*(4), 644–650. https://doi.org/10.1139/cjfas-2019-0238

Lavín, A., Moreno-Ventas, X., Ortiz de Zárate, V., Abaunza, P., & Cabanas, J. M. (2007). Environmental variability in the North Atlantic and Iberian waters and its influence on horse mackerel (Trachurus trachurus) and albacore (Thunnus alalunga) dynamics. *ICES Journal of Marine Science*, *64*(3), 425–438. https://doi.org/10.1093/icesjms/fsl042

Lavín, A., Valdés, L., Sánchez, F., Abaunza, P., Forest, A., Boucher, J., Lazure, P., & Jegou, A. M. (2006). *The Bay of Biscay: The encountering of the ocean and the shelf* (pp. 933–999).

Le Cann, B., & Serpette, A. (2009). Intense warm and saline upper ocean inflow in the southern Bay of Biscay in autumn–winter 2006–2007. *Continental Shelf Research*, *29*(8), 1014–1025. https://doi.org/10.1016/j.csr.2008.11.015

Liermann & Hilborn. (2001). Depensation: Evidence, models and implications. *Fish and Fisheries*, *2*(1), 33–58. https://doi.org/10.1046/j.1467-2979.2001.00029.x

Llope, M., Anadón, R., Viesca, L., Quevedo, M., González-Quirós, R., & Stenseth, N. C. (2006). Hydrography of the southern Bay of Biscay shelf-break region: Integrating the multiscale physical variability over the period 1993–2003. *Journal of Geophysical Research: Oceans*, *111*(C9). https://doi.org/10.1029/2005JC002963

Lockwood, S. J., Nichols, J. H., & Coombs, S. H. (1977). The development rates of mackerel (Scomber scombrus L.) eggs over a range of temperatures. *ICES CM 1977/J:13*, 1–8.

Lorenzo, M. N., Taboada, J. J., & Gimeno, L. (2007). Links between circulation weather types and teleconnection patterns and their influence on precipitation patterns in Galicia (NW Spain). *International Journal of Climatology*, *28*(11), 1493–1505. https://doi.org/10.1002/joc.1646

Lourenço, C. R., Zardi, G. I., McQuaid, C. D., Serrão, E. A., Pearson, G. A., Jacinto, R., & Nicastro, K. R. (2016). Upwelling areas as climate change refugia for the distribution and genetic diversity of a marine macroalga. *Journal of Biogeography*, *43*(8), 1595–1607. https://doi.org/10.1111/jbi.12744

Lucio, P., & Martin, I. (1989). Biological aspects of horse mackerel (Trachurus trachurus L. 1758) in the Bay of Biscay in 1987 and 1988. *ICES CM 1989/H:28*. https://www.ices.dk/sites/pub/CM%20Doccuments/1989/H/1989_H28.pdf

Lucio, P., & Uriarte, A. (1990). Aspects of the reproductive biology of the anchovy (Engraulis encrasicolus L. 1758) during 1987 and 1988 in the Bay of Biscay. *ICES CM 1990/H:27*. https://www.ices.dk/sites/pub/CM%20Doccuments/1990/H/1990_H27.pdf

MacKenzie, B. R. (2000). Turbulence, larval fish ecology and fisheries recruitment: A review of field studies. *Oceanologica Acta*, *23*(4), 357–375. https://doi.org/10.1016/S0399-1784(00)00142-0

MaCoBioS (2024). *Home » MacoBios*. MacoBios. https://macobios.eu/

Macreadie, P. I., Costa, M. D. P., Atwood, T. B., Friess, D. A., Kelleway, J. J., Kennedy, H., Lovelock, C. E., Serrano, O., & Duarte, C. M. (2021). Blue carbon as a natural climate solution. *Nature Reviews Earth & Environment*, *2*(12), Article 12. https://doi.org/10.1038/s43017-021-00224-1

Macreadie, P. I., Jarvis, J., Trevathan-Tackett, S. M., & Bellgrove, A. (2017). Seagrasses and Macroalgae: Importance, Vulnerability and Impacts. In *Climate Change Impacts on Fisheries and Aquaculture* (pp. 729–770). John Wiley & Sons, Ltd. https://doi.org/10.1002/9781119154051.ch22

Marin, M., Bindoff, N. L., Feng, M., & Phillips, H. E. (2021). Slower Long-Term Coastal Warming Drives Dampened Trends in Coastal Marine Heatwave Exposure. *Journal of Geophysical Research: Oceans*, *126*(11), e2021JC017930. https://doi.org/10.1029/2021JC017930

Marin, M., Feng, M., Phillips, H. E., & Bindoff, N. L. (2021). A Global, Multiproduct Analysis of Coastal Marine Heatwaves: Distribution, Characteristics, and Long-Term Trends. *Journal of Geophysical Research: Oceans*, *126*(2), e2020JC016708. https://doi.org/10.1029/2020JC016708

Maroto, J. M., & Moran, M. (2014). Detecting the presence of depensation in collapsed fisheries: The case of the Northern cod stock. *Ecological Economics*, *97*, 101–109. https://doi.org/10.1016/j.ecolecon.2013.11.006

Martínez, B., Afonso Carrillo, J., Anadón, R., Araújo, R., Arenas, F., Arrontes, J., Bárbara, I., Borja, A., Díez, I., Duarte, L., Fernández, C., García Tasende, M., Gorostiaga, J. M., Juanes, J. A., Peteiro, C., Puente, A., Rico, J. M., Sangil, C., Sansón Acedo, M., … Viejo, R. M. (2015). Regresión de las algas marinas en las islas Canarias y en la costa atlántica de la Península Ibérica por efecto del cambio climático. *ALGAS, Boletín Informativo de la Sociedad Española de Ficología*, *49*, 5–12.

Massicotte, P., South, A., & Hufkens, K. (2017). rnaturalearth: World Map Data from Natural Earth. *R Package Version 0.1.0.* https://cran.r-project.org/web/packages/rnaturalearth/index.html

Melet, A., Teatini, P., Le Cozannet, G., Jamet, C., Conversi, A., Benveniste, J., & Almar, R. (2020). Earth Observations for Monitoring Marine Coastal Hazards and Their Drivers. *Surveys in Geophysics*, *41*(6), 1489–1534. https://doi.org/10.1007/s10712-020-09594-5

Mendenhall, E., Hendrix, C., Nyman, E., Roberts, P. M., Hoopes, J. R., Watson, J. R., Lam, V. W. Y., & Sumaila, U. R. (2020). Climate change increases the risk of fisheries conflict. *Marine Policy*, *117*, 103954. https://doi.org/10.1016/j.marpol.2020.103954

Mendiola, D., Alvarez, P., Cotano, U., & Martínezde Murguía, A. (2007). Early development and growth of the laboratory reared north-east Atlantic mackerel Scomber scombrus L. *Journal of Fish Biology*, *70*(3), 911–933. https://doi.org/10.1111/j.1095-8649.2007.01355.x

Mendiola, D., Alvarez, P., Cotano, U., Etxebeste, E., & de Murguia, A. M. (2006). Effects of temperature on development and mortality of Atlantic mackerel fish eggs. *Fisheries Research*, *80*(2), 158–168. https://doi.org/10.1016/j.fishres.2006.05.004

Meneghesso, C., Seabra, R., Broitman, B. R., Wethey, D. S., Burrows, M. T., Chan, B. K. K., Guy-Haim, T., Ribeiro, P. A., Rilov, G., Santos, A. M., Sousa, L. L., & Lima, F. P. (2020). Remotely-sensed L4 SST underestimates the thermal fingerprint of coastal upwelling. *Remote Sensing of Environment*, *237*, 111588. https://doi.org/10.1016/j.rse.2019.111588

Minto, C., Myers, R. A., & Blanchard, W. (2008). Survival variability and population density in fish populations. *Nature*, *452*(7185), Article 7185. https://doi.org/10.1038/nature06605

Montero-Serra, I., Edwards, M., & Genner, M. J. (2015). Warming shelf seas drive the subtropicalization of European pelagic fish communities. *Global Change Biology*, *21*(1), 144–153. https://doi.org/10.1111/gcb.12747

Motos, L., Uriarte, A., & Valencia, V. (1996). The spawning environment of the Bay of Biscay anchovy (Engraulis encrasicolus L.). *Scientia Marina*, *60*.

Muhling, B. A., Gaitán, C. F., Stock, C. A., Saba, V. S., Tommasi, D., & Dixon, K. W. (2018). Potential Salinity and Temperature Futures for the Chesapeake Bay Using a Statistical Downscaling Spatial Disaggregation Framework. *Estuaries and Coasts*, *41*(2), 349–372. https://doi.org/10.1007/s12237-017-0280-8

Müller, R., Laepple, T., Bartsch, I., & Wiencke, C. (2009). *Impact of oceanic warming on the distribution of seaweeds in polar and cold-temperate waters*. *52*(6), 617–638. https://doi.org/10.1515/BOT.2009.080

Myers, R. A. (1998). When Do Environment–recruitment Correlations Work? *Reviews in Fish Biology and Fisheries*, *8*(3), 285–305. https://doi.org/10.1023/A:1008828730759

Myers, R. A., Barrowman, N. J., Hutchings, J. A., & Rosenberg, A. A. (1995). Population Dynamics of exploited fish stocks at lowf population levels. *Science, 269*(5227), pp. 1106–1108. doi:10.1126/science.269.5227.1106.

Nash, R. D. M., Dickey-Collas, M., & Kell, L. T. (2009). Stock and recruitment in North Sea herring (*Clupea harengus*); compensation and depensation in the population dynamics. *Fisheries Research*, *95*(1), 88–97. https://doi.org/10.1016/j.fishres.2008.08.003

Neuwirth, E. (2014). RColorBrewer: ColorBrewer Palettes. *R Package Version 1.1-2*. https://cran.wustl.edu/web/packages/RColorBrewer/

Nicastro, K. R., Zardi, G. I., Teixeira, S., Neiva, J., Serrão, E. A., & Pearson, G. A. (2013). Shift happens: Trailing edge contraction associated with recent warming trends threatens a distinct genetic lineage in the marine macroalga Fucus vesiculosus. *BMC Biology*, *11*(1), 6. https://doi.org/10.1186/1741-7007-11-6

Nychka, D., Furrer, R., Paige, J., Sain, S., Gerber, F., Iverson, M., & Research, U. C. for A. (2017). fields: Tools for Spatial Data. *R Package Version 11.6.* https://cran.r-project.org/web/packages/fields/index.html

O'Leary, J. K., Micheli, F., Airoldi, L., Boch, C., De Leo, G., Elahi, R., Ferretti, F., Graham, N. A. J., Litvin, S. Y., Low, N. H., Lummis, S., Nickols, K. J., & Wong, J. (2017). The Resilience of Marine Ecosystems to Climatic Disturbances. *BioScience*, *67*(3), 208–220. https://doi.org/10.1093/biosci/biw161

Olafsdottir, A. H., Utne, K. R., Jacobsen, J. A., Jansen, T., Óskarsson, G. J., Nøttestad, L., Elvarsson, B. Þ., Broms, C., & Slotte, A. (2019). Geographical expansion of Northeast Atlantic mackerel (Scomber scombrus) in the Nordic Seas from 2007 to 2016 was primarily driven by stock size and constrained by low temperatures. *Deep Sea Research Part II: Topical Studies in Oceanography*, *159*, 152–168. https://doi.org/10.1016/j.dsr2.2018.05.02

Oliver, E. C. J. (2019). Mean warming not variability drives marine heatwave trends. *Climate Dynamics*, *53*(3), 1653–1659. https://doi.org/10.1007/s00382-019-04707-2

Oliver, E. C. J., Benthuysen, J. A., Darmaraki, S., Donat, M. G., Hobday, A. J., Holbrook, N. J., Schlegel, R. W., & Sen Gupta, A. (2021). Marine Heatwaves. *Annual Review of Marine Science*, *13*(1), 313–342. https://doi.org/10.1146/annurev-marine-032720-095144

Oliver, E. C. J., Burrows, M. T., Donat, M. G., Sen Gupta, A., Alexander, L. V., Perkins-Kirkpatrick, S. E., Benthuysen, J. A., Hobday, A. J., Holbrook, N. J., Moore, P. J., Thomsen, M. S., Wernberg, T., & Smale, D. A. (2019). Projected Marine Heatwaves in the 21st Century and the Potential for Ecological Impact. *Frontiers in Marine Science*, *6*. https://www.frontiersin.org/articles/10.3389/fmars.2019.00734

Oliver, E. C. J., Donat, M. G., Burrows, M. T., Moore, P. J., Smale, D. A., Alexander, L. V., Benthuysen, J. A., Feng, M., Sen Gupta, A., Hobday, A. J., Holbrook, N. J., Perkins-Kirkpatrick, S. E., Scannell, H. A., Straub, S. C., & Wernberg, T. (2018). Longer and more frequent marine heatwaves over the past century. *Nature Communications*, *9*(1), Article 1. https://doi.org/10.1038/s41467-018-03732-9

Organization for Economic Co-operation and Development. (2016). The Ocean Economy in 2030. *OECD Publishing, Paris*. https://doi.org/10.1787/9789264251724-en.

Østhagen, A., Spijkers, J., & Totland, O. A. (2020). Collapse of cooperation? The North-Atlantic mackerel dispute and lessons for international cooperation on transboundary fish stocks. *Maritime Studies*, *19*(2), 155–165. https://doi.org/10.1007/s40152-020-00172-4

Otero, P., & Ruiz-Villarreal, M. (2008). Wind forcing of the coastal circulation off north and northwest Iberia: Comparison of atmospheric models. *Journal of Geophysical Research: Oceans*, *113*(C10). https://doi.org/10.1029/2008JC004740

Parrish, R. H., Nelson, C. S., & Bakun, A. (1981). Transport Mechanisms and Reproductive Success of Fishes in the California Current. *Biological Oceanography*, *1*(2), 175–203. https://doi.org/10.1080/01965581.1981.10749438

Parrish, R. H., Serra, R., & Grant, W. S. (1989). The Monotypic Sardines, Sardina and Sardinops: Their Taxonomy, Distribution, Stock Structure, and Zoogeography. *Canadian Journal of Fisheries and Aquatic Sciences, 46*(11), 2019–2036. https://doi.org/10.1139/f89-251

Payne, M. R. (2023). Rethinking the effect of marine heatwaves on fish. *Nature*, *621*(7978), 264–265. https://doi.org/10.1038/d41586-023-02594-6

Pearce, A., Lenanton, R., Jackson, G., Moore, J., Feng, M., & Gaughan, D. (2011). *The "marine heat wave" off Western Australia during the summer of 2010/11.* Department of Fisheries, Western Australia. https://fish.gov.au/Archived-Reports/Documents/Pearce_et_al_2011.pdf

Pebesma, E. (2018). Simple Features for R: Standardized Support for Spatial Vector Data. *The R Journal*, *10*(1), 439–446.

Penn, J. L., & Deutsch, C. (2022). Avoiding ocean mass extinction from climate warming. *Science*, *376*(6592), 524–526. https://doi.org/10.1126/science.abe9039

Pérez, F. F., Padín, X. A., Pazos, Y., Gilcoto, M., Cabanas, M., Pardo, P. C., Doval, M. D., & Farina-Busto, L. (2010). Plankton response to weakening of the Iberian coastal upwelling. *Global Change Biology*, *16*(4), 1258–1267. https://doi.org/10.1111/j.1365-2486.2009.02125.x

Pershing, A., Mills, K., Dayton, A., Franklin, B., & Kennedy, B. (2018). Evidence for Adaptation from the 2016 Marine Heatwave in the Northwest Atlantic Ocean. *Oceanography*, *31*. https://doi.org/10.5670/oceanog.2018.213

Petitgas, P., Alheit, J., Peck, M. A., Raab, K., Irigoien, X., Huret, M., Kooij, J. van der, Pohlmann, T., Wagner, C., Zarraonaindia, I., & Dickey-Collas, M. (2012). Anchovy population expansion in the North Sea. *Marine Ecology Progress Series*, *444*, 1–13. https://doi.org/10.3354/meps09451

Pierce, D. (2019). ncdf4: Interface to Unidata netCDF Format Data Files. *R Package Version 1.17.* https://cran.r-project.org/web/packages/ncdf4/

Piñeiro-Corbeira, C., Barreiro, R., & Cremades, J. (2016). Decadal changes in the distribution of common intertidal seaweeds in Galicia (NW Iberia). *Marine Environmental Research*, *113*, 106–115. https://doi.org/10.1016/j.marenvres.2015.11.012

Pipe, R. K., & Walker, P. (1987). The effect of temperature on development and hatching of scad, Trachurus trachurus L., eggs. *Journal of Fish Biology*, *31*(5), 675–682. https://doi.org/10.1111/j.1095-8649.1987.tb05270.x

Planque, B., Bellier, E., & Lazure, P. (2007). Modelling potential spawning habitat of sardine (Sardina pilchardus) and anchovy (Engraulis encrasicolus) in the Bay of Biscay. *Fisheries Oceanography*, *16*(1), 16–30. https://doi.org/10.1111/j.1365-2419.2006.00411.x

Platt, T., Fuentes-Yaco, C., & Frank, K. T. (2003). Spring algal bloom and larval fish survival. *Nature*, *423*(6938), Article 6938. https://doi.org/10.1038/423398b

Puillat, I., Lazure, P., Jégou, A. M., Lampert, L., & Miller, P. I. (2004). Hydrographical variability on the French continental shelf in the Bay of Biscay, during the 1990s. *Continental Shelf Research*, *24*(10), 1143–1163. https://doi.org/10.1016/j.csr.2004.02.008

Ramos, E., Guinda, X., Puente, A., de la Hoz, C. F., & Juanes, J. A. (2020). Changes in the distribution of intertidal macroalgae along a longitudinal gradient in the northern coast of Spain. *Marine Environmental Research*, *157*, 104930. https://doi.org/10.1016/j.marenvres.2020.104930

Raybaud, V., Bacha, M., Amara, R., & Beaugrand, G. (2017). Forecasting climate-driven changes in the geographical range of the European anchovy (Engraulis encrasicolus). *ICES Journal of Marine Science*, *74*(5), 1288–1299. https://doi.org/10.1093/icesjms/fsx003

Reed, D., Washburn, L., Rassweiler, A., Miller, R., Bell, T., & Harrer, S. (2016). Extreme warming challenges sentinel status of kelp forests as indicators of climate change. *Nature Communications*, *7*(1), Article 1. https://doi.org/10.1038/ncomms13757

Reynolds, R. W., & Chelton, D. B. (2010). Comparisons of Daily Sea Surface Temperature Analyses for 2007–08. *Journal of Climate*, *23*(13), 3545–3562. https://doi.org/10.1175/2010JCLI3294.1

Reynolds, R. W., Smith, T. M., Liu, C., Chelton, D. B., Casey, K. S., & Schlax, M. G. (2007). Daily High-Resolution-Blended Analyses for Sea Surface Temperature. *Journal of Climate*, *20*(22), 5473–5496. https://doi.org/10.1175/2007JCLI1824.1

Rhein, M., Rintoul, S. R., Aoki, S., Campos, E., Chambers, D., Feely, R. A., Gulev, S., Johnson, G. C., Josey, S. A., Kostianoy, A., Mauritzen, C., Roemmich, D., Talley, L. D., & Wang, F. (2013). Observations: Ocean. In *Climate Change 2013—The Physical Science Basis: Contribution of Working Group I to the Fifth Assessment Report of the Intergovernmental Panel on Climate Change* (pp. 255–315). Cambridge University Press. https://www.ipcc.ch/report/ar5/wg1/observations-ocean/

Rochet, M.-J. (2000). A comparative approach to life-history strategies and tactics among four orders of teleost fish. *ICES Journal of Marine Science*, *57*(2), 228–239. https://doi.org/10.1006/jmsc.2000.0641

Rodríguez-Basalo, A., Punzón, A., Ceballos-Roa, E., Jordà, G., González-Irusta, J. M., & Massutí, E. (2022). Fisheries-based approach to disentangle mackerel (Scomber scombrus) migration in the Cantabrian Sea. *Fisheries Oceanography*, *31*(4), 443–455. https://doi.org/10.1111/fog.12594

Rodriguez-Puebla, C., Encinas, A. H., Nieto, S., & Garmendia, J. (1998). Spatial and temporal patterns of annual precipitation variability over the Iberian Peninsula. *International Journal of Climatology*, *18*(3), 299–316. https://doi.org/10.1002/(SICI)1097-0088(19980315)18:3<299::AID-JOC247>3.0.CO;2-L

Ruckelshaus, M., Doney, S. C., Galindo, H. M., Barry, J. P., Chan, F., Duffy, J. E., English, C. A., Gaines, S. D., Grebmeier, J. M., Hollowed, A. B., Knowlton, N., Polovina, J., Rabalais, N. N., Sydeman, W. J., & Talley, L. D. (2013). Securing ocean benefits for society in the face of climate change. *Marine Policy*, *40*, 154–159. https://doi.org/10.1016/j.marpol.2013.01.009

Ruzicka, J., Chiaverano, L., Coll, M., Garrido, S., Tam, J., Murase, H., Robinson, K., Romagnoni, G., Shannon, L., Silva, A., Szalaj, D., & Watari, S. (2024). The role of small pelagic fish in diverse ecosystems: Knowledge gleaned from food-web models. *Marine Ecology Progress Series*, *SPF2*. https://doi.org/10.3354/meps14513

Sáenz, J., Zubillaga, J., & Rodríguez-Puebla, C. (2001). Interannual variability of winter precipitation in northern Iberian Peninsula. *International Journal of Climatology*, *21*(12), 1503–1513. https://doi.org/10.1002/joc.699

Samhouri, J. F., Feist, B. E., Fisher, M. C., Liu, O., Woodman, S. M., Abrahms, B., Forney, K. A., Hazen, E. L., Lawson, D., Redfern, J., & Saez, L. E. (2021). Marine heatwave challenges solutions to human–wildlife conflict. *Proceedings of the Royal Society B: Biological Sciences*, *288*(1964), 20211607. https://doi.org/10.1098/rspb.2021.1607

Santos, A. M. P., de Fátima Borges, M., & Groom, S. (2001). Sardine and horse mackerel recruitment and upwelling off Portugal. *ICES Journal of Marine Science*, *58*(3), 589–596. https://doi.org/10.1006/jmsc.2001.1060

Sanz-Lázaro, C. (2016). Climate extremes can drive biological assemblages to early successional stages compared to several mild disturbances. *Scientific Reports*, *6*(1), Article 1. https://doi.org/10.1038/srep30607

Sargent, R. C., & Gross, M. R. (1985). Parental investment decision rules and the Concorde fallacy. *Behavioral Ecology and Sociobiology*, *17*(1), 43–45. https://doi.org/10.1007/BF00299427

Schickele, A., Goberville, E., Leroy, B., Beaugrand, G., Hattab, T., Francour, P., & Raybaud, V. (2020). European small pelagic fish distribution under global change scenarios. *Fish and Fisheries*, *22*(1), 212–225. https://doi.org/10.1111/faf.12515

Schlegel, R. W. (2017). *Coastal marine heatwaves: Understanding extreme forces*. https://etd.uwc.ac.za:443/xmlui/handle/11394/6445

Schlegel, R. W., & Smit, A. J. (2018). heatwaveR: A central algorithm for the detection of heatwaves and cold-spells. *Journal of Open Source Software*, *3*(27), 821. https://doi.org/10.21105/joss.00821

Schlegel, R. W., Darmaraki, S., Benthuysen, J. A., Filbee-Dexter, K., & Oliver, E. C. J. (2021). Marine cold-spells. *Progress in Oceanography*, *198*, 102684. https://doi.org/10.1016/j.pocean.2021.102684

Schlegel, R. W., Oliver, E. C. J., & Chen, K. (2021). Drivers of Marine Heatwaves in the Northwest Atlantic: The Role of Air–Sea Interaction During Onset and Decline. *Frontiers in Marine Science*, *8*. https://www.frontiersin.org/articles/10.3389/fmars.2021.627970

Schlegel, R. W., Oliver, E. C. J., Hobday, A. J., & Smit, A. J. (2019). Detecting Marine Heatwaves With Sub-Optimal Data. *Frontiers in Marine Science*, *6*. https://www.frontiersin.org/articles/10.3389/fmars.2019.00737

Schlegel, R. W., Oliver, E. C. J., Perkins-Kirkpatrick, S., Kruger, A., & Smit, A. J. (2017). Predominant Atmospheric and Oceanic Patterns during Coastal Marine Heatwaves. *Frontiers in Marine Science*, *4*. https://www.frontiersin.org/articles/10.3389/fmars.2017.00323

Seabra, R., Varela, R., Santos, A. M., Gómez-Gesteira, M., Meneghesso, C., Wethey, D. S., & Lima, F. P. (2019). Reduced Nearshore Warming Associated With Eastern Boundary Upwelling Systems. *Frontiers in Marine Science*, *6*. https://www.frontiersin.org/articles/10.3389/fmars.2019.00104

Seibel, B. A., & Drazen, J. C. (2007). The rate of metabolism in marine animals: Environmental constraints, ecological demands and energetic opportunities. *Philosophical Transactions of the Royal Society of London. Series B, Biological Sciences*, *362*(1487), 2061–2078. https://doi.org/10.1098/rstb.2007.2101

Sibly, R. M., & Hone, J. (2002). Population growth rate and its determinants: An overview. *Philosophical Transactions of the Royal Society of London. Series B: Biological Sciences*, *357*(1425), 1153–1170. https://doi.org/10.1098/rstb.2002.1117

Simon, A., Poppeschi, C., Plecha, S., Charria, G., & Russo, A. (2023). Coastal and regional marine heatwaves and cold-spells in the Northeast Atlantic. *EGUsphere*, 1–25. https://doi.org/10.5194/egusphere-2023-430

Simpson, G. L., & Singmann, H. (2021). gratia: Graceful 'ggplot'-Based Graphics and Other Functions for GAMs Fitted Using 'mgcv'. *R Package Version 0.5.1.* https://cran.r-project.org/web/packages/gratia/

Simpson, J. H., & Sharples, J. (2012). *Introduction to the Physical and Biological Oceanography of Shelf Seas*. Cambridge University Press. https://doi.org/10.1017/CBO9781139034098

Smale, D. A., & Wernberg, T. (2009). Satellite-derived SST data as a proxy for water temperature in nearshore benthic ecology. *Marine Ecology Progress Series*, *387*, 27–37. https://doi.org/10.3354/meps08132

Smale, D. A., & Wernberg, T. (2013). Extreme climatic event drives range contraction of a habitat-forming species. *Proceedings of the Royal Society B: Biological Sciences*, *280*(1754), 20122829. https://doi.org/10.1098/rspb.2012.2829

Smale, D. A., Wernberg, T., Oliver, E. C. J., Thomsen, M., Harvey, B. P., Straub, S. C., Burrows, M. T., Alexander, L. V., Benthuysen, J. A., Donat, M. G., Feng, M., Hobday, A. J., Holbrook, N. J., Perkins-Kirkpatrick, S. E., Scannell, H. A., Sen Gupta, A., Payne, B. L., & Moore, P. J. (2019). Marine heatwaves threaten global biodiversity and the provision of ecosystem services. *Nature Climate Change*, *9*(4), Article 4. https://doi.org/10.1038/s41558-019-0412-1

Smit, A. J., Roberts, M., Anderson, R. J., Dufois, F., Dudley, S. F. J., Bornman, T. G., Olbers, J., & Bolton, J. J. (2013). A Coastal Seawater Temperature Dataset for Biogeographical Studies: Large Biases between In Situ and Remotely-Sensed Data Sets around the Coast of South Africa. *PLOS ONE*, *8*(12), e81944. https://doi.org/10.1371/journal.pone.0081944

Smith-Vanith. (1986). Carangidae. In *Fishes of the North-eastern Atlantic and the Mediterranean—UNESCO Biblioteca Digital* (Whitehead, P.J.P., Bauchot, M.L., Hureau, J.C., Nielsen, J. and Tortonese, E. (eds.), Vol. 2, pp. 815–844). https://unesdoc.unesco.org/ark:/48223/pf0000063661

Smith-Vaniz, W. F., Sidibe, A., Nunoo, F., Lindeman, K., Williams, A. B., Quartey, R., Camara, K., Carpenter, K. E., Montiero, V., de Morais, L., Djiman, R., Sylla, M., & Sagna, A. (2015). Trachurus trachurus. The IUCN Red List of Threatened Species. *2015: E.T198647A43157137*. https://dx.doi.org/10.2305/IUCN.UK.2015-4.RLTS.T198647A43157137.en

Smith, K. E., Aubin, M., Burrows, M. T., Filbee-Dexter, K., Hobday, A. J., Holbrook, N. J., King, N. G., Moore, P. J., Sen Gupta, A., Thomsen, M., Wernberg, T., Wilson, E., & Smale, D. A. (2024). Global impacts of marine heatwaves on coastal foundation species. *Nature Communications*, *15*(1), 5052. https://doi.org/10.1038/s41467-024-49307-9

Smith, K. E., Burrows, M. T., Hobday, A. J., King, N. G., Moore, P. J., Sen Gupta, A., Thomsen, M. S., Wernberg, T., & Smale, D. A. (2023). Biological Impacts of Marine Heatwaves. *Annual Review of Marine Science*, *15*(1), null. https://doi.org/10.1146/annurev-marine-032122-121437

Smith, K. E., Burrows, M. T., Hobday, A. J., Sen Gupta, A., Moore, P. J., Thomsen, M., Wernberg, T., & Smale, D. A. (2021). Socioeconomic impacts of marine heatwaves: Global issues and opportunities. *Science*, *374*(6566), eabj3593. https://doi.org/10.1126/science.abj3593

Solá, A., Motos, L., Franco, C., & Lago De Lanzós, A. (1990). Seasonal ocurrence of pelagic fish egss and larvae in the Cantabrian Sea (VIIIc) and Galicia (IXa) from 1987 to 1989. ICES CM 1990/H:25. https://www.ices.dk/sites/pub/CM%20Doccuments/1990/H/1990_H25.pdf

Somavilla Cabrillo, R., González-Pola, C., Ruiz-Villarreal, M., & Lavín Montero, A. (2011). Mixed layer depth (MLD) variability in the southern Bay of Biscay. Deepening of winter MLDs concurrent with generalized upper water warming trends? *Ocean Dynamics*, *61*(9), 1215–1235. https://doi.org/10.1007/s10236-011-0407-6

South, A., Michael, S., & Massicotte, P. (2017). rnaturalearthdata: World Vector Map Data from Natural Earth Used in 'rnaturalearth'. *R Package Version 0.1.0.* https://cran.r-project.org/web/packages/rnaturalearthdata/index.html

Stobart, B., Downing, N., Buckley, R., & Teleki, K. (2008). Comparison of in situ temperature data from the southern Seychelles with SST data: Can satellite data alone be used to predict coral bleaching events? *Undefined*. https://www.semanticscholar.org/paper/Comparison-of-in-situ-temperature-data-from-the-SST-Stobart-Downing/abeae7a6ce8128d205e543e8a820e827d43b6e44

Stobart, B., Mayfield, S., Mundy, C., Hobday, A. J., & Hartog, J. R. (2015). Comparison of in situ and satellite sea surface-temperature data from South Australia and Tasmania: How reliable are satellite data as a proxy for coastal temperatures in temperate southern Australia? *Marine and Freshwater Research*, *67*(5), 612–625. https://doi.org/10.1071/MF14340

Straub, S. C., Wernberg, T., Thomsen, M. S., Moore, P. J., Burrows, M. T., Harvey, B. P., & Smale, D. A. (2019). Resistance, Extinction, and Everything in Between – The Diverse Responses of Seaweeds to Marine Heatwaves. *Frontiers in Marine Science*, *6*. https://www.frontiersin.org/articles/10.3389/fmars.2019.00763

Sumaila, U. R., & Tai, T. C. (2020). End Overfishing and Increase the Resilience of the Ocean to Climate Change. *Frontiers in Marine Science*, *7*. https://www.frontiersin.org/articles/10.3389/fmars.2020.00523

Taboada, F. G., & Anadón, R. (2015). Determining the causes behind the collapse of a small pelagic fishery using Bayesian population modeling. *Ecological Applications*, *26*(3), 886–898. https://doi.org/10.1890/15-0006

Taboada, F. G., Chust, G., Santos Mocoroa, M., Aldanondo, N., Fontán, A., Cotano, U., Álvarez, P., Erauskin-Extramiana, M., Irigoien, X., Fernandes-Salvador, J. A., Boyra, G., Uriarte, A., & Ibaibarriaga, L. (2024). Shrinking body size of European anchovy in the Bay of Biscay. *Global Change Biology*, *30*(1), e17047. https://doi.org/10.1111/gcb.17047

Thompson, A. R., Ben-Aderet, N. J., Bowlin, N. M., Kacev, D., Swalethorp, R., & Watson, W. (2022). Putting the Pacific marine heatwave into perspective: The response of larval fish off southern California to unprecedented warming in 2014-2016 relative to the previous 65 years. *Global Change Biology*, *28*(5), 1766–1785. https://doi.org/10.1111/gcb.16010

Thoral, F., Montie, S., Thomsen, M. S., Tait, L. W., Pinkerton, M. H., & Schiel, D. R. (2022). Unravelling seasonal trends in coastal marine heatwave metrics across global biogeographical realms. *Scientific Reports*, *12*, 7740. https://doi.org/10.1038/s41598-022-11908-z

Tittensor, D. P., Novaglio, C., Harrison, C. S., Heneghan, R. F., Barrier, N., Bianchi, D., Bopp, L., Bryndum-Buchholz, A., Britten, G. L., Büchner, M., Cheung, W. W. L., Christensen, V., Coll, M., Dunne, J. P., Eddy, T. D., Everett, J. D., Fernandes-Salvador, J. A., Fulton, E. A., Galbraith, E. D., … Blanchard, J. L. (2021). Next-generation ensemble projections reveal higher climate risks for marine ecosystems. *Nature Climate Change*, *11*(11), Article 11. https://doi.org/10.1038/s41558-021-01173-9

Torralba, J., & Besada, M. (2015). A stochastic model for the Iberoatlantic sardine fishery. Global warming and economic effects. *Ocean & Coastal Management*, *114*, 175–184. https://doi.org/10.1016/j.ocecoaman.2015.06.023

Trebilco, R., Fleming, A., Hobday, A. J., Melbourne-Thomas, J., Meyer, A., McDonald, J., McCormack, P. C., Anderson, K., Bax, N., Corney, S. P., Dutra, L. X. C., Fogarty, H. E., McGee, J., Mustonen, K., Mustonen, T., Norris, K. A., Ogier, E., Constable, A. J., & Pecl, G. T. (2022). Warming world, changing ocean: Mitigation and adaptation to support resilient marine systems. *Reviews in Fish Biology and Fisheries*, *32*(1), 39–63. https://doi.org/10.1007/s11160-021-09678-4

Trenkel, V. M., Huse, G., MacKenzie, B. R., Alvarez, P., Arrizabalaga, H., Castonguay, M., Goñi, N., Grégoire, F., Hátún, H., Jansen, T., Jacobsen, J. A., Lehodey, P., Lutcavage, M., Mariani, P., Melvin, G. D., Neilson, J. D., Nøttestad, L., Óskarsson, G. J., Payne, M. R., … Speirs, D. C. (2014). Comparative ecology of widely distributed pelagic fish species in the North Atlantic: Implications for modelling climate and fisheries impacts. *Progress in Oceanography*, *129*, 219–243. https://doi.org/10.1016/j.pocean.2014.04.030

Ullah, H., Nagelkerken, I., Goldenberg, S. U., & Fordham, D. A. (2018). Climate change could drive marine food web collapse through altered trophic flows and cyanobacterial proliferation. *PLoS Biology, 16*(1), e2003446. https://doi.org/10.1371/journal.pbio.2003446

Ummenhofer, C. C., & Meehl, G. A. (2017). Extreme weather and climate events with ecological relevance: A review. *Philosophical Transactions of the Royal Society B: Biological Sciences*, *372*(1723), 20160135. https://doi.org/10.1098/rstb.2016.0135

Urbanek, S. (2013). png: Read and write PNG images. *R Package Version 0.1-7.* https://cran.r-project.org/web/packages/png/index.html

Uriarte, A., & Lucio, P. (2001). Migration of adult mackerel along the Atlantic European shelf edge from a tagging experiment in the south of the Bay of Biscay in 1994. *Fisheries Research*, *50*(1), 129–139. https://doi.org/10.1016/S0165-7836(00)00246-0

Uriarte, A., Alvarez, P., Iversen, S., Molloy, J., Villamor, B., Martíns, M. M., & Myklevoll, S. (2001). Spatial pattern of migration and recruitment of north east atlantic mackerel. *ICES CM 2001/O: 17*.

Uriarte, A., Ibaibarriaga, L., Sánchez-Maroño, S., Abaunza, P., Andrés, M., Duhamel, E., Jardim, E., Pawlowski, L., Prellezo, R., & Roel, B. A. (2023). Lessons learnt on the management of short-lived fish from the Bay of Biscay anchovy case study: Satisfying fishery needs and sustainability under recruitment uncertainty. *Marine Policy*, *150*, 105512. https://doi.org/10.1016/j.marpol.2023.105512

Uriarte, A., Prouzet, P., & Villamor, B. (1996). Bay of Biscay and Ibero Atlantic Anchovy Populations and their Fisheries. *Scientia Marina, 60*.

Valencia, V., Franco, J., Borja, Á., & Fontán, A. (2004). Chapter 7—Hydrography of the southeastern Bay of Biscay. In Á. Borja & M. Collins (Eds.), *Elsevier Oceanography Series* (Vol. 70, pp. 159–194). Elsevier. https://doi.org/10.1016/S0422-9894(04)80045-X

Varela, R., deCastro, M., Costoya, X., Dias, J. M., & Gómez-Gesteira, M. (2024). Influence of the Canary Upwelling System on SST during the unprecedented 2023 North Atlantic Marine Heatwave. *Science of The Total Environment, 949*, 175043. https://doi.org/10.1016/j.scitotenv.2024.175043

Varela, R., Lima, F. P., Seabra, R., Meneghesso, C., & Gómez-Gesteira, M. (2018). Coastal warming and wind-driven upwelling: A global analysis. *Science of The Total Environment*, *639*, 1501–1511. https://doi.org/10.1016/j.scitotenv.2018.05.273

Varela, R., Rodríguez-Díaz, L., de Castro, M., & Gómez-Gesteira, M. (2021). Influence of Eastern Upwelling systems on marine heatwaves occurrence. *Global and Planetary Change*, *196*, 103379. https://doi.org/10.1016/j.gloplacha.2020.103379

Vazquez-Cuervo, J., García-Reyes, M., & Gómez-Valdés, J. (2023). Identification of Sea Surface Temperature and Sea Surface Salinity Fronts along the California Coast: Application Using Saildrone and Satellite Derived Products. *Remote Sensing*, *15*(2), Article 2. https://doi.org/10.3390/rs15020484

Véron, M., Duhamel, E., Bertignac, M., Pawlowski, L., & Huret, M. (2020). Major changes in sardine growth and body condition in the Bay of Biscay between 2003 and 2016: Temporal trends and drivers. *Progress in Oceanography*, *182*, 102274. https://doi.org/10.1016/j.pocean.2020.102274

Viejo, R. M., Martínez, B., Arrontes, J., Astudillo, C., & Hernández, L. (2011). Reproductive patterns in central and marginal populations of a large brown seaweed: Drastic changes at the southern range limit. *Ecography*, *34*(1), 75–84. https://doi.org/10.1111/j.1600-0587.2010.06365.x

Voerman, S. E., Llera, E., & Rico, J. M. (2013). Climate driven changes in subtidal kelp forest communities in NW Spain. *Marine Environmental Research*, *90*, 119–127. https://doi.org/10.1016/j.marenvres.2013.06.006

Wallace, J. M., & Gutzler, D. S. (1981). Teleconnections in the Geopotential Height Field during the Northern Hemisphere Winter. *Monthly Weather Review*, *109*(4), 784–812. https://doi.org/10.1175/1520-0493(1981)109<0784:TITGHF>2.0.CO;2

Wang, Y., Kajtar, J. B., Alexander, L. V., Pilo, G. S., & Holbrook, N. J. (2022). Understanding the Changing Nature of Marine Cold-Spells. *Geophysical Research Letters*, *49*(6), e2021GL097002. https://doi.org/10.1029/2021GL097002

Ware, D. M., & Thomson, R. E. (1991). Link Between Long-Term Variability in Upwelling and Fish Production in the Northeast Pacific Ocean. *Canadian Journal of Fisheries and Aquatic Sciences*, *48*(12), 2296–2306. https://doi.org/10.1139/f91-270

Wernberg, T., & Straub, S. (2016). Impacts and effects of ocean warming on seaweeds. In D. Laffoley & J. M. Baxter (Eds.), *Explaining ocean warming: Causes, scale, effects and consequences* (pp. 87–103). IUCN. : http://dx.doi.org/10.2305/IUCN.CH.2016.08.en

Wernberg, T., Bennett, S., Babcock, R. C., de Bettignies, T., Cure, K., Depczynski, M., Dufois, F., Fromont, J., Fulton, C. J., Hovey, R. K., Harvey, E. S., Holmes, T. H., Kendrick, G. A., Radford, B., Santana-Garcon, J., Saunders, B. J., Smale, D. A., Thomsen, M. S., Tuckett, C. A., … Wilson, S. (2016). Climate-driven regime shift of a temperate marine ecosystem. *Science*, *353*(6295), 169–172. https://doi.org/10.1126/science.aad8745

Wernberg, T., Coleman, M. A., Bennett, S., Thomsen, M. S., Tuya, F., & Kelaher, B. P. (2018). Genetic diversity and kelp forest vulnerability to climatic stress. *Scientific Reports*, *8*(1), Article 1. https://doi.org/10.1038/s41598-018-20009-9

Wernberg, T., Russell, B. D., Moore, P. J., Ling, S. D., Smale, D. A., Campbell, A., Coleman, M. A., Steinberg, P. D., Kendrick, G. A., & Connell, S. D. (2011). Impacts of climate change in a global hotspot for temperate marine biodiversity and ocean warming. *Journal of Experimental Marine Biology and Ecology*, *400*(1), 7–16. https://doi.org/10.1016/j.jembe.2011.02.021

Wernberg, T., Russell, B. D., Thomsen, M. S., Gurgel, C. F. D., Bradshaw, C. J. A., Poloczanska, E. S., & Connell, S. D. (2011). Seaweed Communities in Retreat from Ocean Warming. *Current Biology*, *21*(21), 1828–1832. https://doi.org/10.1016/j.cub.2011.09.028

Wernberg, T., Smale, D. A., Tuya, F., Thomsen, M. S., Langlois, T. J., de Bettignies, T., Bennett, S., & Rousseaux, C. S. (2013). An extreme climatic event alters marine ecosystem structure in a global biodiversity hotspot. *Nature Climate Change*, *3*(1), Article 1. https://doi.org/10.1038/nclimate1627

Wheeler, S. G., Anderson, T. W., Bell, T. W., Morgan, S. G., & Hobbs, J. A. (2017). Regional productivity predicts individual growth and recruitment of rockfishes in a northern California upwelling system. *Limnology and Oceanography*, *62*(2), 754–767. https://doi.org/10.1002/lno.10458

Whitehead, P. J. P., Nelson, G. J., & Wongratana, T. (1988). FAO species catalogue, Vol.7. Clupeoid fishes of the world (Suborder Clupeoidei). An annotated and illustrated catalogue of the herrings, sardines, pilchards, sprats, shads, anchovies, and wolf-herrings. Part 2. Engraulididae. *FAO Fish. Synop*, *7*(125, pt. 2), 305–579.

Wickham, H. (2007). Reshaping Data with the reshape Package. *Journal of Statistical Software*, *21*, 1–20. https://doi.org/10.18637/jss.v021.i12

Wickham, H. (2011). The Split-Apply-Combine Strategy for Data Analysis. *Journal of Statistical Software*, *40*, 1–29. https://doi.org/10.18637/jss.v040.i01

Wickham, H., & Bryan, J. (2019). readxl: Read Excel Files. *R Package Version 1.3.1*. https://cran.r-project.org/web/packages/readxl/index.html

Wickham, H., Averick, M., Bryan, J., Chang, W., McGowan, L. D., François, R., Grolemund, G., Hayes, A., Henry, L., Hester, J., Kuhn, M., Pedersen, T. L., Miller, E., Bache, S. M., Müller, K., Ooms, J., Robinson, D., Seidel, D. P., Spinu, V., … Yutani, H. (2019). Welcome to the Tidyverse. *Journal of Open Source Software*, *4*(43), 1686. https://doi.org/10.21105/joss.01686

Wickham, H., Pedersen, T. L., Seidel, D., Posit, & PBC. (2020). scales: Scale Functions for Visualization. *R Package Version 1.1.1*. https://cran.r-project.org/web/packages/scales/index.html

Wilby, R. L., & Wigley, T. M. L. (1997). Downscaling general circulation model output: A review of methods and limitations. *Progress in Physical Geography: Earth and Environment*, *21*(4), 530–548. https://doi.org/10.1177/030913339702100403

Wilke, C. O. (2020). cowplot: Streamlined Plot Theme and Plot Annotations for 'ggplot2'. *R Package Version 1.1.1*. https://cran.r-project.org/web/packages/cowplot/index.html

Winemiller, K. O. (2005). Life history strategies, population regulation, and implications for fisheries management. *Canadian Journal of Fisheries and Aquatic Sciences*, *62*(4), 872–885. https://doi.org/10.1139/f05-040

Woo, H.-J., & Park, K.-A. (2020). Inter-Comparisons of Daily Sea Surface Temperatures and In-Situ Temperatures in the Coastal Regions. *Remote Sensing*, *12*(10), Article 10. https://doi.org/10.3390/rs12101592

Wood, S. N. (2017). *Generalized Additive Models: An Introduction with R, Second Edition* (2nd ed.). Chapman and Hall/CRC. https://doi.org/10.1201/9781315370279

World Meteorological Organization. (2018). *Guide to climatological practices*. https://library.wmo.int/records/item/28514-guia-de-practicas-climatologicas?language_id=13&back=&offset=

Xiu, P., Chai, F., Curchitser, E. N., & Castruccio, F. S. (2018). Future changes in coastal upwelling ecosystems with global warming: The case of the California Current System. *Scientific Reports*, *8*(1), Article 1. https://doi.org/10.1038/s41598-018-21247-7

Yao, Y., Wang, C., & Fu, Y. (2022). Global Marine Heatwaves and Cold-Spells in Present Climate to Future Projections. *Earth's Future*, *10*(11), e2022EF002787. https://doi.org/10.1029/2022EF002787

Zeileis, A., & Grothendieck, G. (2005). zoo: S3 Infrastructure for Regular and Irregular Time Series. *Journal of Statistical Software*, *14*, 1–27. https://doi.org/10.18637/jss.v014.i06

Ziegler, S. L., Johnson, J. M., Brooks, R. O., Johnston, E. M., Mohay, J. L., Ruttenberg, B. I., Starr, R. M., Waltz, G. T., Wendt, D. E., & Hamilton, S. L. (2023). Marine protected areas, marine heatwaves, and the resilience of nearshore fish communities. *Scientific Reports*, *13*(1), 1405. https://doi.org/10.1038/s41598-023-28507-1

Oviedo, 2024